UNIVERSITY OF CALIFORNIA, SAN DIEGO

Two Studies in Membrane Trafficking: GOLPH3 Binds Phosphatidylinositol-4-phosphate and MYO18A, Connecting the Golgi to the Actin Cytoskeleton and Ubp3p Functions in the Endocytosis of Integral Plasma Membrane Proteins

A dissertation submitted in partial satisfaction of the requirements for the degree Doctor of Philosophy

in

Biological Sciences

by

Holly Christine Dippold

Committee in charge:

Professor Seth J. Field, Chair
Professor Xiangdong Fu
Professor Amy Kiger
Professor Maho Niwa
Professor James Wilhelm

2009

The dissertation of Holly Christine Dippold is approved, and acceptable in quality and form for publication on microfilm and electronically:

(Chair)

University of California, San Diego

2009

TABLE OF CONTENTS

LIST OF FIGURES

LIST OF MOVIES

ACKNOWLEDGEMENTS

I would like to thank my advisor Seth Field for his insightful guidance and innovative ideas.

I would like to acknowledge past and present members of the Field lab for helpful discussions, sharing unpublished data, support, and encouragement. I would especially like to recognize Michelle Ng, Suzette Farber-Katz, Ron Sim, Marshall Peterman, and Patricia Wiharto. Thank you to Michelle M. Ng, Suzette E. Farber-Katz, Sun-Kyung Lee, Monica L. Kerr, Marshall C. Peterman, Ronald Sim, Patricia A. Wiharto, Kenneth A. Galbraith, Swetha Madhavarapu, Greg J. Fuchs, Timo Meerloo, Marilyn G. Farquhar, and Huilin Zhou for allowing me to use material they co-authored. Chapter 1 of this work is a result of experiments done in the Field lab and portions of it have been accepted for publication by *Cell*.

I would like to thank Scott Emr and members of the Emr lab for their help when I was a member of that group. Chapter 2 of this work is the result of experiments done in the Emr lab.

VITA

Education

Doctor of Philosophy, 2009

Division of Biology

University of California, San Diego

Bachelor of Science, Biology, 2002

California State University, Chico

Master of Music, Piano Performance, 1997

Shepherd School of Music

Rice University, Houston, Texas

Bachelor of Music, Piano Performance, 1994

Concordia College, Moorhead, Minnesota

Research Experience

Laboratory of Seth J. Field

University of California, San Diego

2007-present

Laboratory of Scott D. Emr

University of California, San Diego

2003-2007

Laboratory of Leonard Pallanck

University of Washington, Seattle

Summer 2001

Scholarships and Awards

National Cancer Institute Cancer Cell Biology Training Grant

University of California, San Diego

2005-2006

O. and Libby Stansbury Natural Sciences Scholarship

California State University, Chico

2001-2002

Clark Porter Biological Sciences Scholarship

California State University, Chico

2001-2002

Howard Hughes Medical Institute Summer Undergraduate Research Fellowship

University of Washington, Seattle

Summer 2001

Award for Outstanding Achievement and Accomplishment in Organic Chemistry

California State University, Chico

2000-2001

Rice University Shepherd School of Music Scholarship

1994-1997

Concordia College Music Performance Scholarship

1990-1994

Posters

Dippold, H.C., Satterfield, T.F., Jackson, S., Pallanck, L. (2001) Analysis of Genetic and Physical Interactions with a *Drosophila* Ortholog of SCA2. Howard Hughes Medical Institute Summer

Undergraduate Research Program Poster Symposium, University of Washington, Seattle.

Dippold, H.C., Stefan, C.J., Lin, C., Rue, S., Emr, S.D. (2006) The Deubiquitinating Enzyme Ubp3 Functions in the Endocytosis and Downregulation of an Integral Plasma Membrane Protein. Yeast Genetics and Molecular Biology Meeting, July 25-30, Princeton University.

Publication

Dippold, H.C., Ng, M.M., Farber-Katz, S.E., Lee, S.-K., Kerr, M.L., Peterman, M.C., Sim, R., Wiharto, P.A., Galbraith, K.A., Madhavarapu, S., Fuchs, G.J., Meerloo, T., Farquhar, M.G., Zhou, H., Field, S.J. (2009) GOLPH3 Bridges Phosphatidylinositol-4-phosphate and Actomyosin to Stretch and Shape the Golgi to Promote Budding. *Cell,* In Press.

Talk

Dippold, H.C., Ng, M.M., Lee, S.-K., Farber-Katz, S.E., Kerr, M.L., Sim, R., Galbraith, K.A., Madhavarapu, S., Fuchs, G., Zhou, H., and Field, S.J. (2008) A Novel Phosphatidylinositol-4-

phosphate Binding Protein Links the Golgi to the Actin Cytoskeleton and is Essential for Golgi Architecture and Trafficking. The 14th Meeting on Protein Phosphorylation and Cell Signaling, August 15-19, 2008, Salk Institute, La Jolla, California.

ABSTRACT OF THE DISSERTATION

Two Studies in Membrane Trafficking: GOLPH3 Binds Phosphatidylinositol-4-phosphate and MYO18A, Connecting the Golgi to the Actin Cytoskeleton and Ubp3p Functions in the Endocytosis of Integral Plasma Membrane Proteins

by

Holly Christine Dippold

Doctor of Philosophy

University of California, San Diego

Professor Seth J. Field, Chair

Eukaryotic cells maintain a complex organization of vesicular transport pathways through which integral membrane proteins and lipids travel. This allows the cell to maintain the proper functional composition of various intracellular membrane-bound compartments and communication with the external environment via the plasma membrane.

I have studied two facets of vesicular trafficking. Chapter 1 describes the process of vesicle budding from the Golgi and its relationship to the unique morphology of the Golgi. Chapter 2 discusses the regulation of endocytosis and an attempt to find a target for a ubiquitin-specific protease necessary for endocytosis in yeast.

The mechanism underlying the Golgi's flattened structure and its relation to secretory function is an intriguing question in cell biology. Golgi membranes, from yeast to humans, are enriched in phosphatidylinositol-4-phosphate (PtdIns(4)P). In a lipid binding screen, GOLPH3 was identified as a novel PtdIns(4)P-binding protein that depends upon PtdIns(4)P for its Golgi localization. GOLPH3 binds MYO18A, connecting the Golgi to F-actin, thus transmitting a tensile force necessary for Golgi budding and morphology. The same process generating the extended Golgi ribbon observed by fluorescence microscopy and the flattened form observed by electron microscopy drives the formation of transport vesicles.

Integral plasma membrane proteins are down-regulated by endocytosis followed by trafficking to the lysosome for degradation. Can1p is a yeast arginine permease at the plasma membrane and undergoes such regulation. Canavanine is a toxic arginine analog that enters the cell through Can1p. A screen of viable yeast deletion mutants to identify genes which when deleted result in hypersensitivity to canavanine was conducted to identify novel

components involved in down-regulation and internalization of plasma membrane proteins. Three genes identified were ubiquitin-specific proteases. By visual screening, deletion of *UBP3* (UBiquitin-specific Protease 3) was observed to stabilize Can1p-GFP and other endocytic cargoes at the plasma membrane. Rescue experiments show that Ubp3p catalytic activity is necessary for endocytosis. Biochemical experiments indicate that Ubp3p is in a complex with Bre5p, and that Bre5p is also necessary for plasma membrane protein internalization. In conclusion, Ubp3p and its co-factor Bre5p are responsible for deubiquitination and positive regulation of an unidentified protein involved in endocytosis.

Chapter 1: GOLPH3 Binds Phosphatidylinositol-4-phosphate and MYO18A, Connecting the Golgi to the Actin Cytoskeleton

Introduction

Nearly all secretory traffic and the luminal components of most organelles pass through the Golgi. In some secretory cells, the rate of trafficking through the Golgi is fast enough to replace the entire surface area of the plasma membrane (PM) every 10-20 minutes (Kristen and Lockhausen, 1983; Barr and Warren, 1996). This remarkable rate of trafficking requires that the Golgi use a highly efficient mechanism to generate vesicles carrying traffic to its destination. Many of the Golgi components required for trafficking are known, including small GTPases, coat proteins, and lipids (reviewed in De Matteis and Luini, 2008), but the mechanism of the general process of tubulation and budding to form vesicles is unclear.

A perplexing feature of the Golgi is its distinct flattened morphology. Even in yeast, where the Golgi is found dispersed throughout the cytosol, individual cisternae are flat (Preuss et al., 1992). The physical properties of lipids, their asymmetric distribution across the bilayer, curvature-inducing lipid binding proteins, and Golgi matrix proteins have all been proposed to contribute to the unique shape of the Golgi (Peter et al., 2004; Puthenveedu and Linstedt, 2005; Short et al., 2005). Although these may be factors in Golgi

structure, their contribution, if any, to producing flattened cisternae remains uncertain. Beyond the question of the mechanism maintaining Golgi morphology, there remains a larger question of the relationship between this morphology and Golgi secretory function.

The requirement of PtdIns(4)P for Golgi function is evolutionarily conserved from yeast to humans. Genetic experiments in *S. cerevisiae* demonstrate a requirement for the Pik1p PI-4-kinase (Walch-Solimena and Novick, 1999; Audhya et al., 2000) and PtdIns(4)P (Hama et al., 1999) in Golgi secretion. In mammalian cells, PI-4-kinase-IIIβ (Wong et al., 1997) and PI-4-kinase-IIα (Nakagawa et al., 1996) localize to the Golgi, and reporters for the subcellular localization of PtdIns(4)P (composed of a PtdIns(4)P binding domain fused to GFP, reviewed in Varnai and Balla, 2007) indicate that PtdIns(4)P is found predominantly at the Golgi (Godi et al., 2004). In HeLa cells, a dominant-negative PI-4-kinase-IIIβ interferes with reformation of the Golgi complex after washout of Brefeldin A (BFA) (Godi et al., 1999). HEK 293 cells overexpressing PI-4-kinase-IIIβ show enhanced trafficking from the Golgi to the PM (Hausser et al., 2005) and knockdown of PI-4-kinase-IIα impairs trafficking from the Golgi to the PM (Wang et al., 2003). Taken together, the evidence for a role for PtdIns(4)P in Golgi function is compelling, but the crucial targets of PtdIns(4)P important for Golgi function are unclear.

A few direct PtdIns(4)P binding proteins are known, including OSBP (OxySterol Binding Protein), FAPP (phosphatidylinositol-Four-P AdaPtor

Protein), CERT (CERamide Transporter), and their homologs. All contain PH (Pleckstrin Homology) domains that bind specifically to PtdIns(4)P, mediating their Golgi localization (Dowler et al., 2000; Levine and Munro, 2002). Recent evidence demonstrates a role for these PtdIns(4)P binding proteins in non-vesicular trafficking of lipids. OSBP transports cholesterol (Im et al., 2005; Raychaudhuri and Prinz, 2006), FAPP2 transports glucosylceramide (Halter et al., 2007; D'Angelo et al., 2007), and CERT transports ceramide (Hanada et al., 2003). However, the FAPP proteins and CERT are not conserved in *S. cerevisiae*, and simultaneous mutation of all PH domain-containing OSBPs in yeast has little effect, certainly not copying the lethality due to deletion of the *PIK1* PI-4-kinase (Beh et al., 2001).

Many undiscovered PtdIns(4)P binding proteins mediating the effects of PtdIns(4)P at the Golgi may exist and these could provide new insight into the biology of the Golgi. Through large-scale screening of the *Drosophila* proteome for new phosphoinositide binding proteins, GOLPH3 was identified as a novel PtdIns(4)P binding protein. GOLPH3 is an abundant protein conserved from yeast to humans, but contains no previously known phosphoinositide binding domains. GOLPH3 and the yeast homolog Vps74p localize to the Golgi by binding PtdIns(4)P. GOLPH3 also interacts with the unconventional myosin, MYO18A, linking Golgi membranes to the actin cytoskeleton. This interaction provides a tensile force that is required for

normal Golgi vesicle trafficking and architecture, demonstrating an unexpected role for PtdIns(4)P at the Golgi.

Results

An *in vitro* Lipid Binding Screen Identifies GOLPH3 as a Novel PtdIns(4)P Binding Protein

To identify novel phosphoinositide binding proteins, a high throughput proteomic screen based on the lipid blot assay of Dowler et al., 2000 was designed. This assay involves spotting phosphoinositides on a membrane, blotting with a protein of interest, extensive washing, and detecting bound protein. The assay was optimized for use with proteins produced by *in vitro* transcription and translation (IVT) in the presence of ^{35}S-methionine to allow detection.

Critical to the reliability of this assay is the quality of the phosphoinositides. Individual lots of lipids from commercial suppliers were screened by thin layer chromatography (TLC) and each binding assay was validated with a panel of positive control lipid binding proteins.

The *D. melanogaster* proteome was chosen for this screen because it is compact but contains examples of the known phosphoinositide-modifying enzymes and phosphoinositide-dependent signaling pathways found in higher organisms. The *Drosophila* Gene Collection provides an arrayed set of 15,466 cDNAs of known sequence under the control of T7 promoters, allowing for IVT

(Stapleton et al., 2002). To date, a screen of approximately 4000 unique cDNAs from this collection has scored positive hits for many previously identified PH, PX, FYVE, Tub, and Proppin family proteins, validating the method (Figure 1.1). The screen has also identified some unique phosphoinositide binding proteins. One of these, a PtdIns(4)P binding protein (clone ID LD23816, FBgn0010704), lacks any homology to known phosphoinositide binding proteins. The mammalian homolog has been named GOLPH3 (Genbank), GPP34 (Bell et al., 2001), GMx33 (Wu et al., 2000), or MIDAS (Nakashima-Kamimura et al., 2005), and the yeast homolog is Vps74p (Bonangelino et al., 2002).

GOLPH3 is conserved from yeast to humans. It was first identified in a proteomic characterization of the rat Golgi and later suggested to be a Golgi matrix protein (Wu et al., 2000; Bell et al., 2001; Snyder et al., 2006), although its mechanism of interaction with the Golgi and function were not determined. GOLPH3 was recently identified as an oncogene amplified in many human cancers (Scott et al., 2009).

Deletion of *VPS74* in *S. cerevisiae* resulted in defective trafficking of vacuolar proteases in a large-scale screen (Bonangelino et al., 2002). More recently, Vps74p was found localized to the Golgi and necessary for the localization of glycosyltransferases, glycosylation, and normal secretory function of the Golgi in yeast (Schmitz et al., 2008; Tu et al., 2008).

To validate the results of screen, GOLPH3 was confirmed to bind PtdIns(4)P. The *D. melanogaster*, *H. sapiens,* and *S. cerevisiae* orthologs of GOLPH3 expressed in rabbit reticulocyte lysates all bind tightly and specifically to PtdIns(4)P in our lipid blot assay (Figure 1.1). Using *E. coli* expressed and purified GOLPH3 shows the binding to PtdIns(4)P is direct (Figure 1.2). Binding of GOLPH3 to small unilamellar vesicles further demonstrates specific binding to PtdIns(4)P (Figure 1.11).

PtdIns(4)P is Required for GOLPH3 Localization to the Golgi

If GOLPH3 binding to PtdIns(4)P is functionally important *in vivo*, then it should localize to the Golgi, as other groups have previously reported (Wu et al., 2000; Bell et al., 2001; Snyder et al., 2006; Schmitz et al., 2008). Specifically, GOLPH3 was shown by immunofluorescence microscopy to colocalize with *trans* Golgi markers and found by immunoelectron microscopy at the rim of the *trans* Golgi (Wu et al., 2000) and enriched in budding vesicles and tubules (Snyder et al., 2006). Using antibodies raised in our lab to GOLPH3, endogenous GOLPH3 is seen to colocalize with the endogenous *trans* Golgi network (TGN) markers TGN46 and p230 (Figure 1.3), but somewhat less with the *cis* Golgi marker GM130, in several mammalian cell lines (data not shown). In yeast, EGFP-Vps74p colocalizes with the late Golgi marker Sec7p-dsRed (Figure 1.4).

If GOLPH3 binds PtdIns(4)P *in vivo*, then the subcellular localization of the two should coincide. Coexpression of the PtdIns(4)P reporter EYFP-FAPP1-PH (Godi et al., 2004) with mCherry-GOLPH3 in HeLa cells, shows using time-lapse confocal fluorescence microscopy that the two proteins fully colocalize over space and time (Movie 1.1). Both EYFP-FAPP1-PH and mCherry-GOLPH3 were enriched on tubules and vesicles leaving the Golgi, similar to previous results localizing PtdIns(4)P (Godi et al., 2004) and GOLPH3 (Snyder et al., 2006).

If GOLPH3 binds PtdIns(4)P *in vivo*, then reduction of PtdIns(4)P at the Golgi should result in GOLPH3 dissociation from the Golgi. PtdIns(4)P was depleted by expressing a mutant of the lipid phosphatase Sac1 (Sac1-K2A) that constitutively localizes to the Golgi, dephosphorylating PtdIns(4)P without affecting other phosphoinositide pools (Rohde et al., 2003). In HeLa cells, expression of EGFP-Sac1-K2A resulted in loss of GOLPH3 from the Golgi (Figure 1.5), although the Golgi remained intact and other markers remained at the Golgi including p230, TGN46, β-1,4-galactosyltransferase-EYFP, and α-mannosidase II-EGFP (Figure 1.5 and data not shown).

In *S. cerevisiae* the PI-4-kinase Pik1p produces PtdIns(4)P at the Golgi. A temperature sensitive mutant allele of *PIK1*, *pik1-83*^{ts}, is functional at 26°C but inactivated at 37°C, resulting in depletion of PtdIns(4)P at the Golgi (Audhya et al., 2000). In *pik1-83*^{ts} cells, EGFP-Vps74p dissociates from the

Golgi (marked by Sec7p-dsRed) in under ten minutes after shift to 37°C, but remains at the Golgi in wild type cells (Figure 1.6 and Movie 1.2).

Finally, highly over-expressed EYFP-FAPP1-PH displaces endogenous GOLPH3 from the Golgi (Figure 1.7). In conclusion, PtdIns(4)P must be present and available for interaction for GOLPH3 to localize to the Golgi.

GOLPH3 binds PtdIns(4)P via a positively charged binding pocket on the hydrophobic face of the protein

Because GOLPH3 contains no domains found in previously characterized phosphoinositide binding proteins, the minimal domain required for PtdIns(4)P binding was mapped. A series of truncations of *Drosophila* GOLPH3 tested for binding to PtdIns(4)P by lipid blot assay showed that binding to PtdIns(4)P requires amino acids 30-293 (Figure 1.8). This corresponds to the most evolutionarily conserved portion of the protein, and has been termed the GPP34 domain by PFAM. This series of truncations was fused to EGFP and expressed in HEK 293 cells. The GPP34 domain is also the minimal domain required for localization to the Golgi (Figure 1.9).

Using the crystal structure of yeast Vps74p (Schmitz et al., 2008), a positively charged pocket on the hydrophobic face of the GPP34 domain was identified (Figure 1.10). To test the role of this pocket, mutations were made in human GOLPH3 designed to neutralize its charge yet retain proper folding. Two independent mutations of the pocket (R90L and R171A/R174L) each

impaired binding to PtdIns(4)P in the lipid blot assay (data not shown) and the vesicle binding assay (Figure 1.11). Immunofluorescence of 3xHA-tagged wild type and mutant GOLPH3 expressed in HeLa cells shows that the binding pocket mutants also lose Golgi localization (Figure 1.12). This further demonstrates the requirement for PtdIns(4)P binding for Golgi localization.

Deletion of *VPS74* in yeast leads to a growth defect

In order to determine the function of Vps74p in yeast, *VPS74* was deleted in diploid cells and replaced with the *HIS3* gene, as in Longtine et al., 1998. Following sporulation and dissection of tetrads, it was observed that each tetrad consisted of 2 spores that grew into large colonies and 2 spores that grew into small colonies (Figure 1.13). Replica plating onto plates lacking histidine revealed that these small colonies were from spores able to grow in the absence of histidine, or containing the *HIS3* gene (Figure 1.13). Cells from large colonies were unable to grow without added histidine. PCR analysis confirmed that the His^+ cells from the smaller colonies were indeed deleted for *VPS74*, while the His^- cells from the larger colonies were not (data not shown).

Yeast cells deleted for *VPS74* show abnormal secretion and recycling

Given the major role of the Golgi in secretion, the first goal was to determine if Vps74p is required for this function. Can1p is an amino acid permease found at the plasma membrane in yeast (Grenson et al., 1966;

Hoffmann, 1985). After synthesis in the ER, it travels via membrane transport through the Golgi secretory pathway (Roberg et al., 1997) to the plasma membrane where it imports arginine. Trafficking of GFP-tagged Can1p was examined by fluorescence microscopy in wild type and *Δvps74* cells. Can1p-GFP was observed to accumulate within the cell at slightly greater levels in *Δvps74* cells than in wild type cells (Figure 1.14).

In a large-scale yeast two-hybrid screen, Vps74p was found to interact with the retromer component Vps26p (Ito et al., 2001). More recently, human GOLPH3 interacted with another retromer component Vps35 in a yeast two-hybrid screen of a human fetal brain cDNA library (Scott et al., 2009). Two cargoes known to recycle between the late Golgi and endosome in yeast, and thus dependent upon a functional retromer complex, are Kex2p and Vps10p. Kex2p is a resident late Golgi protein responsible for the cleavage of many pro-proteins to mature form before secretion (Gluschankof and Fuller, 1994). GFP-tagged Kex2p was observed in *Δvps74* cells and found to accumulate in a location and manner different from wild type cells (Figure 1.15).

Yeast α-factor is processed by Kex2p at the late Golgi and secreted by MATα cells. When streaked on a lawn of MATa cells hypersensitive to α-factor, the growth of the MATa lawn is normally suppressed around the MATα streak. Spores from dissection of *VPS74/Δvps74* tetrads carrying the *HIS3* gene that were determined to be MATα by process of elimination (mating type segregates 2:2) failed to arrest the growth of a lawn of a MATa mating type

tester strain hypersensitive to α-factor (Figure 1.16). This indicates that either α-factor is not properly processed, or not efficiently secreted in *Δvps74* cells.

Vps10p is a membrane-bound receptor responsible for trafficking of the soluble vacuolar protease carboxypeptidase Y (CPY) from the late Golgi to the endosome, where the protease is sorted via the multivesicular body (MVB) pathway and delivered to the vacuole. Upon delivery of CPY to the MVB, Vps10p recycles back to the late Golgi. The receptor is mislocalized to the vacuolar limiting membrane in cells deleted for retromer components, which are unable to return it to the Golgi (Seaman et al., 1997; Seaman et al., 1998). Examination of GFP-tagged Vps10p (Burda et al., 2002) in *Δvps74* cells showed its localization to be different from that seen in wild type cells, although not necessarily at the vacuole limiting membrane (Figure 1.17).

VPS74 shares its upstream region with the upstream region of *FRQ1*, a gene encoding a regulator of the Golgi PI-4-kinase Pik1p

To demonstrate that a phenotype seen upon deletion of a particular gene is due to the loss of function of only that gene and not of effects on expression of other genes, a wild type copy of the gene on a single-copy plasmid is transformed into the deletion strain and compared to the deletion strain carrying only vector without the gene. The aberrant phenotype of the deletion strain is rescued to wild type if the phenotype is due only to deletion of the target gene. Wild type cells or cells deleted for *VPS74* and transformed

with wild type *VPS74* on a single copy plasmid or empty vector were serially diluted and spotted on plates lacking the amino acid expressed by the vector. Plates were examined after 2, 3, and 4 days. In comparison to wild type cells transformed with either vector, the growth of *VPS74* deletion cells transformed with empty vector was significantly sparser (Figure 1.18). Growth of deletion cells transformed with *VPS74*-expressing vector was also significantly sparser compared to that of wild type cells (Figure 1.18).

This result indicated that something other than Vps74p is affected by *VPS74* deletion. Examination of a chromosomal map around the area of the *VPS74* gene revealed on the opposite strand, 610 base pairs upstream of the 5' end of *VPS74,* the 5' end of *FRQ1* (Figure 1.19). This arrangement suggested that the two genes likely share a promoter region or one gene contains regulatory sequence for expression of the other and vice versa. Frq1p is an N-myristoylated Golgi-localized protein that recruits the essential PI-4-kinase Pik1p to the Golgi membrane and stimulates its activity (Hendricks et al., 1999; Strahl et al., 2005).

Ultimately, to determine if deletion of *VPS74* is affecting expression of *FRQ1*, thereby causing the phenotype seen in *VPS74* deletion cells, one would need to express the entire chromosomal segment containing *VPS74* and *FRQ1* on a single copy plasmid, although this has not been done. If this were to rescue the *VPS74* deletion phenotype, *FRQ1* would need to be

expressed extra-chromosomally under the control of a different promoter at endogenous levels in experiments involving deletion of *VPS74*.

GOLPH3 is an Abundant Protein

To determine a role for GOLPH3 in Golgi function, its abundance was estimated using quantitative Western blotting of HeLa whole cell lysates. Signal intensity from lysates of known numbers of HeLa cells was compared to known quantities of purified bacterial expressed GOLPH3. It is estimated that each HeLa cell expresses 25+/-5 fg (mean+/-SEM, n=4) or 500,000+/-100,000 molecules of GOLPH3, making it a highly abundant protein (Figure 1.20). This abundance suggests that GOLPH3 is a major target of PtdIns(4)P, likely to be of general importance in Golgi function.

GOLPH3 is Required for Anterograde Trafficking from the Golgi to the Plasma Membrane

To determine the requirement for GOLPH3 in Golgi function, the effect of reducing its levels by siRNA knockdown was examined. By Western blot, three different GOLPH3-specific siRNA oligos reduced GOLPH3 levels by at least 70-90% in HeLa or HEK 293 cells (Figure 1.21 and data not shown).

Using the cargo ts045-VSVG-EGFP (Hirschberg et al., 2000), anterograde trafficking was examined in cells depleted of GOLPH3. Transport of ts045-VSVG-EGFP from the ER to the Golgi was unaltered by knockdown

of GOLPH3 (data not shown). Immunofluorescence of unpermeabilized cells using an antibody specific to the extracellular domain of VSVG, allowing unambiguous detection at the PM (Bossard et al., 2007), showed that knockdown of GOLPH3 impaired trafficking from the Golgi to the PM (Figure 1.22). Delivery to the PM was quantified by summing exofacial fluorescence over the volume of each cell and normalizing to total ts045-VSVG-EGFP fluorescence, and a highly significant ($p<10^{-7}$, t-test) defect in delivery of ts045-VSVG-EGFP to the PM was observed in GOLPH3 knockdown cells (Figure 1.23) [control=6.5+/-0.3 (n=13), GOLPH3 knockdown=3.5+/-0.2 (n=12), arbitrary normalized fluorescence units, mean+/-SEM].

GOLPH3 is Required for the Normal Extended Golgi Ribbon

Golgi morphology was next examined by immunofluorescence in GOLPH3 knockdown cells. Depletion of GOLPH3 levels altered the Golgi ribbon, changing it from its normal appearance of extending partially around the nucleus, to condensing it at one end of the nucleus (Figure 1.24). Quantification of Golgi extent around the nucleus, measured as the fraction of nuclear perimeter encompassed by the Golgi, demonstrated a highly significant condensation of the Golgi upon knockdown of GOLPH3 by each of three specific siRNA oligos ($p<10^{-12}$ for each versus control, t-test, Figure 1.25). Several peripheral membrane and transmembrane Golgi markers were examined, and all revealed condensation of *cis*, *medial*, and *trans* Golgi as

well as the TGN upon knockdown of GOLPH3 in HeLa, HEK 293, and NIH 3T3 cells (data not shown).

Rescue of Golgi Morphology in GOLPH3 Knockdown Cells Requires the Ability of GOLPH3 to Bind PtdIns(4)P

To further confirm specificity of the siRNA knockdown phenotype, silent mutations were made in GOLPH3 to allow for expression resistant to our most potent siRNA oligo. Expression of siRNA-resistant wild type GOLPH3 completely rescued the normal extended Golgi ribbon morphology (Figures 1.26, 1.27, and 1.28). An siRNA-resistant construct with the R90L PtdIns(4)P binding mutation was also produced. This mutant, as expected, did not localize to the Golgi, and was incapable of rescuing Golgi morphology (Figure 1.27 and 1.28). These results validate that the effects seen on the Golgi upon knockdown of GOLPH3 are specific to the function of GOLPH3 and further demonstrate that PtdIns(4)P binding is essential to GOLPH3 function at the Golgi.

GOLPH3 Links the Golgi to the Actin Cytoskeleton

The condensation of the Golgi observed upon knockdown of GOLPH3 suggested that GOLPH3 may serve to mediate the application of a tensile force to the Golgi, pulling the Golgi ribbon around the nucleus. A cytoskeletal motor would likely be needed to apply such a force. The dyneins and kinesins

act on microtubules and the myosins act on F-actin. The effect of using nocodazole to depolymerize microtubules results in dispersal of the Golgi (Rogalski and Singer, 1984), quite different from the effect of GOLPH3 knockdown.

The role of actin at the Golgi is poorly understood. To examine the effect of actin depolymerization on Golgi morphology, HEK 293 cells expressing a Golgi marker were treated with Latrunculin B while performing live cell imaging. Treatment with Latrunculin B led to rapid condensation of the Golgi (Movie 1.3), recapitulating a published report (Lázaro-Diéguez et al., 2006) and the effect of GOLPH3 knockdown.

The effects of Latrunculin B treatment or GOLPH3 knockdown on the Golgi were compared by immunofluorescence microscopy. Knockdown of GOLPH3 results in compaction of the Golgi without altering the pattern of F-actin (Figure 1.29). Depolymerization of actin by Latrunculin B leads to compaction of the Golgi without affecting the Golgi association of GOLPH3 (Figure 1.29). Simultaneous knockdown of GOLPH3 and treatment with Latrunculin B produced a similar compaction of the Golgi, but without an additive effect (Figures 1.29 and 1.30). These results raised the possibility that GOLPH3 may in some way link the Golgi to the actin cytoskeleton, exerting a tensile force on the Golgi.

GOLPH3 Binds MYO18A

To determine how GOLPH3 might link the Golgi to actin, thus affecting Golgi structure, an open-ended approach was taken and large-scale immunoprecipitation of GOLPH3 from HeLa whole-cell lysates performed. Analysis by mass spectrometry of two prominent bands near 250 kDa identified the unconventional myosin, MYO18A as a candidate GOLPH3 interacting protein (Figure 1.31).

MYO18A (type XVIIIA, also known as MysPDZ) has been observed to localize to the Golgi (Furusawa et al., 2000; Mori et al., 2003; Mori et al., 2005) and to bind actin filaments (Isogawa et al., 2005). Recently, MYO18A was shown to form a tripartite complex with MRCK and LRAP35a in regulation of actomyosin retrograde flow in cell protrusion and migration (Tan et al., 2008).

The interaction between GOLPH3 and a Golgi-localized myosin suggested a model to explain a role for GOLPH3 in linking the Golgi to the actin cytoskeleton (Figure 1.32). This model builds upon GOLPH3 binding to PtdIns(4)P at the Golgi and suggests that GOLPH3 further interacts with MYO18A, bringing it to the Golgi and thus linking the Golgi to the actin cytoskeleton.

To confirm the interaction between GOLPH3 and MYO18A, GOLPH3 was immunoprecipitated from HeLa whole cell lysates and Western blotted with a MYO18A-specific antibody. MYO18A coimmunoprecipitated specifically with GOLPH3 (Figure 1.33). The interaction is not mediated by actin, as it was

not disrupted by actin depolymerization by Latrunculin B treatment (Figures 1.33 and 1.34). The Golgi-localized myosins MYO2B and MYO6 did not coimmunoprecipitate with GOLPH3 (Figure 1.33), indicating that GOLPH3 interacts uniquely with MYO18A. The GOLPH3/MYO18A complex is likely distinct from the MYO18A/LRAP35a/MRCK complex (Tan et al., 2008), as no MRCKβ was detected in GOLPH3 immunoprecipitates (Figure 1.33) and only a fraction of MYO18A coimmunoprecipitated with GOLPH3 (data not shown).

Next, a direct interaction between GOLPH3 and MYO18A was tested. The N-terminal, Middle, and C-terminal segments of MYO18A were tagged with 6xHis-SUMO, expressed in bacteria, and purified on nickel beads. Incubation of each MYO18A fragment with purified bacterial expressed GOLPH3 and GST (negative control) showed that GOLPH3 was specifically pulled down by the N-terminal and Middle fragments of MYO18A, but not by the C-terminal fragment or 6xHis-SUMO alone (Figure 1.35). This pull-down of GOLPH3 with two fragments of MYO18A indicates a bipartite interaction, suggesting the interaction with intact MYO18A in living cells may be particularly strong.

In examination of the subcellular localization of MYO18A by immunofluorescence, endogenous MYO18A was observed at the Golgi, colocalizing with endogenous GOLPH3 and p230 in cells treated with control siRNA (Figure 1.36). Localization of GOLPH3 at the Golgi is independent of MYO18A, as shown by its Golgi localization upon knockdown of MYO18A.

However, MYO18A no longer localized to the Golgi upon knockdown of GOLPH3, indicating that MYO18A depends on GOLPH3 for Golgi localization and providing confirmation of the biochemical interaction.

Depletion of PtdIns(4)P Phenocopies Knockdown of GOLPH3

The model predicts that depletion of PtdIns(4)P should also result in a condensed Golgi ribbon. In Figure 1.5, depletion of PtdIns(4)P by expression of EGFP-Sac1-K2A caused dissociation of GOLPH3 from the Golgi. Immunofluorescence to p230 reveals that depletion of PtdIns(4)P also causes the Golgi ribbon to condense into a compact ball (Figure 1.5). Quantification of Golgi extent around the nuclear perimeter confirmed that the Golgi compaction was highly significant ($p<10^{-8}$, t-test, Figure 1.37). Similar results were observed with the Golgi reporter α-mannosidase II-EGFP (data not shown) and indicate that depletion of PtdIns(4)P phenocopies knockdown of GOLPH3 and both are essential for an extended Golgi ribbon.

Knockdown of MYO18A Phenocopies Knockdown of GOLPH3

To determine if knockdown of MYO18A causes the same condensed Golgi phenotype, siRNA was used to knock down MYO18A expression in HeLa cells (Figure 1.38). Immunofluorescence to endogenous GOLPH3 and p230 showed that each of three MYO18A-specific siRNAs produced the condensed Golgi phenotype (Figure 1.39). Quantification of Golgi extent

confirmed that the Golgi compaction in MYO18A knockdown cells was highly significant and similar to GOLPH3 knockdown ($p<10^{-10}$, t-test, Figure 1.40). Similar results were observed in HEK 293 cells (data not shown).

Rescue of MYO18A Knockdown Requires an Intact MYO18A ATP-binding Pocket

To confirm the specificity of the MYO18A siRNA phenotype, GFP-tagged wild type mouse MYO18A, predicted to be resistant to our human siRNA oligos, was expressed to rescue the compact Golgi phenotype. Overexpressed mouse MYO18A-EGFP was diffuse in the cell, but fully rescued Golgi morphology resulting from knockdown of human MYO18A (Figures 1.41 and 1.42).

Mutation of the MYO18A ATPase pocket was recently demonstrated to result in a dominant negative effect on actomyosin retrograde flow (Tan et al., 2008). The ability to rescue human MYO18A knockdown with mouse MYO18A-EGFP allowed testing of the function of a mutation in conserved residues in the MYO18A ATP-binding pocket. The G520S/K521A ATPase mutant of mouse MYO18A failed to rescue the condensed Golgi phenotype (Figures 1.41 and 1.42). The ability of MYO18A to generate force on actin has not been formally demonstrated, however since MYO18A is homologous to other myosins, especially in important functional regions, and fails to function when the ATP-binding pocket is mutated (Figures 1.41 and 1.42 and Tan et

al., 2008), it is likely that MYO18A functions, like other myosins, to generate force on F-actin.

trans Golgi Cisternae are Dilated in Cells Depleted of GOLPH3 or MYO18A

The data shown here demonstrate that GOLPH3 functions to bind specifically to Golgi membranes by binding to PtdIns(4)P and also to MYO18A, which likely generates a pulling force, one consequence of which is to stretch the Golgi around the nucleus. Interfering with this apparatus could also produce ultrastructural changes. Depolymerization of actin has been shown to cause rounding of the normally flat Golgi cisternae (Lázaro-Diéguez et al., 2006). Examination of Golgi ultrastructure in control, GOLPH3, or MYO18A knockdown cells by electron microscopy showed that knockdown of GOLPH3 or MYO18A produced dilated Golgi cisternae, frequently dramatically so (Figure 1.43). Cells appeared similar to those observed upon depolymerization of actin (Lázaro-Diéguez et al., 2006). The dilation persists despite cycloheximide treatment, suggesting it is not due to filling of cisternae with protein (data not shown). Cisternal dilation was observed as asymmetrically localized to one side of the Golgi (Figure 1.43). Because PtdIns(4)P (Godi et al., 2004) and GOLPH3 (this study and Wu et al., 2000) localize to the *trans* Golgi, these dilated cisternae likely represent the *trans* Golgi. The thickness of individual cisternae were measured in control,

GOLPH3, and MYO18A knockdown cells, and the difference in cisternal thickness at the *trans* Golgi was found to be highly statistically significant ($p<10^{-4}$, unpaired t-test, Figure 1.44). It is thus concluded that GOLPH3, MYO18A, and F-actin are required to maintain the familiar flattened appearance of the *trans* Golgi.

A Complex of PtdIns(4)P, GOLPH3, MYO18A, and F-actin is Required for Efficient Vesicle Budding

The data demonstrate that PtdIns(4)P, GOLPH3, MYO18A, and F-actin form a molecular apparatus to pull on *trans* Golgi membranes. The purpose of this apparatus may be to contribute to the efficient extraction of tubules or vesicles from the Golgi, and thus may be required for normal Golgi vesicle trafficking. If true, interfering with any component of the apparatus depicted in Figure 1.32 should impair trafficking. Indeed, knockdown of GOLPH3 significantly impaired trafficking of ts045-VSVG-EGFP from the Golgi to the PM (Figures 1.22 and 1.23).

The effect of actin depolymerization, GOLPH3 knockdown, or MYO18A knockdown on the rate of tubule or vesicle exit from the Golgi was examined by measuring the effect on vesicles bearing PtdIns(4)P. Live time-lapse fluorescence microscopy of cells expressing low levels of EYFP-FAPP1-PH was performed. Images were obtained and tubules or vesicles emanating from the Golgi identified (Movie 1.4). The number of vesicles or tubules

leaving the Golgi was counted from the same cells before and after treatment with Latrunculin B. Depolymerization of actin caused a dramatic reduction in the frequency of Golgi exit events (Figure 1.45), consistent with previously reported results (Lázaro-Diéguez et al., 2007). Furthermore, knockdown of GOLPH3 or MYO18A each caused a similar reduction in the frequency of tubule and vesicle exit from the Golgi (Figure 1.45). These results were further validated by measuring the rate of exit of tubules and vesicles marked with the cargo ts045-VSVG-EGFP (data not shown). Thus, GOLPH3, MYO18A, and F-actin are all required for efficient exit from the Golgi.

The requirement for GOLPH3 binding to PtdIns(4)P for efficient Golgi trafficking was next tested. Rescue of EYFP-FAPP1-PH trafficking in siRNA knockdown of GOLPH3 was attempted with siRNA-resistant wild type or R90L mutant GOLPH3. Wild type GOLPH3 rescued efficient EYFP-FAPP1-PH trafficking, but the R90L PtdIns(4)P binding mutant did not (Figure 1.46). Thus, efficient exit from the Golgi depends on the ability of GOLPH3 to bind PtdIns(4)P.

The model indicates that the extension of the Golgi ribbon around the nucleus is a consequence of a tensile force applied via GOLPH3, and that this force is necessary for extracting tubules and vesicles from the Golgi. If true, tubules and vesicles should exit the Golgi on a trajectory parallel to the path of the Golgi ribbon around the nucleus. As above, low levels of EYFP-FAPP1-PH were expressed to mark PtdIns(4)P-bearing vesicles and tubules and the

angle between the trajectory of exit from the Golgi and a tangent to the Golgi ribbon at the point of exit was measured (Figure 1.47 and Movie 1.4). The trajectory angles were graphed for 99 exit events observed in eight cells (Figure 1.48). These angles clustered highly significantly near 0° and 180°, or parallel to the Golgi ($p<0.01$, Kolmogorov-Smirnov). Trafficking of ts045-VSVG-EGFP was also observed, and the angles again clustered around 0° and 180°, as predicted ($p<0.01$, Kolmogorov-Smirnov, data not shown).

Taken together, these data indicate that exit of traffic from the Golgi depends on interaction of PtdIns(4)P, GOLPH3, MYO18A, and F-actin. The initial trajectory of vesicle exit follows the orientation of the tensile force that extends the Golgi ribbon and flattens Golgi cisternae. This force is produced by MYO18A and F-actin and transmitted to the Golgi by GOLPH3 and PtdIns(4)P. The molecular apparatus diagrammed in Figures 1.32 and 1.49 functions to attach the Golgi to the actin cytoskeleton and is necessary to pull tubules and vesicles from it.

Summary and Discussion

A Novel Phosphoinositide Binding Domain

By proteomic screening GOLPH3 has been identified as a PtdIns(4)P binding protein. The specificity of binding is conserved among yeast, flies, and humans. GOLPH3 Golgi localization is a consequence of its interaction with PtdIns(4)P. The highly conserved GOLPH3 proteins represent a family of

phosphoinositide binding proteins with a unique structure (Schmitz et al., 2008) unlike other known phosphoinositide binding proteins, and their ability to bind PtdIns(4)P could not have been predicted before this screen. The confirmation of GOLPH3 as a PtdIns(4)P binding protein and characterization of its critical role at the Golgi provides strong validation of the screen and the hypothesis that many undiscovered phosphoinositide binding proteins exist and knowing their identity and properties will illuminate fundamental cell functions.

Function of GOLPH3 at the Golgi

These data indicate that PtdIns(4)P, GOLPH3, MYO18A, and F-actin are all necessary for extension of the Golgi around the nucleus. The compact Golgi phenotype is unusual and not described in many other manipulations of the Golgi, including in response to nocodazole, brefeldin A, knockdown of Golgi proteins such as Arl1 (Lu et al., 2004), GCC185 (Derby et al., 2007), p230, (Yoshino et al., 2005), GM130 or GRASP65 (Puthenveedu et al., 2006), COG1, COG2, or COG5 (Oka et al., 2005), or knockdown of other PtdIns(4)P binding proteins such as FAPP1, FAPP2 (Godi et al., 2004), or CERT (Giussani et al., 2008). Golgi compaction is a distinct result of depletion of PtdIns(4)P, knockdown of GOLPH3, knockdown of MYO18A, or depolymerization of F-actin, consistent with the interactions depicted in the model (Figure 1.32).

GOLPH3 functions at the Golgi by binding directly and specifically to Golgi membranes through PtdIns(4)P, although it remains formally possible that an additional Golgi factor may help to recruit GOLPH3 to the Golgi. GOLPH3 also binds MYO18A, linking the Golgi to actin filaments. Based on homology and the requirement for an intact ATP-binding pocket, MYO18A is likely functioning as an active motor, although it is possible that MYO18A functions only to link to F-actin, and the generation of tension involves a more complicated mechanism.

Actin and Myosin at the Golgi

A role for F-actin at the Golgi has been suggested previously. In *S. cerevisiae,* vesicles trafficking from the Golgi in the polarized secretory pathway travel along actin cables in a process dependent on the Pik1p PI-4-kinase (Finger and Novick, 1998; Walch-Solimena and Novick, 1999; Hsu et al., 2004; Pruyne et al., 2004).

In mammalian cells, F-actin and actin-associated proteins have been found at the Golgi (for reviews see Egea et al., 2006 and De Matteis and Luini, 2008). Egea and colleagues have published a series of studies showing that depolymerization of actin alters Golgi morphology and trafficking, although a compelling mechanism was not identified (Egea et al., 2006; Lázaro-Diéguez et al., 2007). These data and model provide an explanation for their results.

Previous studies have identified other myosins at the Golgi. In mammalian cells, MYO1, MYO2, and MYO6 have been implicated in Golgi secretory function (for review see Allan et al., 2002). Our mass spectrometry and coimmunoprecipitation data reveal that GOLPH3 couples specifically to MYO18A in mammalian cells.

In mammalian cells, the demonstration that vesicles leaving the Golgi follow a path that colocalizes with microtubules (Cooper et al., 1990) has led to a popular model whereby vesicles are carried by microtubules. A growing number of proteins serve to bridge microtubules and F-actin (reviewed in Rodriguez et al., 2003), providing potential synthesis between the F-actin model favored in yeast and these data, and the microtubule model that has been favored in the mammalian system.

Conservation to *S. cerevisiae*

Vps74p binds PtdIns(4)P *in vitro* and is downstream of *PIK1 in vivo*. Furthermore, human GOLPH3 can partially rescue a *vps74* mutant (Tu et al., 2008), and so they likely function similarly. In mammals, GOLPH3 functions through its interaction with MYO18A, but the *S. cerevisiae* genome does not encode an ortholog of MYO18A, having only type I, II, and V myosins (Berg et al., 2001). There are many examples in *S. cerevisiae* where a small number of primordial myosins perform the range of functions that in higher organisms are partitioned between a larger number of more specialized myosins (for

review see Berg et al., 2001), and thus Vps74p could be expected link to one of these. In fact, Pik1p-dependent polarized secretion is proposed to be dependent on the type V myosin, Myo2p (Walch-Solimena and Novick, 1999; Pruyne et al., 2004), making it a good candidate.

Two groups recently reported that in yeast Vps74p is involved in maintaining the steady-state localization of *cis* and *medial* Golgi-localized glycosyltransferases that function in cell wall biosynthesis (Schmitz et al., 2007; Tu et al., 2007). In mammalian cells, GOLPH3 localizes to the *trans* Golgi (Wu et al., 2000; Snyder et al., 2006 and current study). The specific glycosyltransferases studied in yeast are not conserved beyond fungi. Several mammalian glycosyltransferases were examined in our lab and neither interaction with GOLPH3 nor mislocalization upon knockdown of GOLPH3 has been seen (data not shown). It is possible that this represents a species difference.

The Role of PtdIns(4)P at the Golgi

Based on high abundance of GOLPH3 (~500,000 molecules per HeLa cell) and high conservation from *S. cerevisiae* to humans, it is a major target of PtdIns(4)P. Other well-documented targets of PtdIns(4)P include OSBP, FAPP, and CERT which function in the non-vesicular transport of cholesterol, glucosylceramide, and ceramide, respectively (Im et al., 2005; Raychaudhuri and Prinz, 2006; Halter et al., 2007; D'Angelo et al., 2007; Hanada et al.,

2003). Notably, these proteins all function to regulate the composition of Golgi membranes and therefore are expected to regulate the mechanical properties of the membrane. Thus, PtdIns(4)P has targets that simultaneously regulate the tensile force on the membrane and its mechanical properties, including presumably its elasticity and elastic limit, thereby determining behavior of the membrane when subjected to tension. The coordinate regulation of a tensile force and the mechanical properties of the membrane provides an ideal arrangement to control the ability to pull vesicles from the Golgi and consequently, to generate the morphology uniquely characteristic of the Golgi. This model provides a simple explanation for all available data and an appealing link between the process of vesicle budding and Golgi morphology.

Future Directions

The purification of GOLPH3 followed by mass spectrometry identified GOLPH3 interactors other than MYO18A (Figure 1.50). One of these, Golgi-localized optineurin (also called HYPL, FIP-2, NRP, or TFIII-IntP), is an interesting candidate for further study. It has been implicated in processes as diverse as transcription (Moreland et al., 2000), cell shape (Hattula and Peränen, 2000), cell survival (De Marco et al., 2006), secretion (Sahlender et al, 2005; del Toro et al., 2009), Golgi morphology (Park et al., 2006), and NF-κB signaling (Li et al., 1998; Zhu et al., 2007; Mrowka et al, 2008). Mutations in the OPTN gene are associated with glaucoma (Rezaie et al., 2002; Park et

al., 2006) and the interaction of optineurin with huntingtin links it to Huntington's disease (Faber et al., 1998; Hattula and Peränen, 2000; del Toro et al., 2009).

Optineurin is a 67 kDa protein with multiple coiled-coil domains, two leucine zippers, a zinc finger, and a UBAN domain. UBAN is a Ubiquitin-Binding domain in ABIN proteins and NEMO (Wagner et al., 2008) and the UBAN motif of NEMO (NF-κB Essential MOdulator) bound to ubiquitin has been crystallized and shown to form a parallel coiled-coil dimer, selectively binding two linear diubiquitin molecules (Rahighi et al., 2009). The yeast GOLPH3 homolog Vps74p was identified in a screen of the entire yeast proteome for ubiquitinated proteins (Peng et al 2003), and so we reason that GOLPH3 is likely ubiquitinated and that optineurin binds ubiquitinated GOLPH3.

A few preliminary experiments have indicated that GOLPH3 and optineurin interact in the same pathway, possibly through the binding of ubiquitinated GOLPH3 by optineurin. The interaction between optineurin and GOLPH3 was first confirmed by immunoprecipitation of GOLPH3 followed by western blot using an antibody specific to optineurin. Immunoprecipitation from HeLa whole cell lysates was performed with GOLPH3-specific or pre-immune serum. Western blot indicates that optineurin coimmunoprecipitates only when GOLPH3 is immunoprecipitated (Figure 1.51). Like the interaction between MYO18A and GOLPH3, the interaction between optineurin and

GOLPH3 is not dependent upon actin filaments, as the interaction is retained in Latrunculin B-treated cells (Figure 1.51).

Next, optineurin levels were knocked down in HeLa cells by siRNA. Using three different optineurin-specific siRNA oligos, Western blot shows that optineurin can be knocked down to less than 10% of normal levels (Figure 1.52). Immunofluorescence to cells prepared in parallel shows that knockdown of optineurin with two of the three oligos results in a compact Golgi phenotype. It is not clear at this point why one oligo seems to have no effect, but we suspect it may relate to the extent of knockdown or to off-target effects.

Experiments to directly detect ubiquitinated GOLPH3 are being optimized, but one experiment already performed indicates that ubiquitination of GOLPH3 may strengthen its interaction with optineurin. N-ethylmaleimide (NEM) inhibits ubiquitin-specific proteases by creating disulfide bonds with the catalytic cysteines, and is often used in biochemical experiments to detect ubiquitin and ubiquitination. In a coimmunoprecipitation to test whether or not the addition of NEM to the immunoprecipitation buffer made a difference in how much optineurin coimmunoprecipitates with GOLPH3, a considerable difference between the two conditions was seen. Immunoprecipitation of GOLPH3 in the presence of NEM resulted in far more optineurin coimmunoprecipitating with GOLPH3 than in buffer without NEM (Figure 1.54). For now, our working model is that GOLPH3 undergoes ubiquitination and that

this allows binding by optineurin. In some way, optineurin is required for GOLPH3 function in maintaining Golgi morphology.

Acknowledgements

Thank you to Seth Field for starting this project and guiding the research. Thank you to Michelle Ng, Suzette Farber-Katz, Sun-Kyung Lee, and Marshall Peterman for sharing unpublished data. Thank you to Ronald Sim and Patricia Wiharto for technical support. Thank you to Michelle M. Ng, Suzette E. Farber-Katz, Sun-Kyung Lee, Monica L. Kerr, Marshall C. Peterman, Ronald Sim, Patricia A. Wiharto, Kenneth A. Galbraith, Swetha Madhavarapu, Greg J. Fuchs, Timo Meerloo, Marilyn G. Farquhar, and Huilin Zhou for allowing me to use material they co-authored. Portions of this chapter have been accepted for publication in *Cell*.

Figures

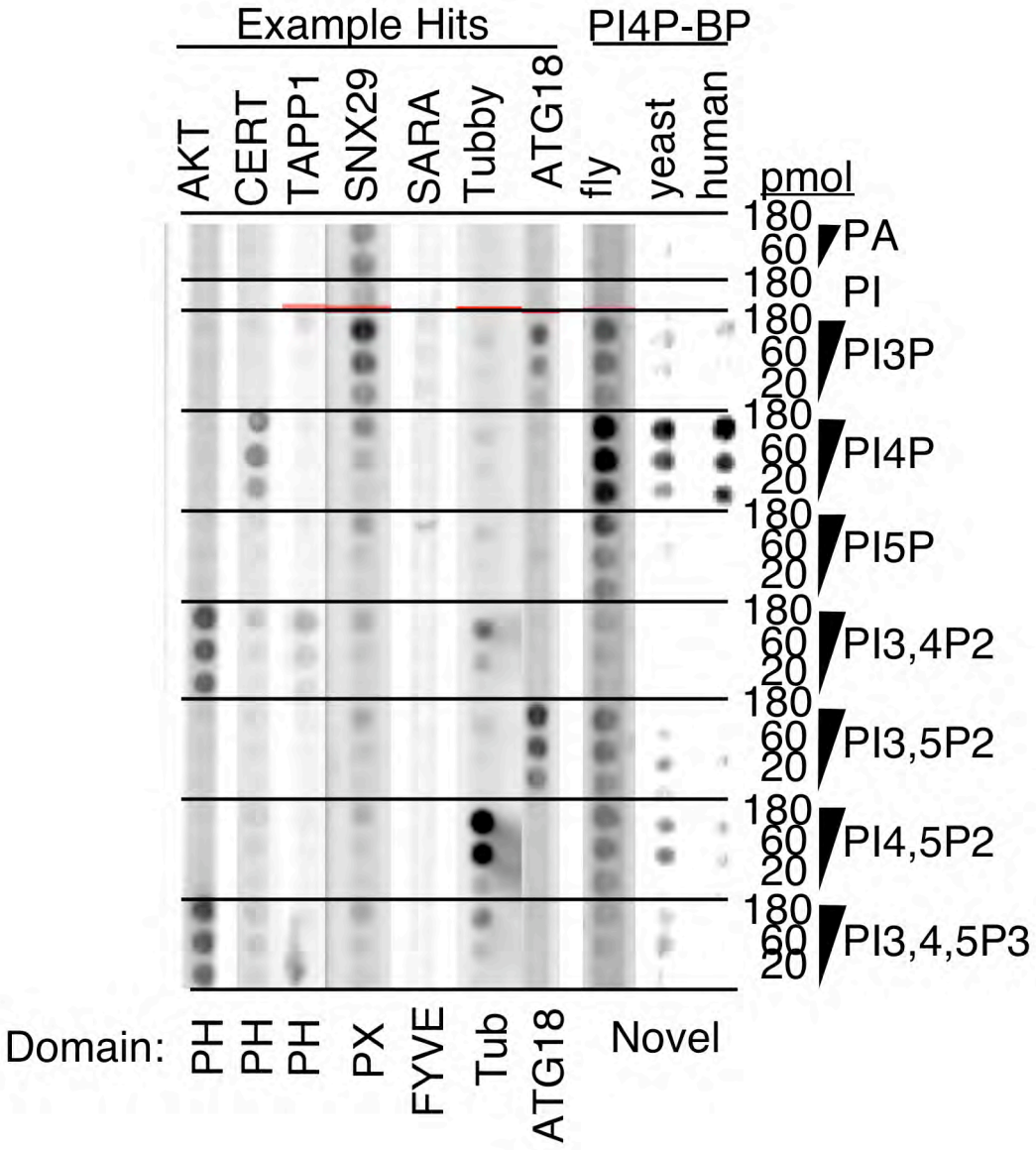

Figure 1.1. Screening of the *Drosophila* Gene Collection for lipid binding. Example hits correspond to previously well-validated lipid binding proteins with known binding domains. The screen also identified novel lipid binding proteins. Shown is novel PtdIns(4)P binding protein, GOLPH3. The yeast (Vps74p) and human orthologs also bind PtdIns(4)P.

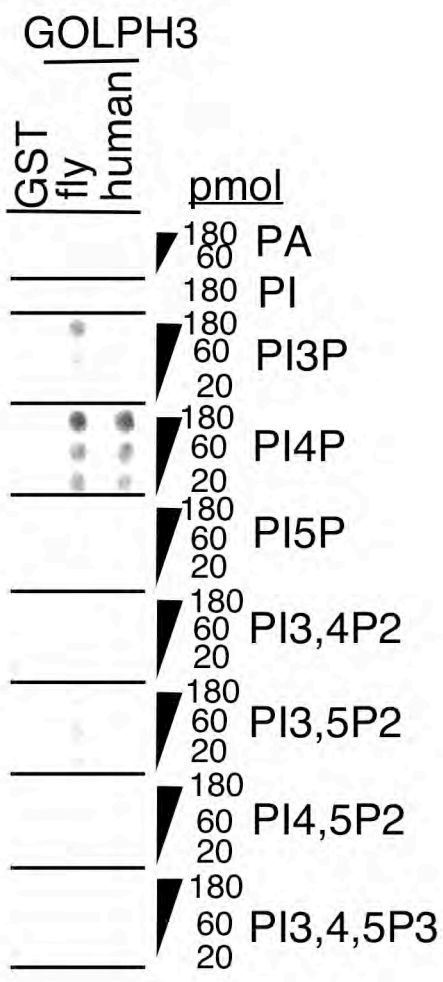

Figure 1.2. Purified *Drosophila* and human GOLPH3 bind PtdIns(4)P *in vitro.* Bacterial expressed and purified GST fusions of *Drosophila* and human GOLPH3 specifically bind PtdIns(4)P *in vitro* by lipid blot assay.

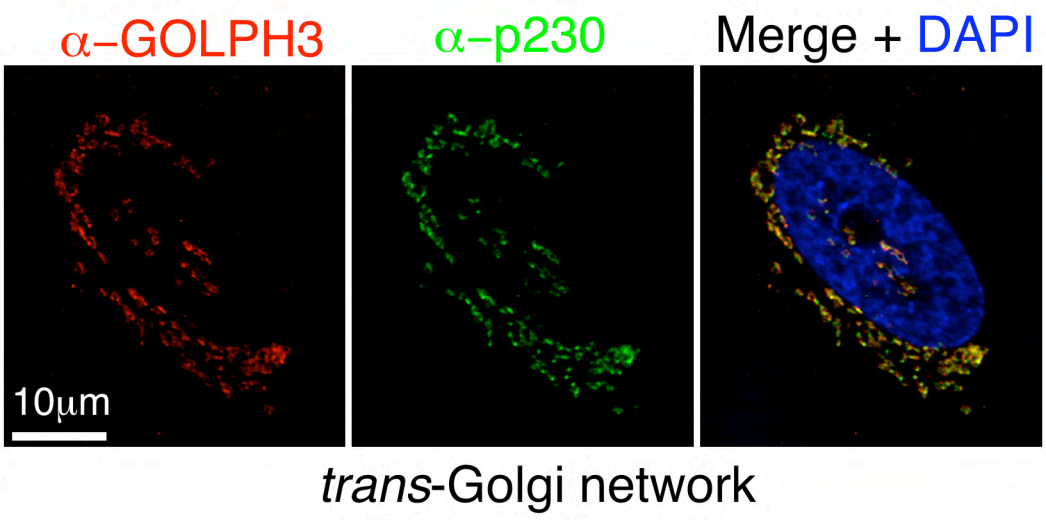

Figure 1.3. Endogenous GOLPH3 (green) colocalizes with endogenous p230 (red) in HeLa cells. Yellow in merge indicates colocalization.

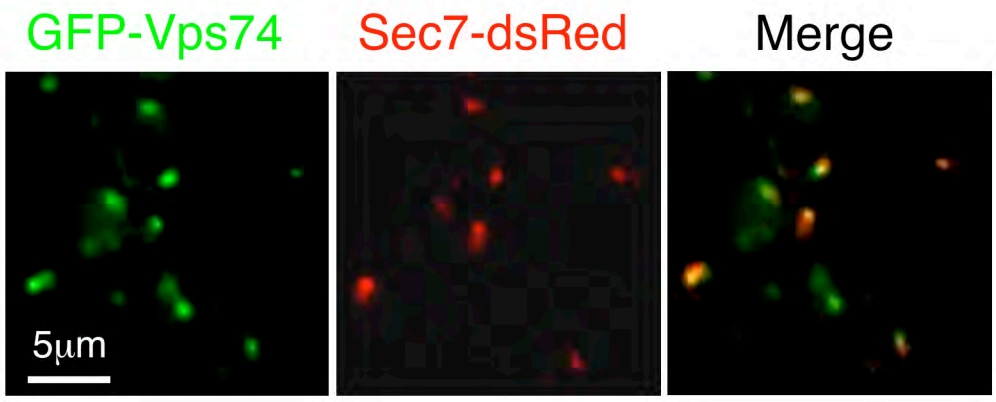

Figure 1.4. In yeast, GFP-Vps74p (GOLPH3 homolog) colocalizes with co-expressed late Golgi marker Sec7p-dsRed. Yellow in merge indicates colocalization.

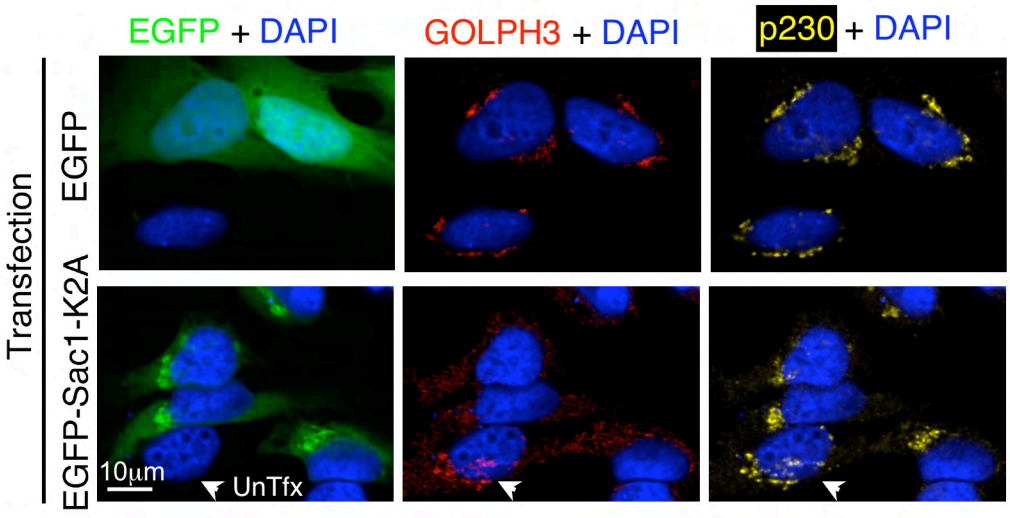

Figure 1.5. Depletion of PtdIns(4)P results in the dissociation of GOLPH3 from the Golgi. HeLa cells expressing EGFP-tagged phosphatase Sac1-K2A or EGFP (control) stained for endogenous GOLPH3 (red), TGN marker p230 (yellow), and DAPI (blue). In control and untransfected cells, GOLPH3 and p230 co-localize at the Golgi, but EGFP-Sac1-K2A renders GOLPH3 staining diffuse and distinct from p230.

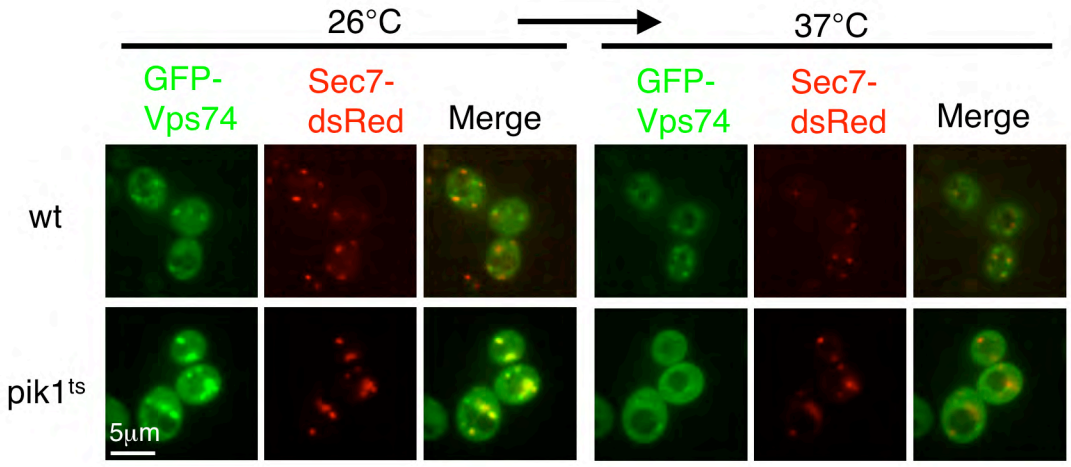

Figure 1.6. PtdIns(4)P is depleted in *S. cerevisiae* expressing temperature sensitive allele *pik1-83*^{ts} upon shift to 37°C. In wild type, GFP-Vps74p remains colocalized with late Golgi marker Sec7p-dsRed at both temperatures. In *pik1-83*^{ts}, GFP-Vps74p dissociates from the Golgi upon shift to 37°C (also see Movie 1.2).

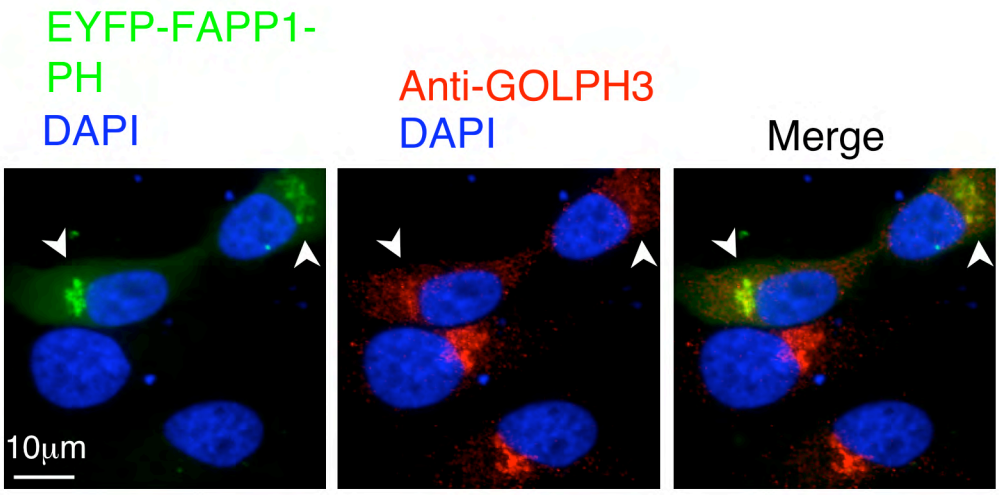

Figure 1.7. Overexpression of EYFP-FAPP1-PH displaces endogenous GOLPH3 from the Golgi. White arrowheads indicate cells expressing EYPF-FAPP1-PH (green) in which anti-GOLPH3 staining (red) is diffuse vs. adjacent untransfected cells.

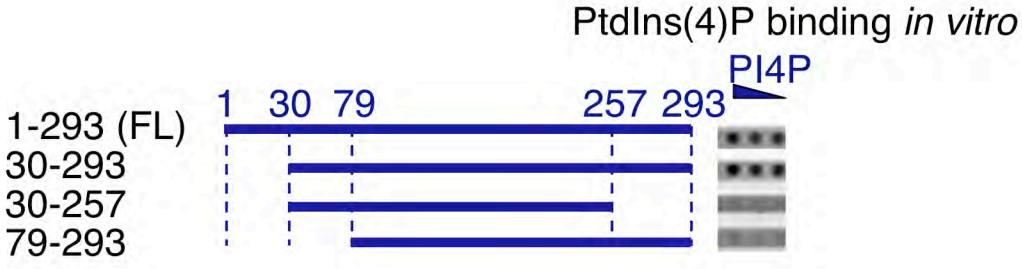

Figure 1.8. Lipid blot with truncations of *Drosophila* GOLPH3 expressed *in vitro* show amino acids 30-293 make up the minimal PtdIns(4)P binding domain.

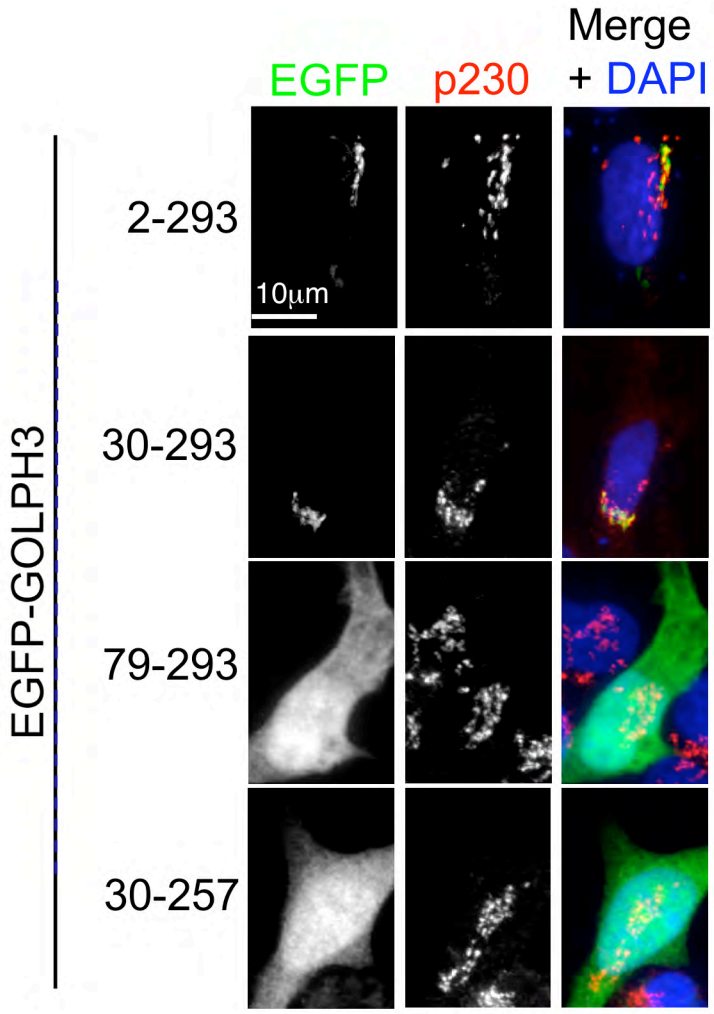

Figure 1.9. Truncations of *Drosophila* GOLPH3 expressed in HEK 293 cells for fluorescence microscopy show that the minimal PtdIns(4)P binding domain is also the minimal domain required for Golgi localization.

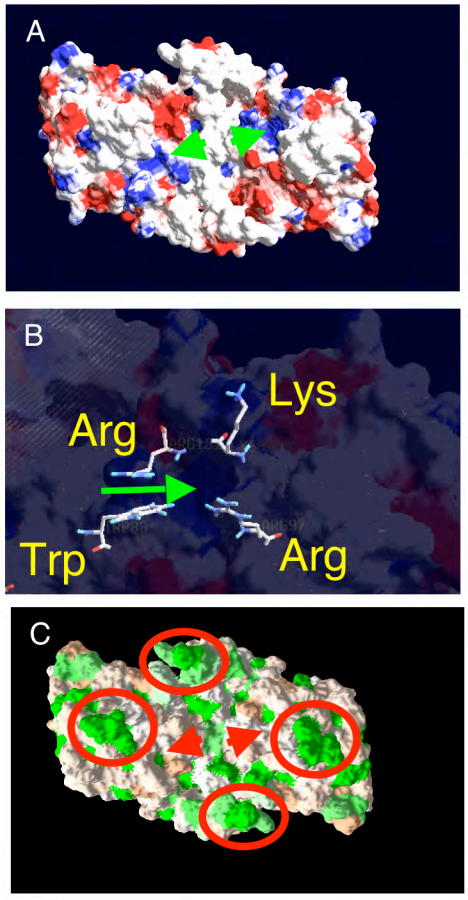

Figure 1.10. (A) Electrostatic surface rendering (red=acidic, blue=basic) of the Vps74p core homodimer reveals in each subunit a basic pocket (green arrows) that could accommodate a phosphoinositide head group. (B) Residues lining the pocket (green arrow) include the conserved Arg97 at the bottom of the pocket, conserved Lys178 and Arg181 at the sides of the pocket, and conserved Trp88 at the side of the pocket. Note that in other classes of phosphoinositide binding domains, a common feature of the binding pocket are conserved basic amino acids that ligate the phosphates and hydroxyls on the inositol ring, and often a conserved aromatic residue (such as Trp) that forms stacking interactions with the inositol ring. (C) Hydrophobic surface rendering (green=hydrophobic, orange=hydrophilic) of the Vps74p core homodimer reveals that residues extending up (toward the viewer) beyond the plane of the two putative phosphoinositide binding pockets (red arrows) are highly hydrophobic (red circles), consistent with an interaction with the lipid bilayer that would occur if the molecule were engaged by two molecules of PtdIns(4)P in the two binding pockets of the homodimer.

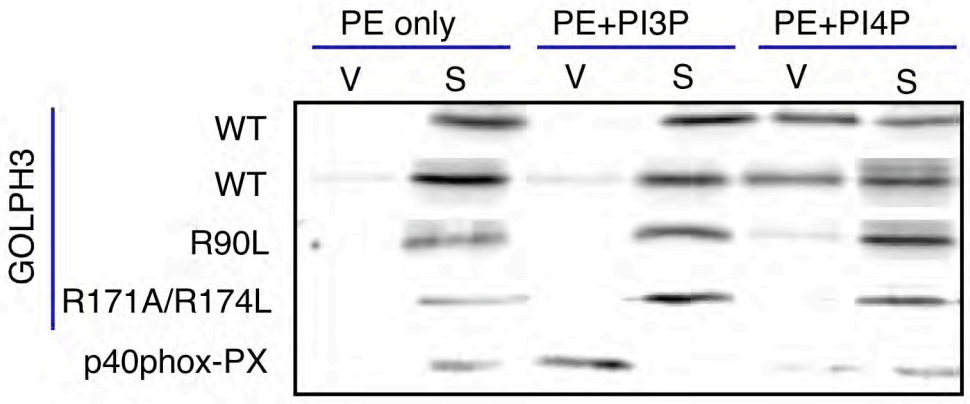

Figure 1.11. Lipid vesicle binding shows the specificity of wild type GOLPH3 for PtdIns(4)P, but not for PtdIns(3)P. R90L and R171A/R174L mutants do not bind PtdIns(4)P-enriched vesicles. The p40phox-PX control binds PtdIns(3)P, but not PtdIns(4)P vesicles. (V=vesicle, S=soluble)

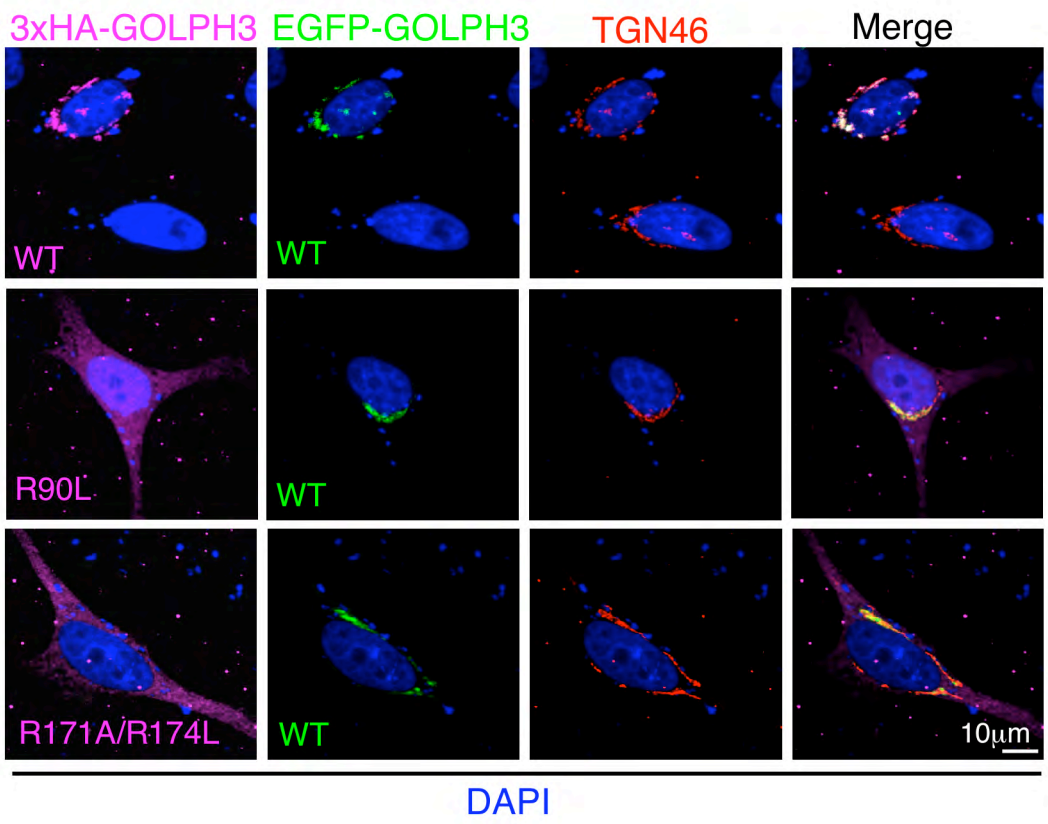

Figure 1.12. In HeLa cells, R90L and R171A/R174L mutations of GOLPH3 (magenta) mislocalize to the cytosol, but coexpressed wild type EGFP-GOLPH3 (green) remains at the Golgi as marked by TGN46 (red). DAPI in blue.

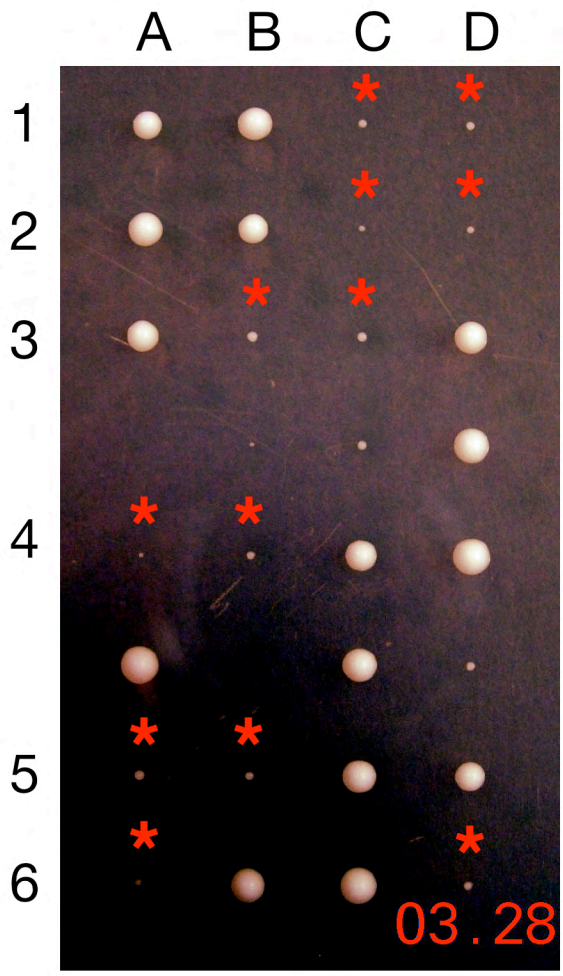

Figure 1.13. Germination of spores from dissection of six complete tetrads from *VPS74/Δvps74::HIS3* diploid strain on rich media. Red asterisks denote colonies from cells that are His^+, or deleted for *VPS74*.

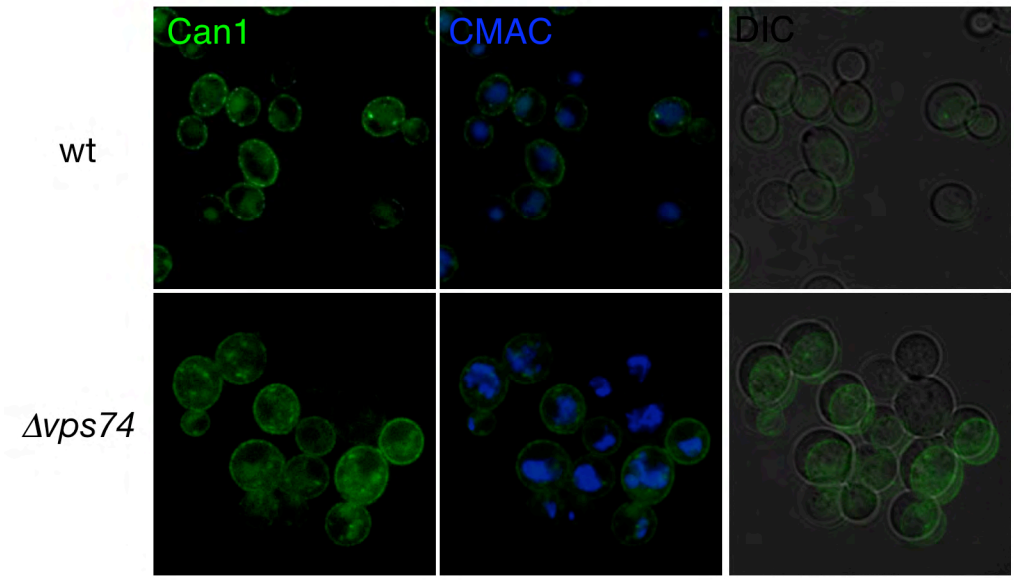

Figure 1.14. Cells deleted for *VPS74* show slightly more internal Can1p-GFP accumulation than wild type cells. CMAC stains the vacuole/lysosome.

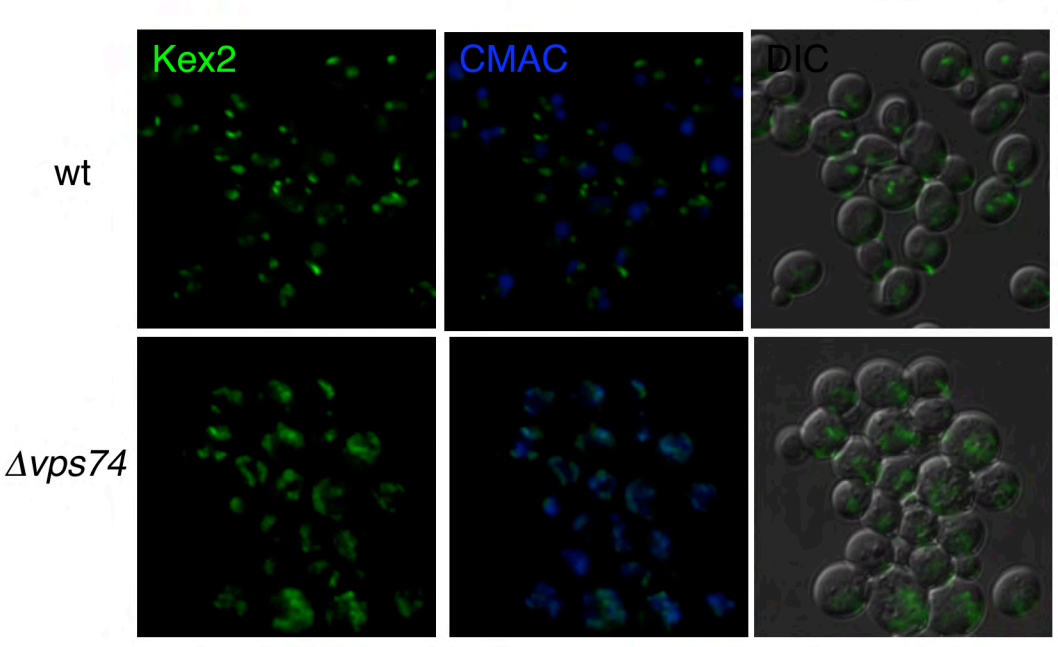

Figure 1.15. Cells deleted for *VPS74* show a different Kex2p-GFP pattern of localization than wild type cells. CMAC stains the vacuole/lysosome.

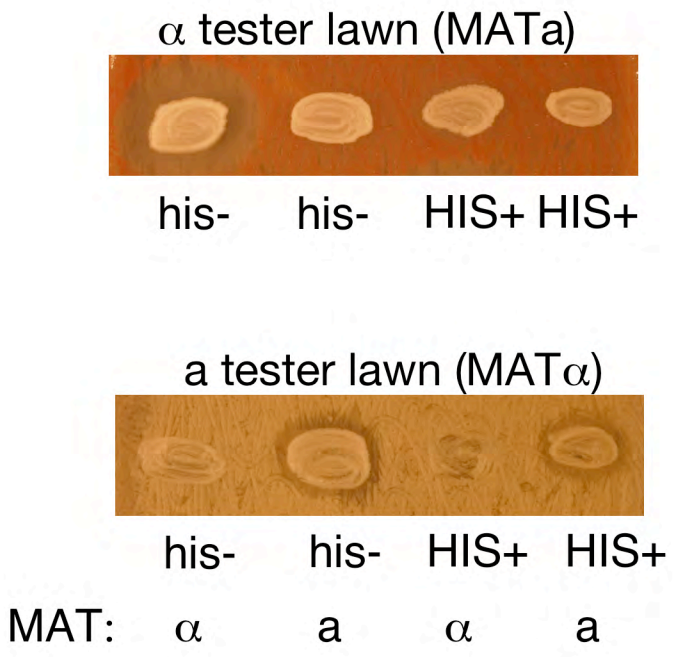

Figure 1.16. MATα cells deleted for *VPS74* do not suppress growth of a lawn of α-factor hypersensitive MATa cells, indicating that α-factor is not being secreted or not fully processed in *Δvps74* cells.

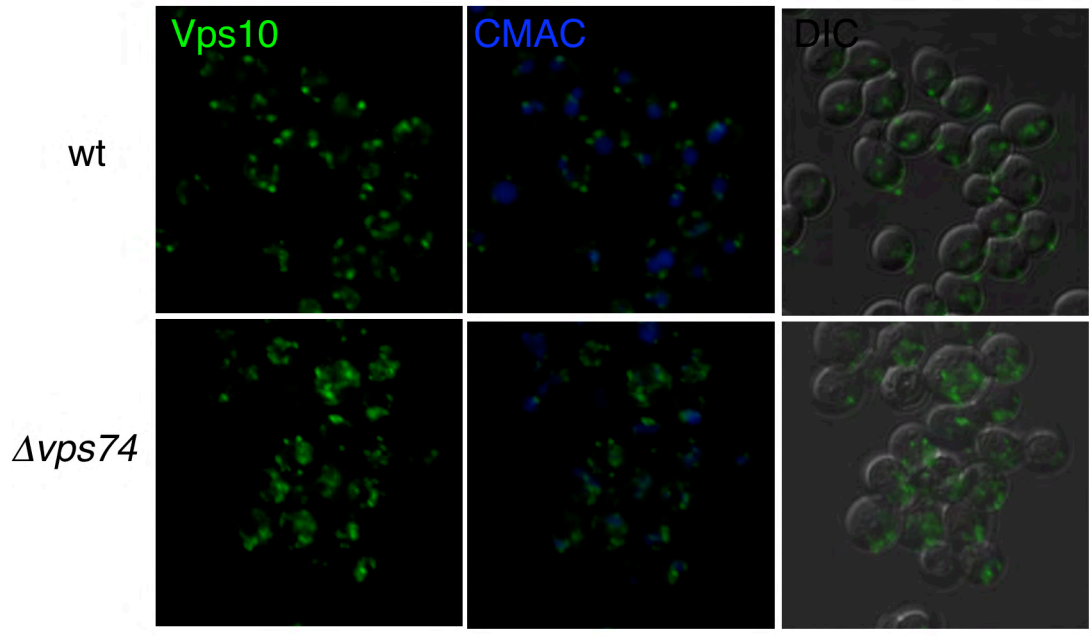

Figure 1.17. Vps10p-GFP, the yeast CPY receptor shows a different pattern of localization in *Δvps74* cells in comparison to wild type cells. CMAC stains the vacuole/lysosome.

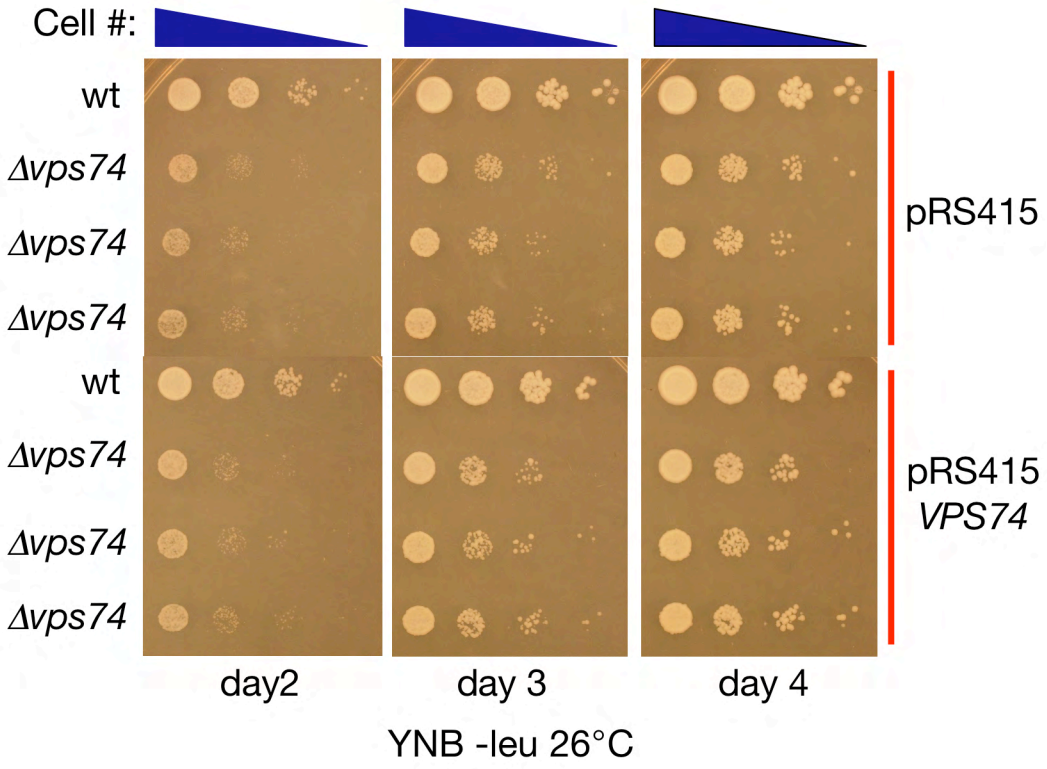

Figure 1.18. Serial dilutions of cells spotted onto plates show that the growth defect of *Δvps74* cells is not rescued by expression of wild type *VPS74* from a single-copy vector. Wild type cells transformed with empty vector or vector carrying *VPS74* grow at approximately equal rates. *VPS74* deletion cells transformed with empty vector or vector carrying *VPS74* grow at approximately equal rates, but more slowly than wild type.

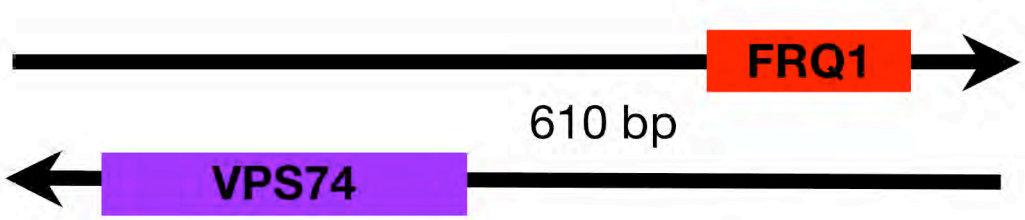

Figure 1.19. The 5' end of *FRQ1* is 610 base pairs upstream of the 5' end of *VPS74*, indicating that the two genes likely share a promoter region. Deletion of *VPS74* may affect expression of *FRQ1.*

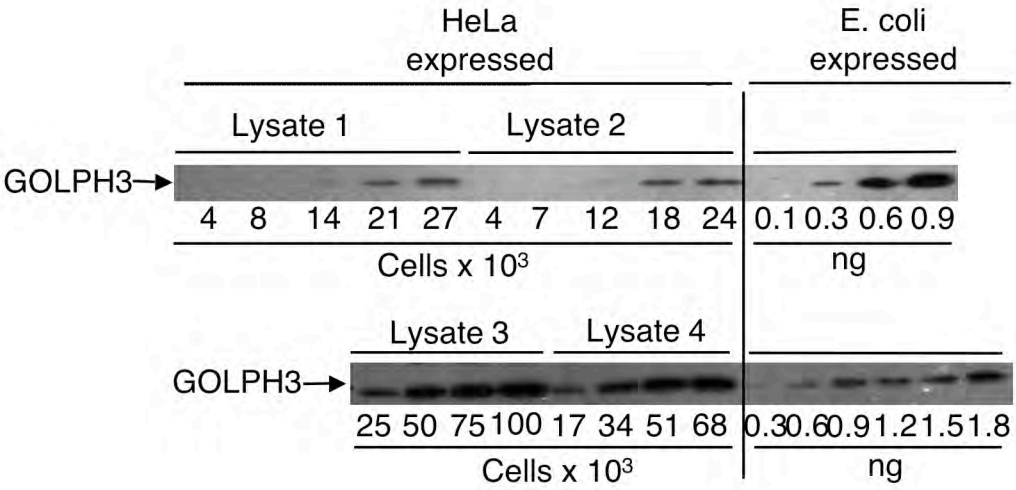

Figure 1.20. An estimation of GOLPH3 abundance in HeLa cells. Western blot with GOLPH3 antiserum was used to compare levels of GOLPH3 in whole-cell SDS lysates from pre-determined numbers of HeLa cells to purified *E. coli* expressed GOLPH3 of known quantities. Calculations indicate that each HeLa cell contains 25+/-5 fg, or 500,000+/-100,000 molecules of GOLPH3 (mean+/-SEM, n=4).

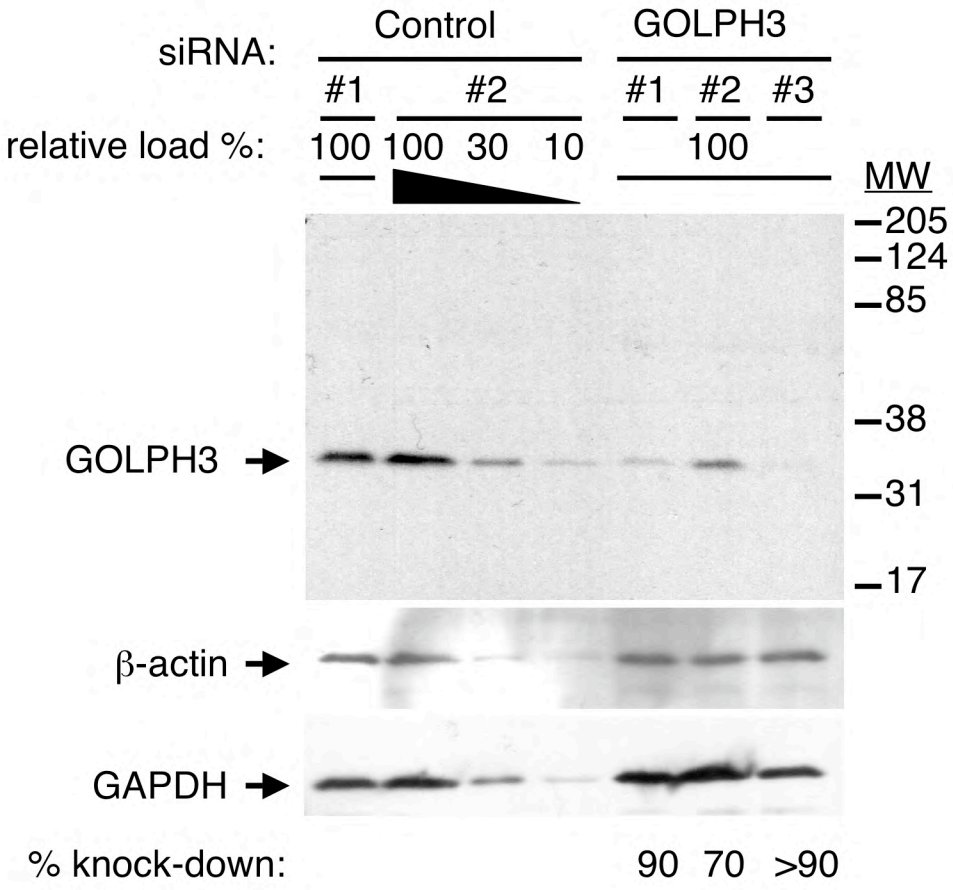

Figure 1.21. Western blot of HeLa lysates shows GOLPH3 is knocked down 70-90% by each specific siRNA. GOLPH3 antiserum recognizes a single band at 34 kDa in control lysates. Decreasing amounts of control lysate were loaded to allow for quantification of knockdown. Blots for β-actin and glyceraldehyde-3-phosphate dehydrogenase (GAPDH) verify equal loading.

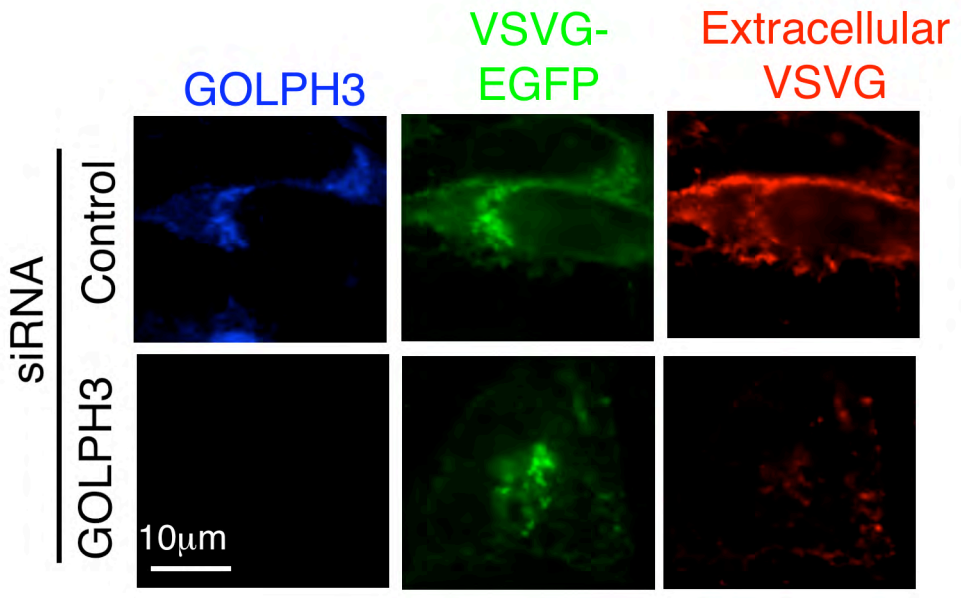

Figure 1.22. Trafficking of ts045-VSVG-EGFP, through the Golgi to the PM is impaired by the knockdown of GOLPH3. HeLa cells were serially transfected with GOLPH3 or control siRNA, then with ts045-VSVG-EGFP expression vector, incubated at 40°C overnight, then shifted to 32°C for 2 hours. Arrival at the PM was determined unambiguously with an antibody to the extracellular domain of VSVG applied to unpermeabilized cells.

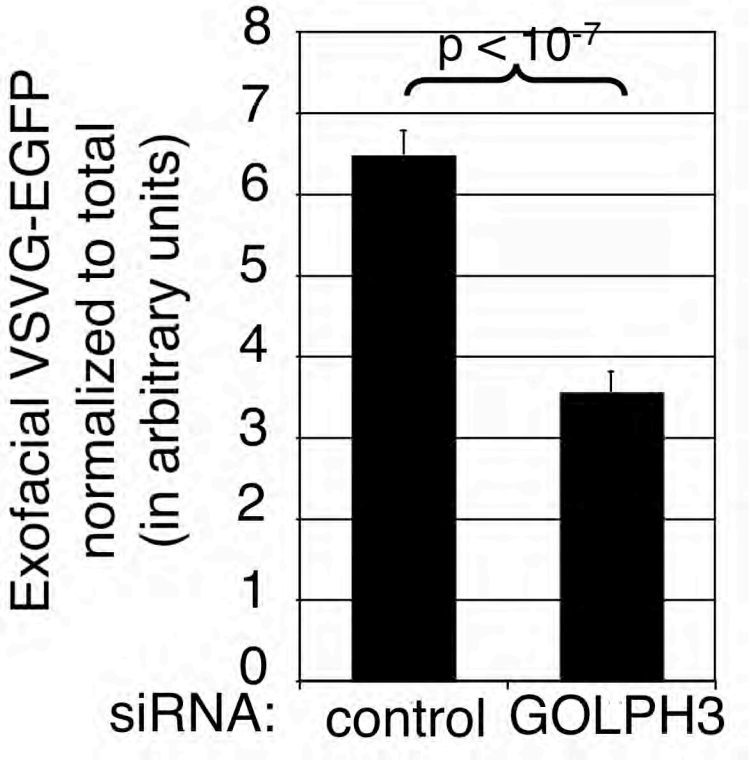

Figure 1.23. GOLPH3 knockdown cells have less ts045-VSVG-EGFP at the surface than control cells, as detected by an antibody to the external portion of VSVG in unpermeabilized cells.

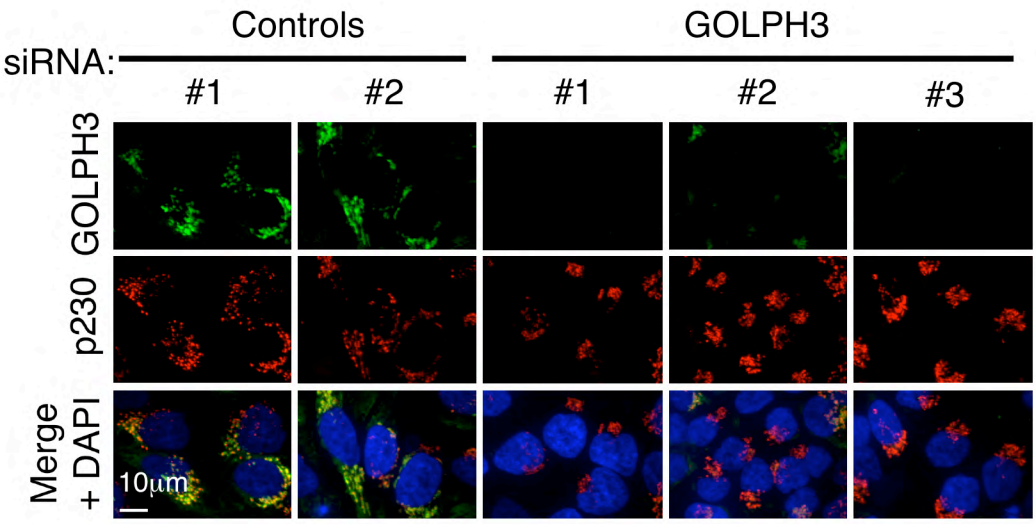

Figure 1.24. Knockdown of GOLPH3 causes condensation of the Golgi ribbon. Control siRNA transfected cells show a normal extended Golgi ribbon as detected by GOLPH3 (green) and p230 (red). GOLPH3 siRNA reduces GOLPH3 levels and causes condensation of the Golgi (p230). DAPI in blue. Imaging parameters identical in all.

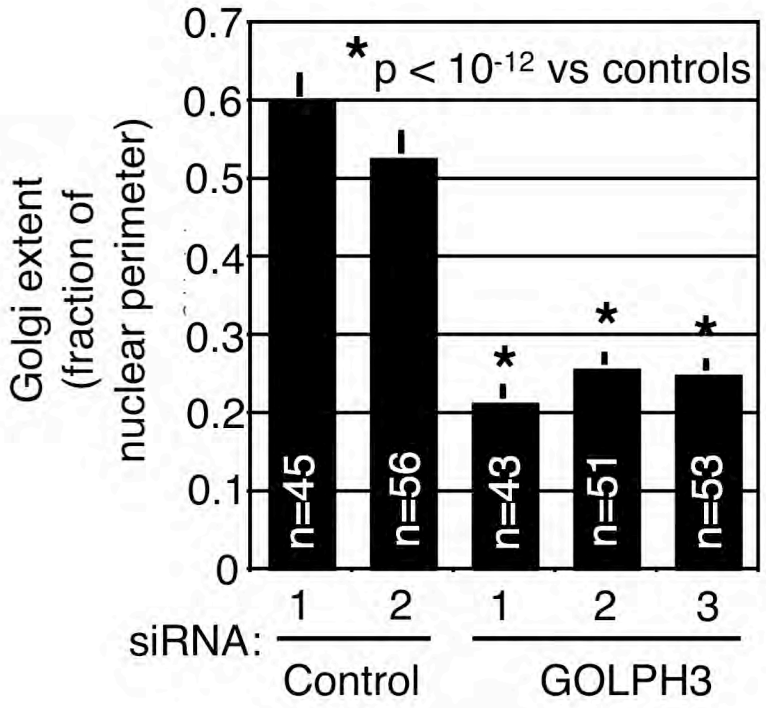

Figure 1.25. Quantification of Golgi extent around the nucleus (Golgi length relative to nuclear perimeter, mean/SEM graphed) demonstrates a significant change with depletion of GOLPH3 ($p<10^{-12}$, t-test).

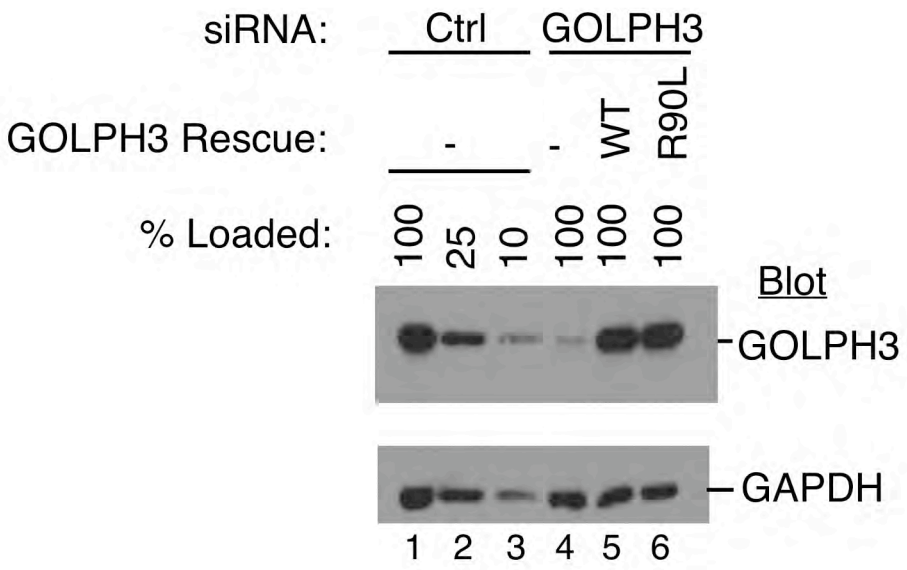

Figure 1.26. Western blot shows knockdown of GOLPH3 (lane 4) and restoration by siRNA-resistant wild type (lane 5) and R90L (lane6) GOLPH3. Blot for GAPDH shows equal loading.

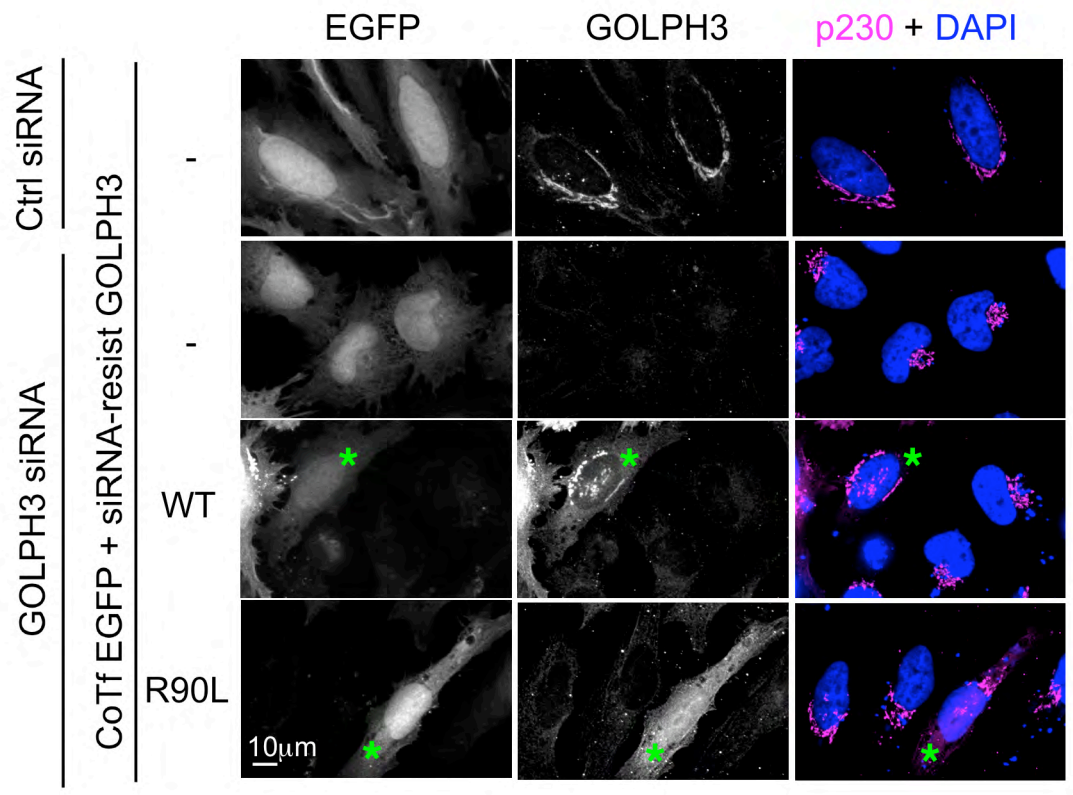

Figure 1.27. Expression of siRNA-resistant GOLPH3 (near endogenous levels, cotransfected with EGFP) rescues the compact Golgi phenotype, resulting in an extended Golgi ribbon and validating GOLPH3 siRNA specificity. Expression of siRNA-resistant GOLPH3 PtdIns(4)P binding pocket mutant does not rescue the condensed Golgi phenotype. Asterisks indicate transfected cells.

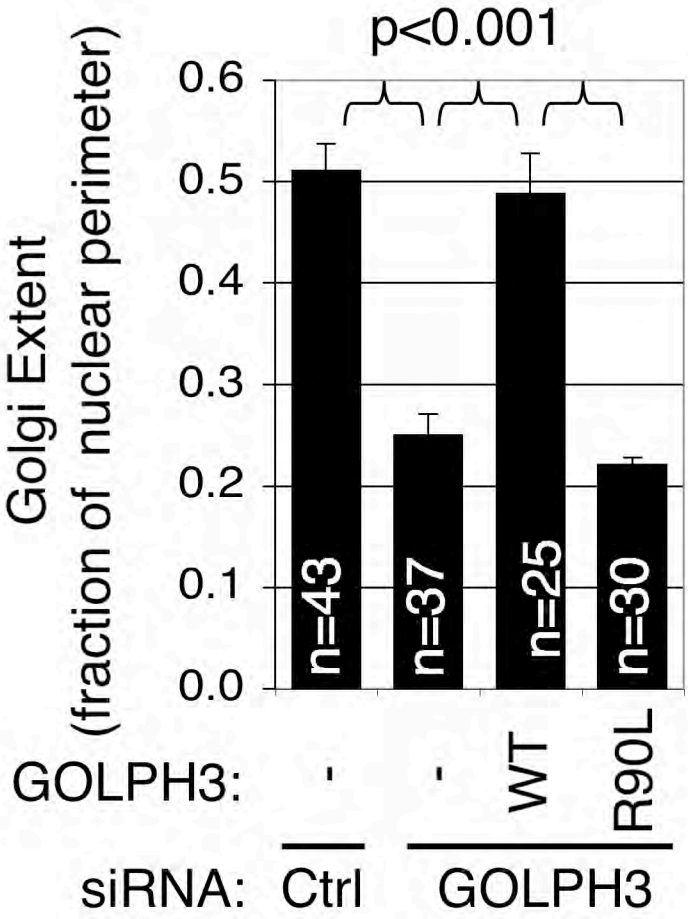

Figure 1.28. Quantification of Golgi extent around the nucleus (mean/SEM) demonstrates a significant rescue of Golgi compaction by wild type, but not R90L GOLPH3 ($p<0.001$ for indicated comparisons, t-test).

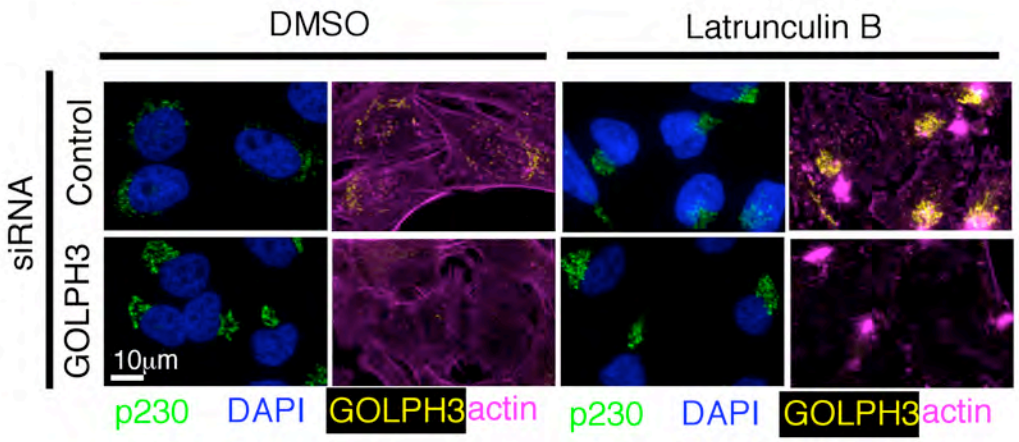

Figure 1.29. HeLa cells treated with control siRNA and DMSO show a normal extended Golgi morphology (p230, green and GOLPH3, yellow) and normal F-actin (Texas red phalloidin, magenta). Control siRNA + Latrunculin B causes loss of F-actin (stress fibers and peripheral actin) and Golgi condensation, but GOLPH3 remains at Golgi. GOLPH3 siRNA + DMSO causes a loss of GOLPH3 and Golgi condensation, but F-actin remains normal. Combined GOLPH3 siRNA + Latrunculin B causes loss of F-actin and GOLPH3, with Golgi condensation.

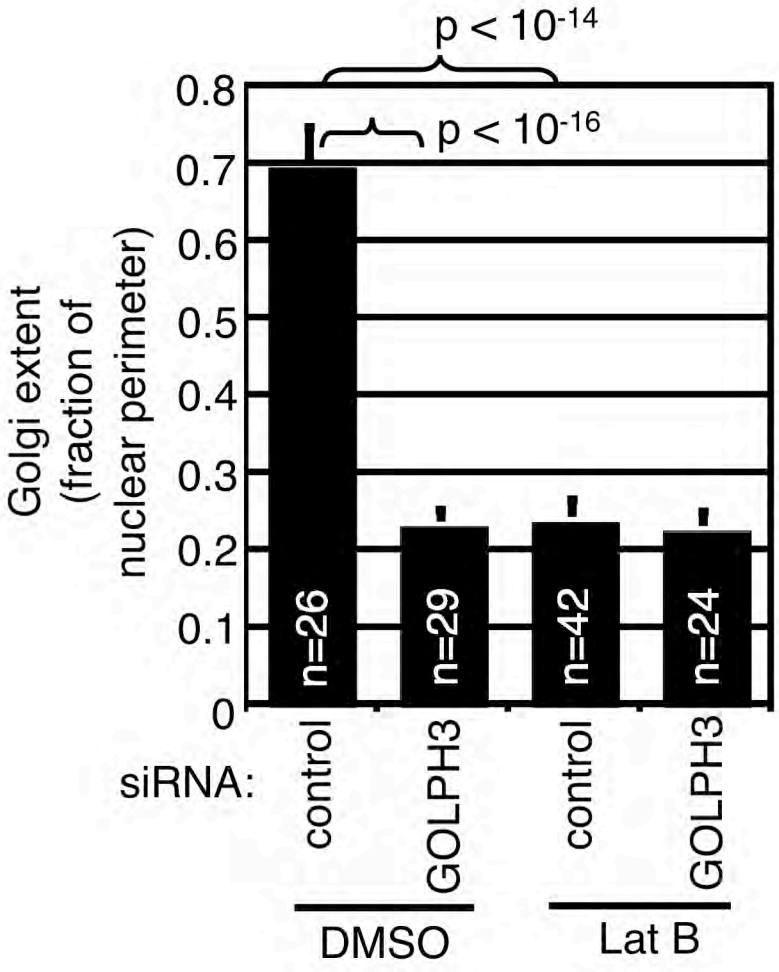

Figure 1.30. Measurement of Golgi extent around the nucleus (from 1.29) indicates that no additional effects on Golgi are seen in combining GOLPH3 siRNA and Latrunculin B.

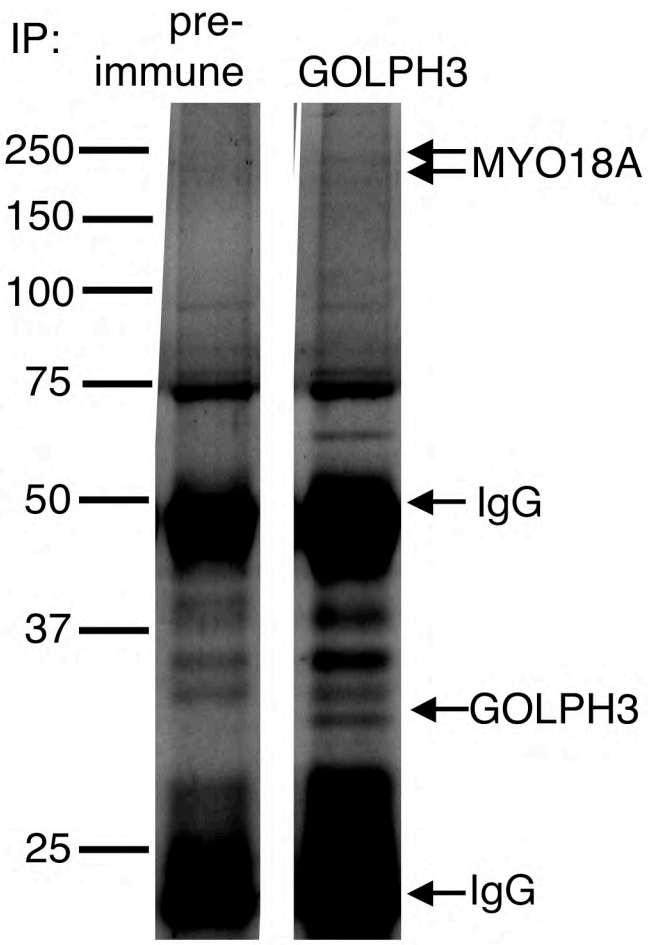

Figure 1.31. Large scale anti-GOLPH3 (or control) immunoprecipitation of HeLa whole-cell lysates separated by SDS-PAGE and stained with Coomassie blue. Bands specific to anti-GOLPH3 immunoprecipitation (indicated by arrows) were excised and identified by mass spectrometry. These included GOLPH3 (at ~34KDa), and a doublet at ~250 KDa that represents isoforms of MYO18A.

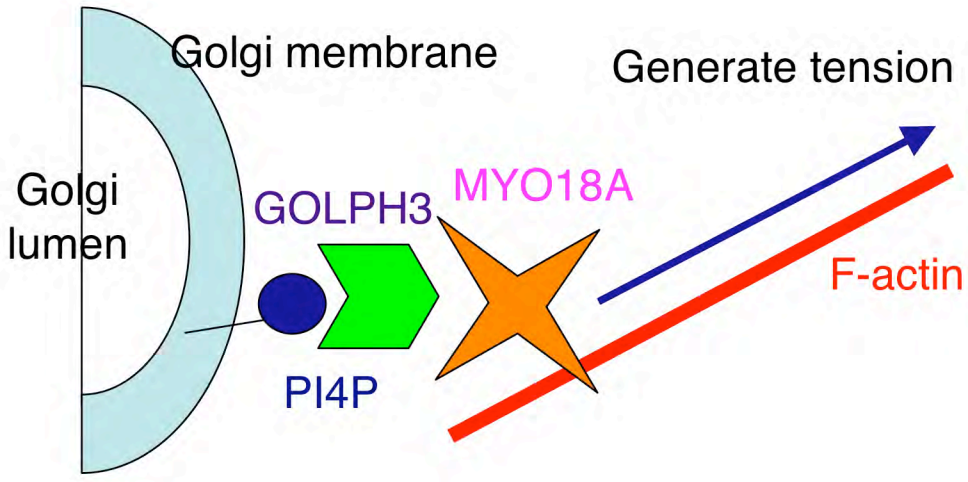

Figure 1.32. Proposed model: GOLPH3 binds Golgi membrane PtdIns(4)P and MYO18A, linking the Golgi to the cytoskeleton.

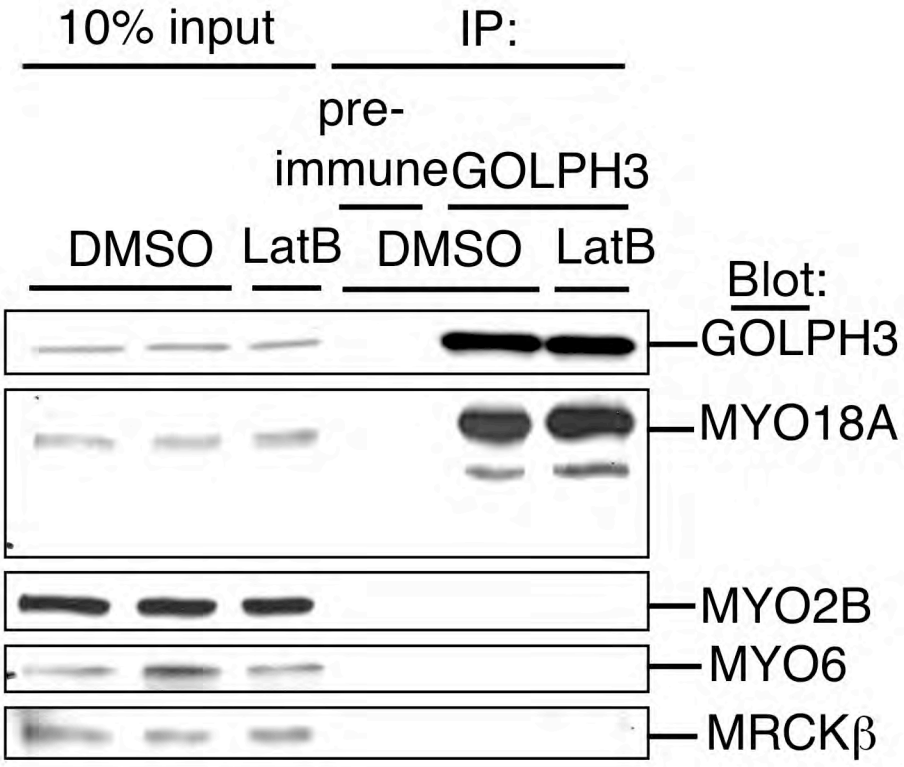

Figure 1.33. Western blot shows that MYO18A coimmunoprecipitates specifically with GOLPH3 even when actin is depolymerized by Latrunculin B (Figure 1.34). Golgi-localized myosins, MYO2B and MYO6, and MRCKβ did not coimmunoprecipitate with GOLPH3.

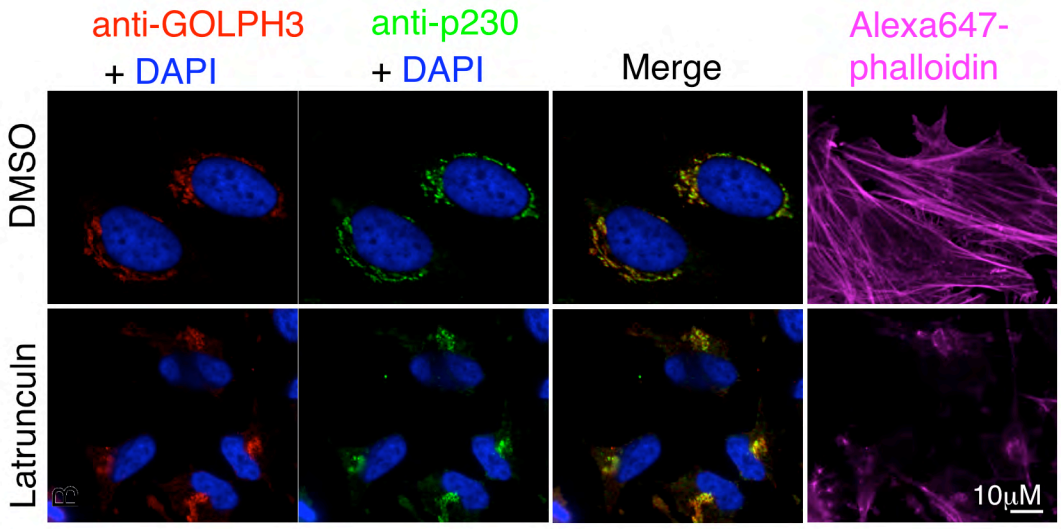

Figure 1.34. HeLa cells were treated with Latrunculin B to depolymerize actin prior to immunoprecipitation with GOLPH3 antiserum (Figure 1.33). Latrunculin B treated cells are observed to have a condensed Golgi as shown by GOLPH3 and p230 staining, and depolymerized actin as indicated by lack of stress fibers and peripheral F-actin observed by phalloidin staining.

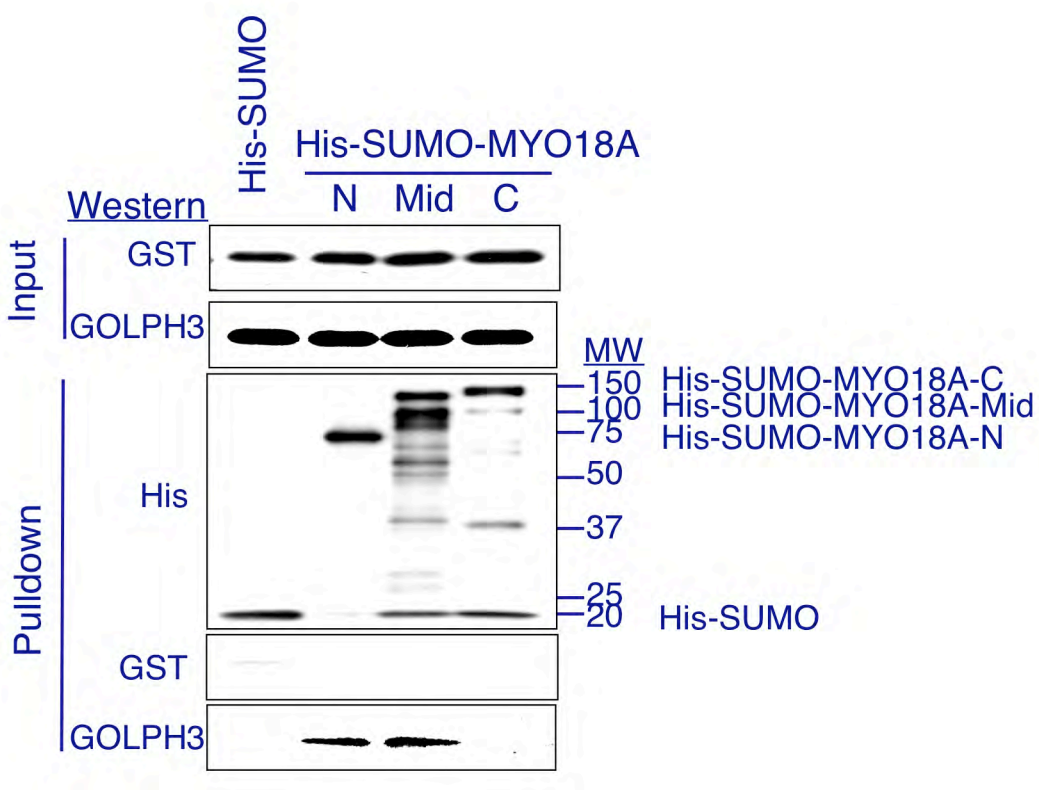

Figure 1.35. Purified, bacterial expressed GOLPH3 (but not GST) binds His-SUMO-tagged N-terminal and Middle fragments of MYO18A but not the C-terminal fragment or His-SUMO alone bound to nickel beads.

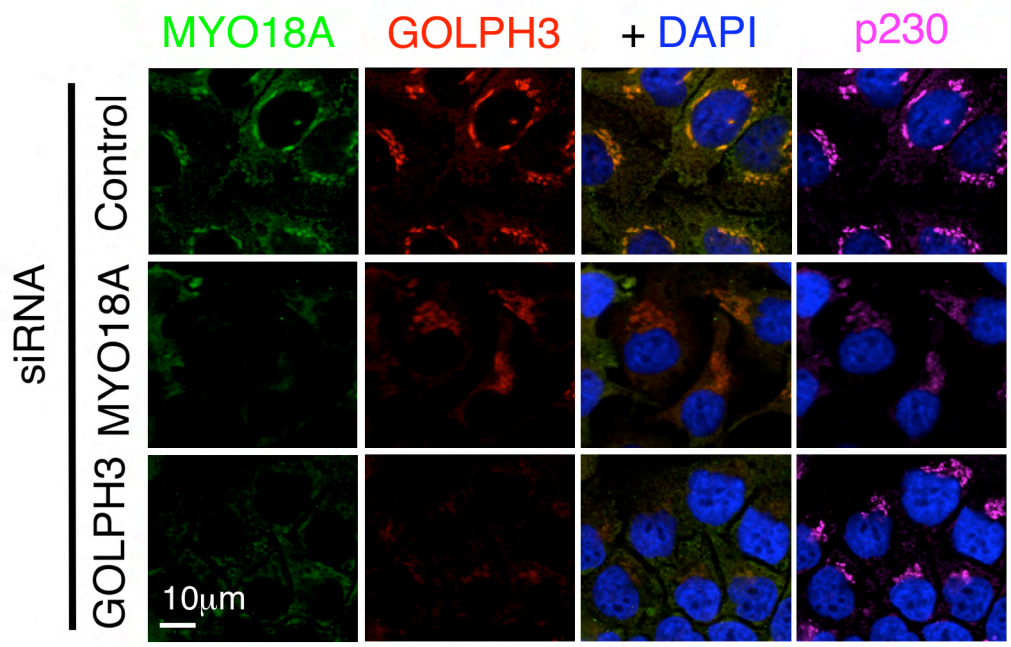

Figure 1.36. MYO18A (green) colocalizes with GOLPH3 (red) and p230 (magenta) in HeLa cells. DAPI in blue. Knockdown of MYO18A shows the specificity of the MYO18A antibody for immunofluorescence. Knockdown of GOLPH3 causes loss of MYO18A from Golgi.

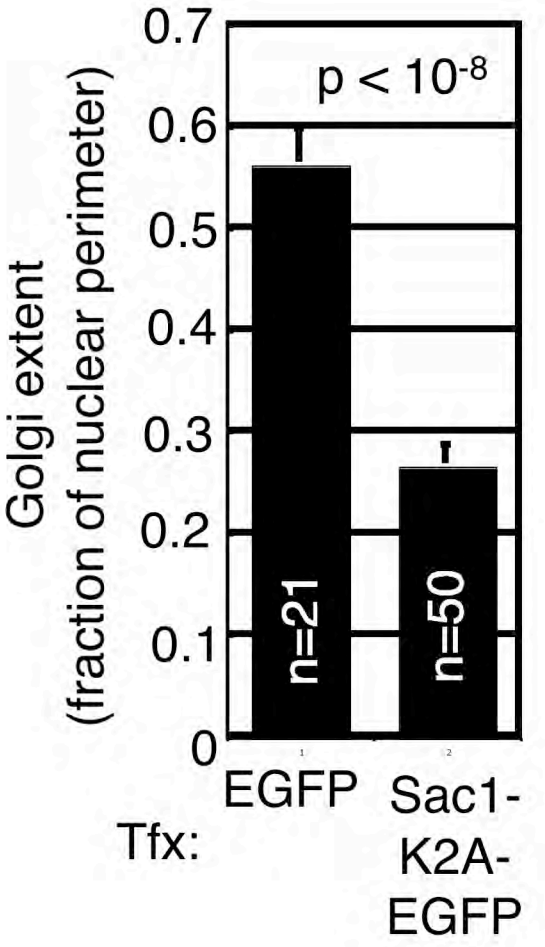

Figure 1.37. Depletion of PtdIns(4)P causes condensation of the Golgi. Quantification of Golgi extent measured as a fraction of the nuclear perimeter from cells in randomly chosen fields from Figure 1.5. Graph indicates mean and standard error. Expression of EGFP-Sac1-K2A causes a statistically significant decrease in Golgi extent around the nucleus ($p<10^{-8}$, t-test).

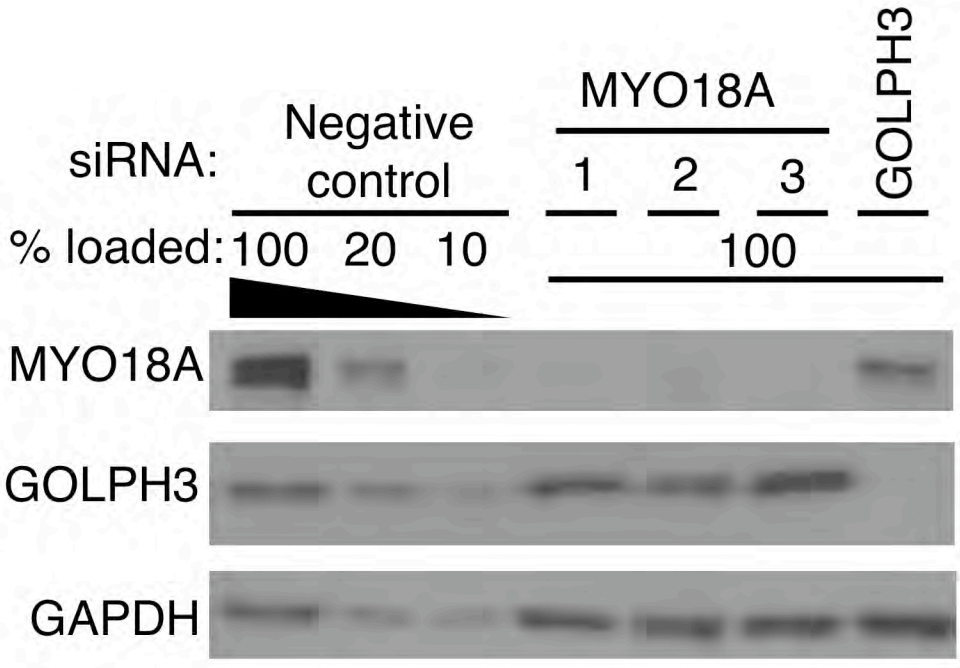

Figure 1.38. Western blot of HeLa lysates shows that MYO18A is knocked down >90% by each specific siRNA oligo. GAPDH blot verifies equal loading.

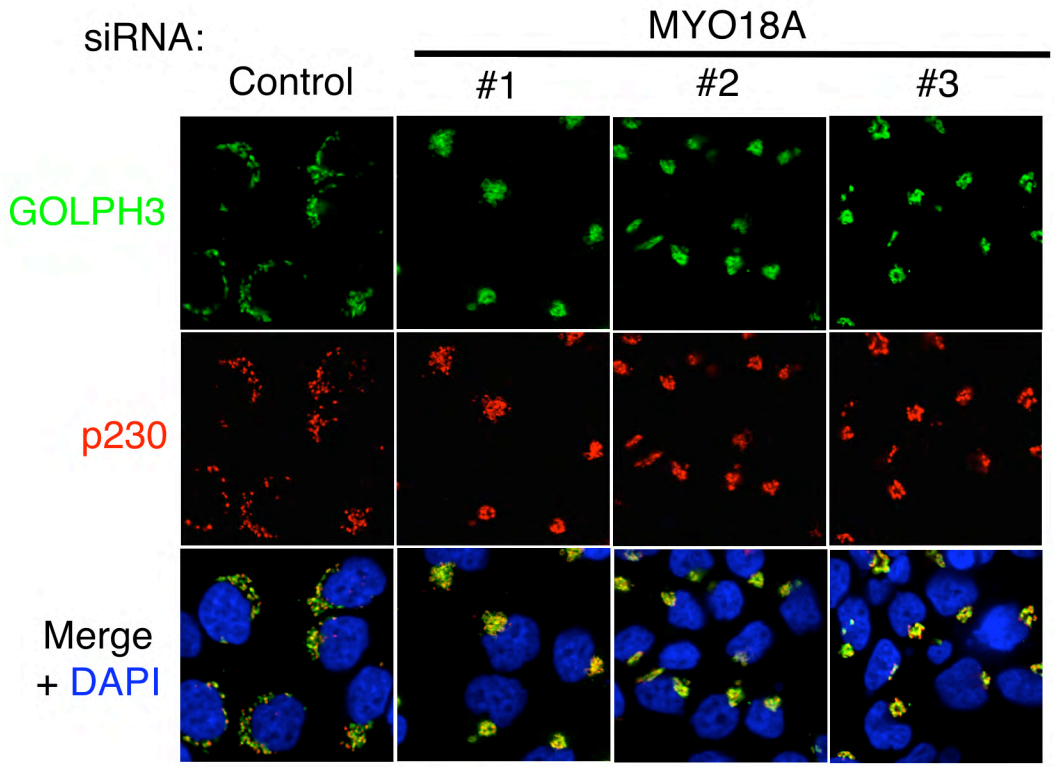

Figure 1.39. Knockdown of MYO18A with each specific siRNA results in a condensed Golgi as shown by immunofluorescence to GOLPH3 (green) and p230 (red). DAPI in blue. Similar results are seen in HeLa (shown) and HEK 293 cells.

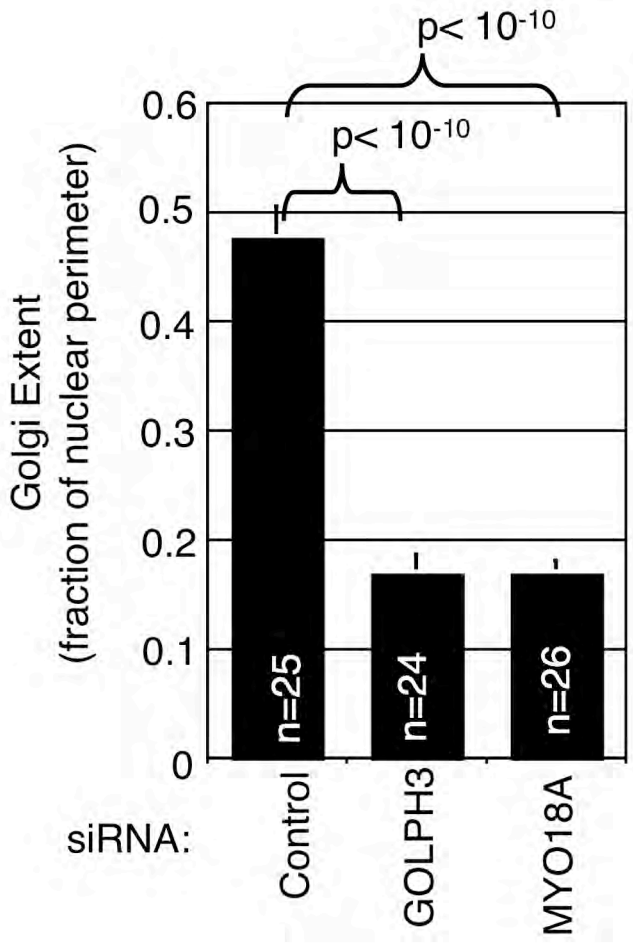

Figure 1.40. Quantification of Golgi extent (length relative to nuclear perimeter, mean/SEM graphed) demonstrates a significant compaction of the Golgi ($p<10^{-10}$, t-test) in MYO18A knockdown cells.

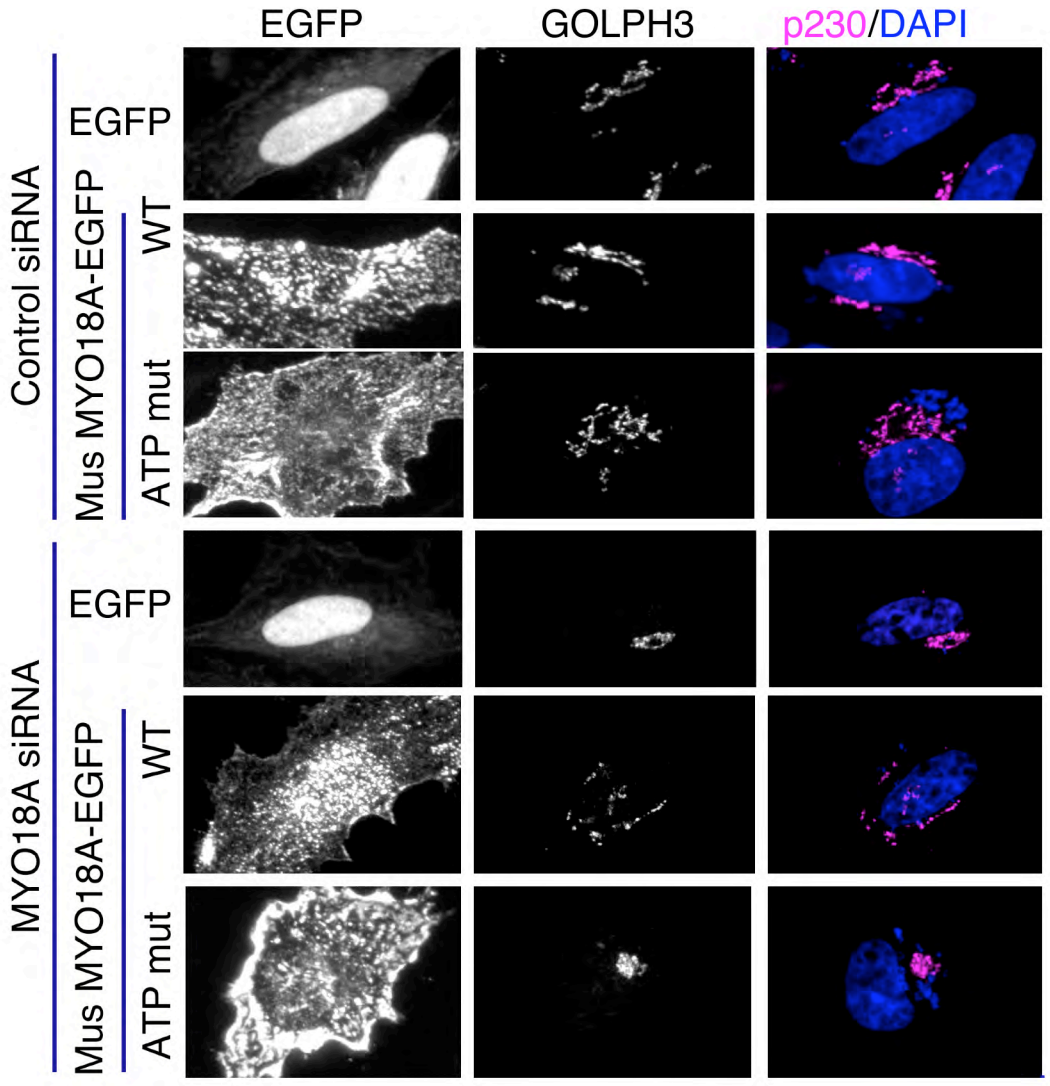

Figure 1.41. GFP-tagged wild type mouse MYO18A, but not an ATP-binding mutant or EGFP alone, rescues the Golgi phenotype of MYO18A knockdown in HeLa cells as shown by immunofluorescence to GOLPH3 and p230 (magenta). DAPI shown in blue.

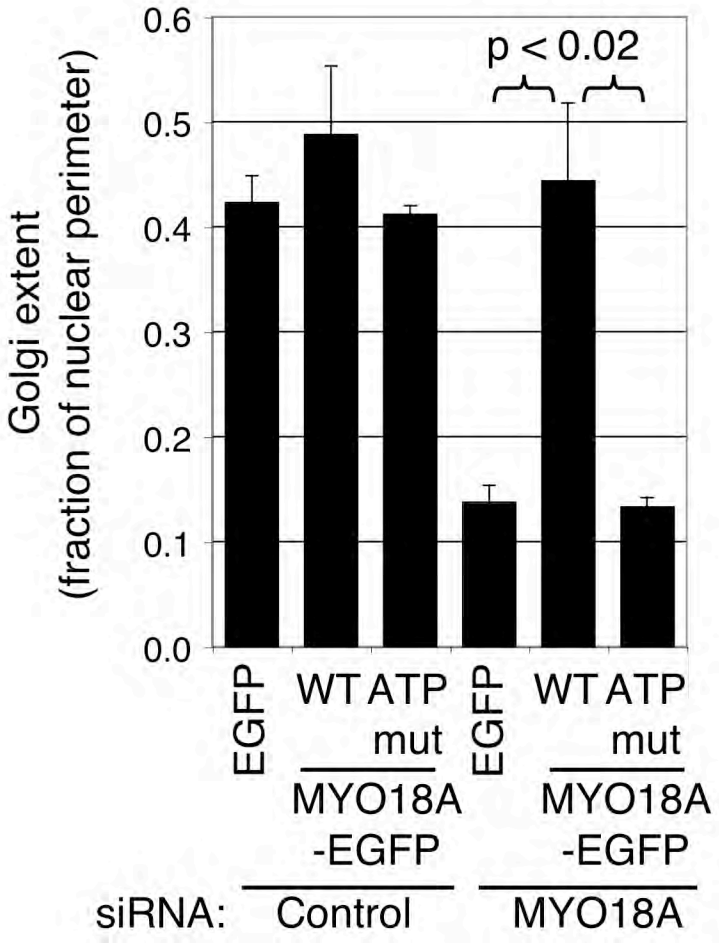

Figure 1.42. Quantification of Golgi extent around the nucleus (mean/SEM graphed) demonstrates significant rescue of Golgi morphology by wild type mouse MYO18A, but not by ATP-binding mutant mouse MYO18A ($p<0.02$ for indicated comparisons, t-test).

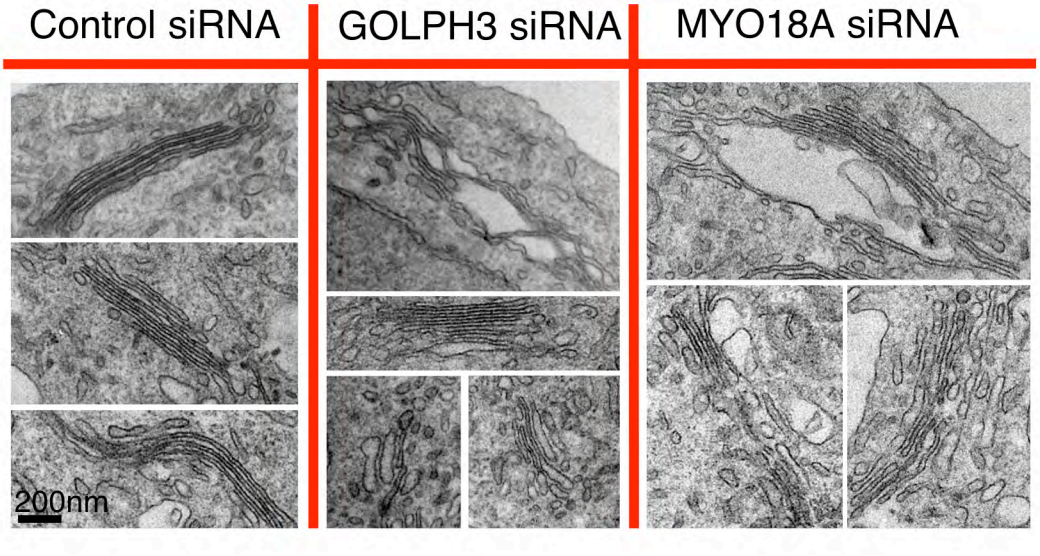

Figure 1.43. Electron micrographs of negative control, GOLPH3, and MYO18A siRNA-treated HeLa cells (two different oligos for each). Control cells show flat Golgi cisternae arranged in neat stacks. Knockdown of GOLPH3 or MYO18A (verified by Western blot of parallel samples) results in dilated, frequently completely aberrant Golgi cisternae, especially on the *trans* face (see text). (scale bar = 200 nm)

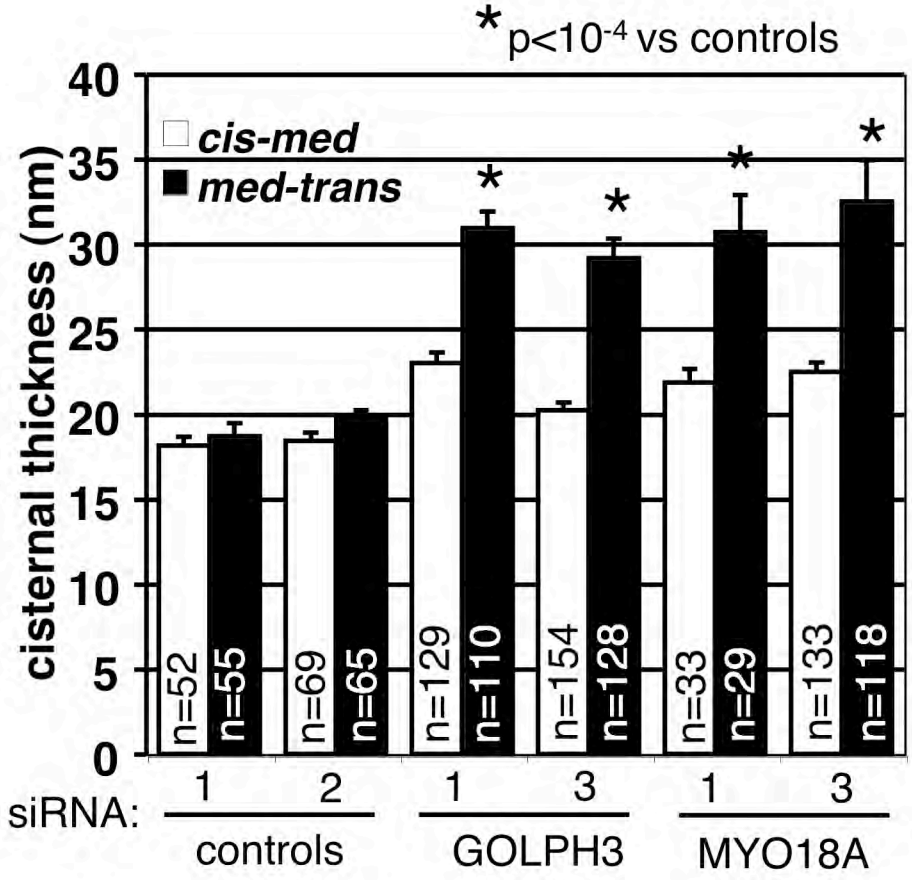

Figure 1.44. The cisternae in each stack were divided into the *cis-medial* and *medial-trans* halves and the thickness of each cisterna measured. The differences between control and knockdown are highly significant for *medial-trans* cisternae ($p<10^{-4}$, t-test, mean/SEM graphed).

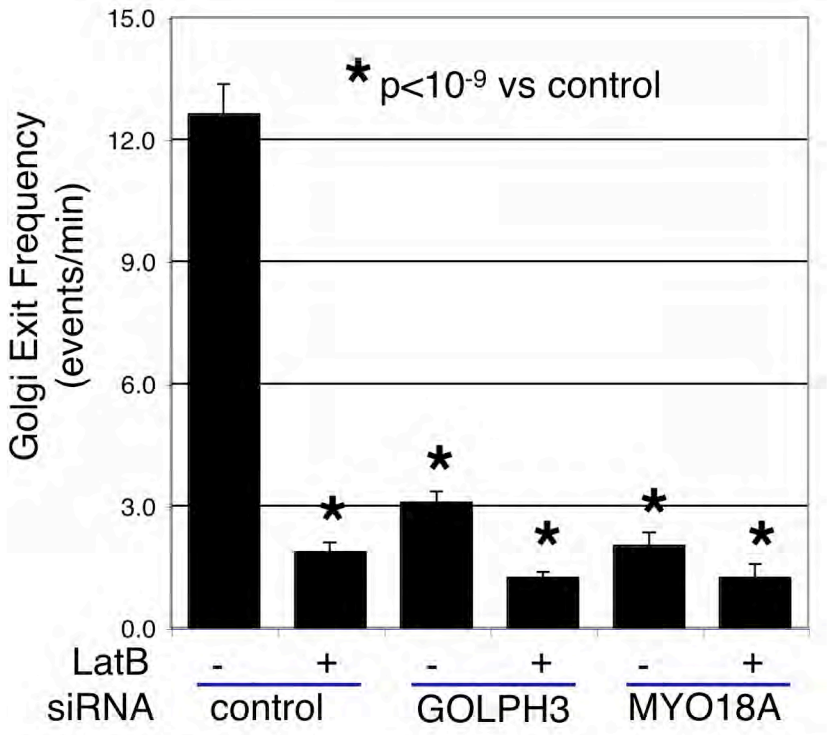

Figure 1.45. Knockdown of GOLPH3, MYO18A, or depolymerization of actin each impair Golgi vesicle exit. HeLa cells expressing low levels of EYFP-FAPP1-PH to mark PtdIns(4)P-rich membranes were imaged live before and after Latrunculin B treatment. Vesicles or tubules exiting the Golgi were counted (10-15 cells per siRNA, counting 100-1500 exit events per siRNA, pooling two experiments). Differences from control are highly significant ($p<10^{-9}$, t-test).

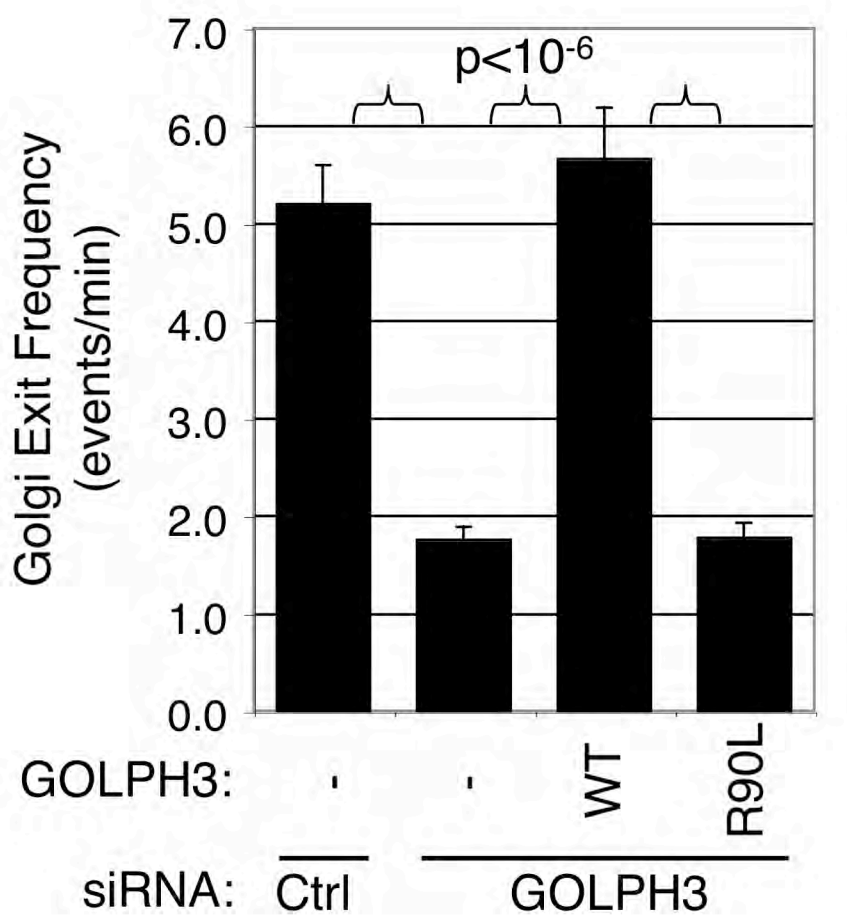

Figure 1.46. siRNA-resistant wild-type GOLPH3, but not the R90L mutant defective in binding PtdIns(4)P, rescues the Golgi trafficking defect. Differences are significant ($p<10^{-6}$ by t-test, 20-30 cells each, counting 900-2400 exit events, pooling two experiments).

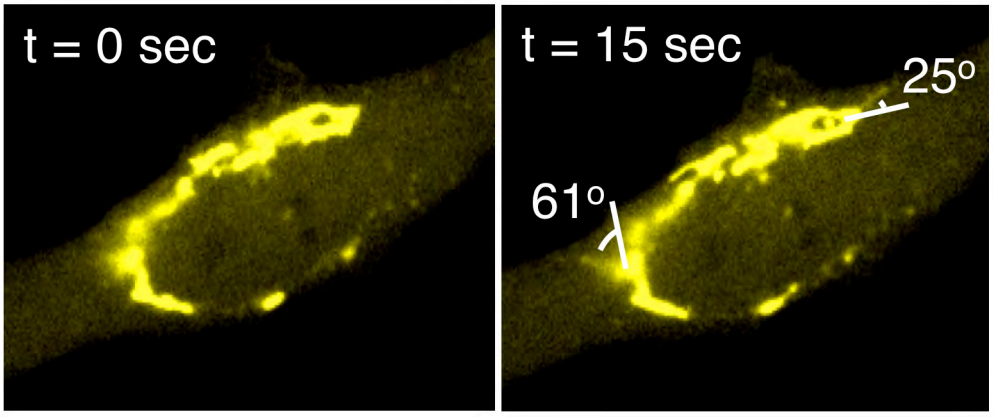

Figure 1.47. Measurement of the angle of exit of tubules/vesicles from the Golgi. Live imaging of EYFP-FAPP1-PH shows two PtdIns(4)P-rich tubules leaving the Golgi (see also Movie 1.4) and measurement of initial trajectory angles relative to the direction of the Golgi ribbon at point of exit.

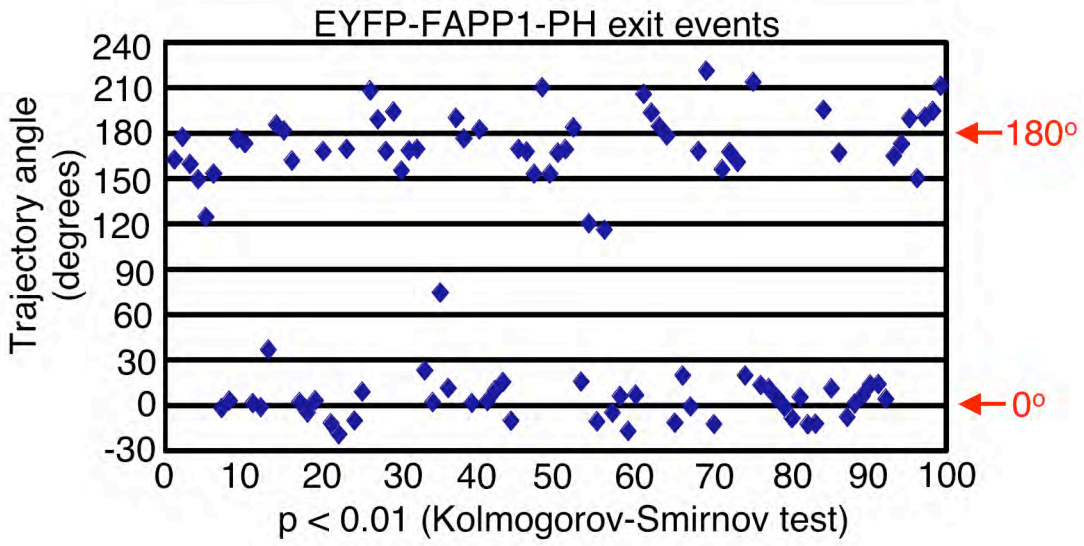

Figure 1.48. Initial trajectories of PtdIns(4)P-rich tubules or vesicles were plotted for 99 exit events collected from independent imaging of 8 HeLa cells. Clustering around 0° and 180°, or parallel to the plane of the Golgi, is highly significant ($p<0.01$, Kolmogorov-Smirnov test).

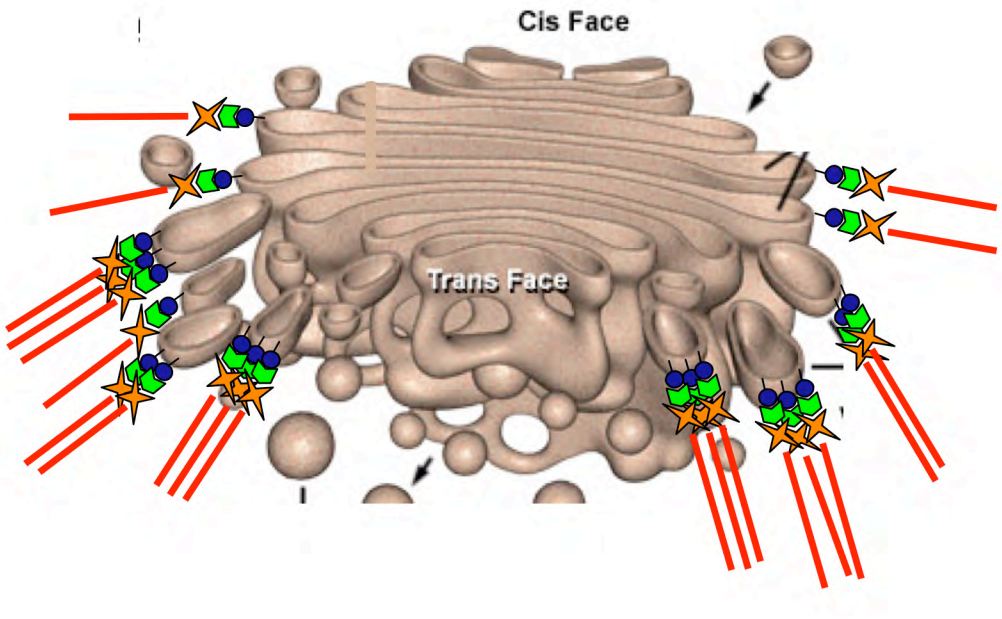

Figure 1.49. Diagram of the Golgi (used with permission (Davidson, 2004)) superimposed with Model: GOLPH3 binds PtdIns(4)P and links to MYO18A, transducing a tensile force to pull vesicles from the Golgi, contributing to its flattened form.

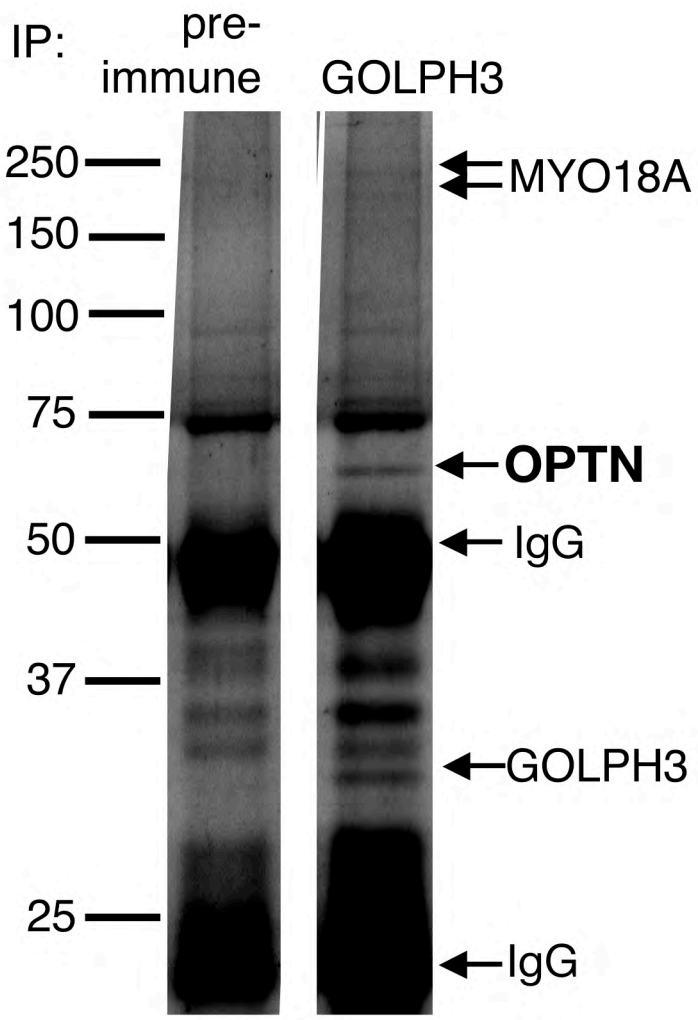

Figure 1.50. Optineurin was also identified as a GOLPH3 interactor by mass spectrometry.

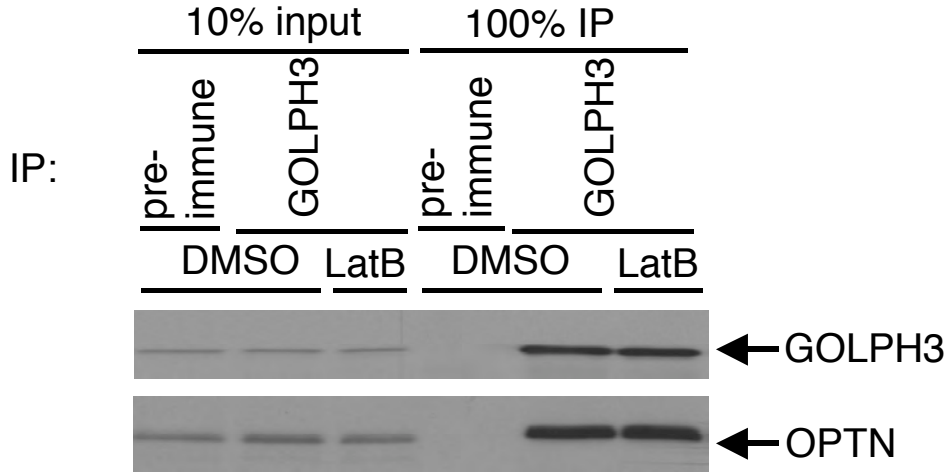

Figure 1.51. Western blot with an antibody specific to optineurin shows that it coimmunoprecipitates specifically with GOLPH3 from HeLa whole cell lysates. Pre-treatment of cells with latrunculin B shows that the interaction is not dependent upon actin filaments.

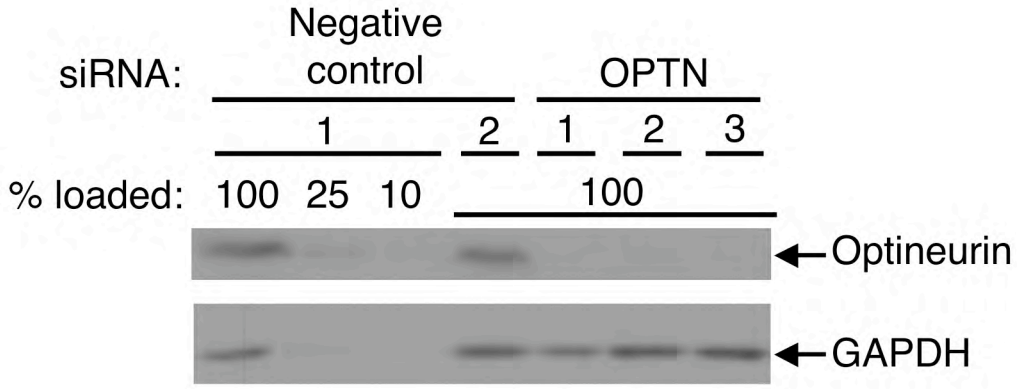

Figure 1.52. Optineurin can be knocked down by more than 90% with 3 different optineurin-specific siRNA oligos. HeLa cells were treated with 20nM siRNA for 72 hours and lysed by boiling in SDS.

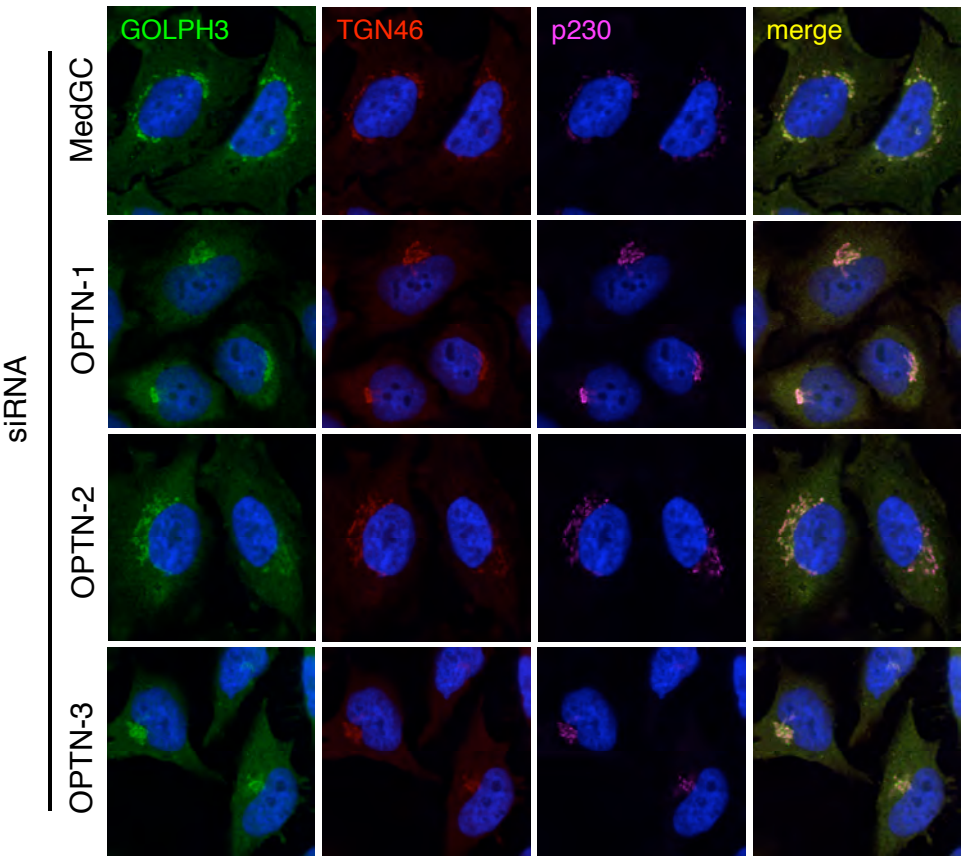

Figure 1.53. Knockdown of optineurin with 2 of 3 optineurin-specific siRNA oligos results in a compact Golgi, as seen with staining to endogenous Golgi markers GOLPH3 (green), TGN46 (red), and p230 (magenta). HeLa cells were treated with 20nM siRNA for 72 hours. Blue is DAPI staining.

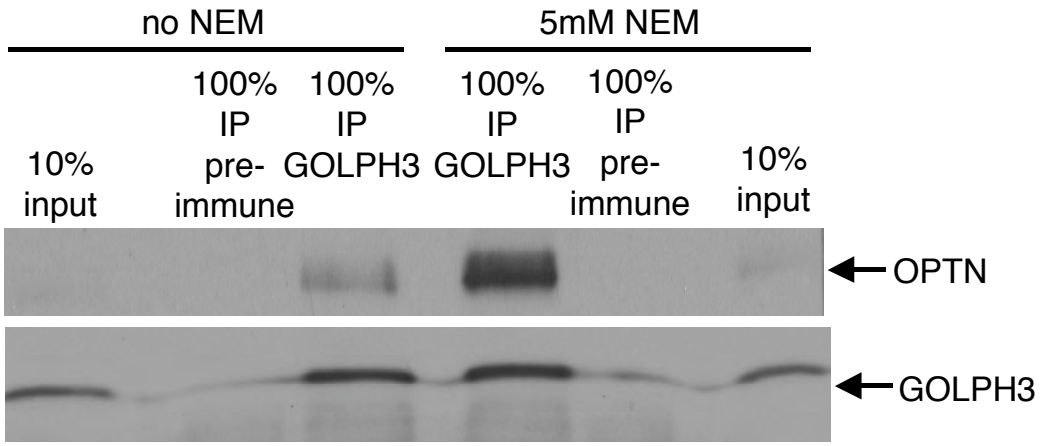

Figure 1.54. More optineurin coimmunoprecipitates with GOLPH3 from HeLa whole cell lysates when immunoprecipitation buffer contains 5mM NEM than in buffer without NEM.

References

Allan, V.J., Thompson, H.M., and McNiven, M.A. (2002) Motoring around the Golgi. Nat. Cell Biol. 4, E236-242.

Audhya, A., Foti, M. and Emr, S.D. (2000) Distinct roles for the yeast phosphatidylinositol 4-kinases, Stt4p and Pik1p, in secretion, cell growth, and organelle membrane dynamics. Mol. Biol. Cell 11, 2673-2689.

Barr, F.A. and Warren, G. (1996) Disassembly and reassembly of the Golgi apparatus. Semin. Cell Dev. Biol. 7, 505-510.

Beh, C.T., Cool, L., Phillips, J., and Rine, J. (2001) Overlapping functions of the yeast oxysterol-binding protein homologs. Genetics 157, 1117-1140.

Bell, A.W., Ward, M.A., Blackstock, W.P., Freeman, H.N.M., Choudhary, J.S., Lewis, A.P., Chotai, D., Fazel, A., Gushue, J.N., Paiement, J., Palcy, S., Chevet, E., Lafrenière-Roula, M., Solari, R., Thomas, D.Y., Rowley, A., and Bergeron, J.J.M. (2001) Proteomics characterization of abundant Golgi membrane proteins. J. Biol. Chem. 276, 5152-5165.

Berg, J.S., Powell, B.C., and Cheney, R.E. (2001) A millennial myosin census. Mol. Biol. Cell 12, 780-794.

Bonangelino, C.J., Chavez, E.M., and Bonifacino, J.S. (2002) Genomic screen for vacuolar protein sorting genes in *Saccharomyces cerevisiae*. Mol. Biol. Cell 13, 2486-2501.

Bossard, C., Bresson, D., Polishchuk, R.S., and Malhotra, V. (2007) Dimeric PKD regulates membrane fission to form transport carriers at the TGN. J. Cell Biol. 179, 1123-1131.

Burda, P., Padilla, S.M., Sarkar, S., and Emr, S.D. (2002) Retromer function in endosome-to-Golgi retrograde transport is regulated by the yeast Vps34 PtdIns 3-kinase. J. Cell. Sci. 115, 3889-3900.

Cooper, M.S., Cornell-Bell, A.H., Chernjavsky, A., Dani, J.W., and Smith, S.J. (1990) Tubulovesicular processes emerge from *trans*-Golgi cisternae, extend along microtubules, and interlink adjacent *trans*-Golgi elements into a reticulum. Cell 61, 135-145.

D'Angelo, G., Polishchuk, E., Di Tullio, G., Santoro, M., Di Campli, A., Godi, A., West, G., Bielawski, J., Chuang, C.-C., van der Spoel, A.C., Platt, F.M.,

Hannun, Y.A., Polishchuk, R., Mattjus, P., and De Matteis, M.A. (2007) Glycosphingolipid synthesis requires FAPP2 transfer of glucosylceramide. Nature 449, 62-67.

Davidson, M.W. (2004) Molecular expressions cell biology: The Golgi apparatus. Website: http://micro.magnet.fsu.edu/cells/golgi/golgiapparatus.html

De Marco, N., Buono, M., Troise, F., and Diez-Roux, G. (2006) Optineurin increases cell survival and translocates to the nucleus in a Rab8-dependent manner upon an apoptotic stimulus. J. Biol. Chem. 281, 16147-16156.

De Matteis, M.A. and Luini, A. (2008) Exiting the Golgi complex. Nat. Rev. Mol. Cell Biol. 9, 273-284.

del Toro, D., Alberch, J., Lázaro-Diéguez, F., Martín-Ibáñez, R., Xifró, X., Egea, G., and Canals, J.M. (2009) Mutant Huntingtin impairs post-Golgi trafficking to lysosomes by delocalizing Optineurin/Rab8 complex from the Golgi apparatus. Mol. Biol. Cell 20, 1478-1492.

Derby, M.C., Lieu, Z.Z., Brown, D., Stow, J.L., Goud, B., and Gleeson, P.A. (2007) The *trans*-Golgi network golgin, GCC185, is required for endosome-to-Golgi transport and maintenance of Golgi structure. Traffic 8, 758-773.

Dowler, S., Currie, R.A., Campbell, D.G., Deak, M., Kular, G., Downes, C.P., and Alessi, D.R. (2000) Identification of pleckstrin-homology-domain-containing proteins with novel phosphoinositide-binding specificities. Biochem. J. 351, 19-31.

Egea, G., Lázaro-Diéguez, F., and Vilella, M. (2006) Actin dynamics at the Golgi complex in mammalian cells. Curr. Opin. Cell Biol. 18, 168-178.

Faber, P.W., Barnes, G.T., Srinidhi, J., Chen, J., Gusella, J.F., and MacDonald, M.E. (1998) Huntingtin interacts with a family of WW domain proteins. Hum. Mol. Genet. 7, 1463-1474.

Finger, F.P. and Novick, P. (1998) Spatial regulation of exocytosis: lessons from yeast. J. Cell Biol. 142, 609-612.

Furusawa, T., Ikawa, S., Yanai, N., and Obinata, M. (2000) Isolation of a novel PDZ-containing myosin from hematopoietic supportive bone marrow stromal cell lines. Biochem. Biophys. Res. Commun. 270, 67-75.

Giussani, P., Colleoni, T., Brioschi, L., Bassi, R., Hanada, K., Tettamanti, G., Riboni, L., and Viani, P. (2008) Ceramide traffic in C6 glioma cells: evidence for CERT-dependent and independent transport from ER to the Golgi apparatus. Biochim. Biophys. Acta 1781, 40-51.

Gluschankof, P, and Fuller, R.S. (1994) A C-terminal domain conserved in precursor processing proteases is required for intramolecular N-terminal maturation of pro-Kex2 protease. EMBO J. 13, 2280-2288.

Godi, A., Pertile, P., Meyers, R., Marra, P., Di Tullio, G., Iurisci, C., Luini, A., Corda, D., and De Matteis, M.A. (1999) ARF mediates recruitment of PtdIns-4-OH kinase-β and stimulates synthesis of PtdIns(4,5)P_2 on the Golgi complex. Nat. Cell Biol. 1, 280-287.

Godi, A., Di Campli, A., Konstantakopoulos, A., Di Tullio, G., Alessi, D.R., Kular, G.S., Daniele, T., Marra, P., Lucocq, J.M., and De Matteis, M.A. (2004) FAPPs control Golgi-to-cell-surface membrane traffic by binding to ARF and PtdIns(4)P. Nat. Cell Biol. 6, 393-404.

Grenson, M., Mousset, M., Wiame, J.M., Bechet, J. (1966) Multiplicity of the amino acid permeases in *Saccharomyces cerevisiae*. I. Evidence for a specific arginine-transporting system. Biochim. Biophys. Acta 127, 325-38.

Halter, D., Neumann, S., van Dijk, S.M., Wolthoorn, J., de Mazière, A.M., Vieira, O.V., Mattjus, P., Klumperman, J., van Meer, G., and Sprong, H. (2007) Pre- and post-Golgi translocation of glucosylceramide in glysosphingolipid synthesis. J. Cell Biol. 179, 101-115.

Hama, H., Schnieders, E.A., Thorner, J., Takemoto, J.Y., and DeWald, D.B. (1999) Direct involvement of phosphatidylinositol 4-phosphate in secretion in the yeast *Saccharomyces cerevisiae*. J. Biol. Chem. 274, 34294-34300.

Hanada, K., Kumagai, K., Yasuda, S., Miura, Y., Kawano, M., Fukasawa, M., and Nishijima, M. (2003) Molecular machinery for non-vesicular trafficking of ceramide. Nature 426, 803-809.

Hattula, K., and Peränen, J. (2000) FIP-2, a coiled-coil protein, links Huntingtin to Rab8 and modulates cellular morphogenesis. Curr. Biol. 10, 1603-1606.

Hausser, A., Storz, P., Märtens, S., Link, G., Toker, A., and Pfizenmaier, K. (2005) Protein kinase D regulates vesicular transport by phosphorylating and activating phosphatidylinositol-4 kinase IIIβ at the Golgi complex. Nat. Cell Biol. 7, 880-886.

Hendricks, K.B., Wang, B.Q., Schnieders, E.A., and Thorner, J. (1999) Yeast homologue of neuronal frequenin is a regulator of phosphatidylinositol-4-OH kinase. Nat. Cell Biol. 1, 234-241.

Hirschberg, K., Phair, R.D., and Lippincott-Schwartz, J. (2000) Kinetic analysis of intracellular trafficking in single living cells with vesicular stomatitis virus protein G-green fluorescent protein hybrids. Methods Enzymol. 327, 69-89.

Hoffmann, W. (1985) Molecular characterization of the *CAN1* locus in Saccharomyces cerevisiae. A transmembrane protein without N-terminal hydrophobic signal sequence. J. Biol. Chem. 260, 11831-7.

Hsu, S.-C., TerBush, D., Abraham, M., and Guo, W. (2004) The exocyst complex in polarized exocytosis. Int. Rev. Cytol. 233, 243-265.

Im, Y.J., Raychaudhuri, S., Prinz, W.A., and Hurley, J.H. (2005) Structural mechanism for sterol sensing and transport by OSBP-related proteins. Nature 437, 154-158.

Isogawa, Y., Kon, T., Inoue, T., Ohkura, R., Yamakawa, H., Ohara, O., and Sutoh, K. (2005) The N-terminal domain of MYO18A has an ATP-insensitive actin-binding site. Biochemistry 44, 6190-6196.

Ito, T., Chiba, T., Ozawa, R., Yoshida, M., Hattori, M., and Sakaki, Y. (2001) A comprehensive two-hybrid analysis to explore the yeast protein interactome. Proc.Natl. Acad. Sci. 98, 4569-74.

Kristen, U. and Lockhausen, J. (1983) Estimation of Golgi membrane flow rates in ovary glands of *Aptenia cordifolia* using cytochalasin B. Eur. J. Cell Biol. 29, 262-267.

Lázaro-Diéguez, F., Jiménez, N., Barth, H., Koster, A.J., Renau-Piqueras, J., Llopis, J.L., Burger, K.N.J., and Egea, G. (2006) Actin filaments are involved in the maintenance of Golgi cisternae morphology and intra-Golgi pH. Cell Motil. Cytoskeleton 63, 778-791.

Lázaro-Diéguez, F., Colonna, C., Cortegano, M., Calvo, M., Martínez, S.E., and Egea, G. (2007) Variable actin dynamics requirement for the exit of different cargo from the *trans*-Golgi network. FEBS Lett. 581, 3875-3881.

Levine, T.P. and Munro, S. (2002) Targeting of Golgi-specific pleckstrin homology domains involves both PtdIns 4-kinase-dependent and – independent components. Curr. Biol. 12, 695-704.

Li, Y., Kang, J., and Horwitz, M.S. (1998) Interaction of an adenovirus E3 14.7-kilodalton protein with a novel tumor necrosis factor alpha-inducible cellular protein containing leucine zipper domains. Mol. Cell. Biol. 18, 1601-1610.

Longtine, M.S., McKenzie III, A., Demarini, D.J., Shah, N.G., Wach, A., Brachat, A., Philippsen, P., and Pringle, J.R. (1998) Additional modules for versatile and economical PCR-based gene deletion and modification in *saccharomyces cerevisiae.* Yeast 14, 953-961.

Lu, L., Guihua, T., and Hong, W. (2004) Autoantigen Golgin-97, an effector of Arl1 GTPase, participates in traffic from the endosome to the *trans*-Golgi network. Mol. Biol. Cell 15, 4426-4443.

Moreland, R.J., Dresser, M.E., Rodgers, J.S., Roe, B.A., Conaway, J.W., Conaway, R.C., and Hanas, J.S. (2000) Identification of a transcription factor IIIA-interacting protein. Nucleic Acids Res. 28, 1986-1993.

Mori, K., Furusawa, T., Okubo, T., Inoue, T., Ikawa, S., Yanai, N., Mori, K.J., and Obinata, M. (2003) Genome structure and differential expression of two isoforms of a novel PDZ-containing myosin (MysPDZ) (Myo18A). J. Biochem. 133, 405-413.

Mori, K., Matsuda, K., Furusawa, T., Kawata, M., Inoue, T., and Obinata, M. (2005) Subcellular localization and dynamics of MysPDZ (Myo18A) in live mammalian cells. Biochem. Biophys. Res. Comm. 326, 491-498.

Mrowka, R., Blüthgen, N., and Fähling, M. (2008) Seed-based systematic discovery of specific transcription factor target genes. FEBS J. 275, 3178-3192.

Nakagawa, T., Goto, K., and Kondo, H. (1996) Cloning, expression, and localization of 230-kDa phosphatidylinositol 4-kinase. J. Biol. Chem. 271, 12088-12094.

Nakashima-Kamimura, N., Asoh, S., Ishibashi, Y., Mukai, Y., Shidara, Y., Oda, H., Munakata, K., Goto, Y., and Ohta, S. (2005) MIDAS/GOLPH3, a nuclear gene product, regulates total mitochondrial mass in response to mitochondrial dysfunction. J. Cell. Sci. 118, 5357-5367.

Oka, T., Vasile, E., Penman, M., Novina, C.D., Dykxhoorn, D.M., Ungar, D., Hughson, F.M., and Krieger, M. (2005) Genetic analysis of the subunit organization and function of the conserved oligomeric Golgi (COG) complex. J. Biol. Chem. 280, 32736-32745.

Park, B.-C., Shen, X., Samaraweera, M., and Yue, B.Y.J.T. (2006) Studies of Optineurin, a glaucoma gene: Golgi fragmentation and cell death from overexpression of wild-type and mutant Optineurin in two ocular cell types. Am. J. Pathol. 169, 1976-1989.

Peng, J., Schwartz, D., Elias, J.E., Thoreen, C.C., Cheng, D., Marsischky, G., Roelofs, J., Finley, D., and Gygi, S.P. (2003) A proteomics approach to understanding protein ubiquitination. Nat. Biotechnol. 21, 921-26.

Peter, B.J., Kent, H.M., Mills, I.G., Vallis, Y., Butler, P.J.G., Evans, P.R., and McMahon, H.T. (2004) BAR domains as sensors of membrane curvature: the amphiphysin BAR structure. Science 303, 495-499.

Preuss, D., Mulholland, J., Franzusoff, A., Segev, N., and Botstein, D. (1992) Characterization of the *Saccharomyces* Golgi complex through the cell cycle by immunoelectron microscopy. Mol. Biol. Cell 3, 789-803.

Pruyne, D., Legesse-Miller, A., Gao, L., Dong, Y., and Bretscher, A. (2004) Mechanisms of polarized growth and organelle segregation in yeast. Annu. Rev. Cell Dev. Biol. 20, 559-591.

Puthenveedu, M.A. and Linstedt, A.D. (2005) Subcompartmentalizing the Golgi apparatus. Curr. Opin. Cell Biol. 17, 369-375.

Puthenveedu, M.A., Bachert, C., Puri, S., Lanni, F., and Linstedt, A.D. (2006) GM130 and GRASP65-dependent lateral cisternal fusion allows uniform Golgi-enzyme distribution. Nat. Cell Biol. 8, 238-248.

Rahighi, S., Ikeda, F., Kawasaki, M., Akutsu, M., Suzuki, N., Kato, R., Kensche, T., Uejima, T., Bloor, S., Komander, D., Randow, F., Wakatsuki, S., and Dikic, I. (2009) Specific recognition of linear ubiquitin chains by NEMO is important for NF-κB activation. Cell 136, 1098-1109.

Raychaudhuri, S. and Prinz, W.A. (2006) Uptake and trafficking of exogenous sterols in *Saccharomyces cerevisiae.* Biochem. Soc. Trans. 34, 359-362.

Rezaie, T., Child, A., Hitchings, R., Brice, G., Miller, L., Coca-Prados, M., Héon, E., Krupin, T., Ritch, R., Kreutzer, D., Crick, R.P., and Sarfarazi, M.

(2002) Adult-onset primary open-angle glaucoma caused by mutations in Optineurin. Science 295, 1077-1079.

Roberg, K.J., Bickel, S., Rowley, N., Kaiser, C.A. (1997) Control of amino acid permease sorting in the late secretory pathway of Saccharomyces cerevisiae by SEC13, LST4, LST7 and LST8. Genetics 147, 1569-84.

Rodriguez, O.C., Schaefer, A.W., Mandato, C.A., Forscher, P., Bement, W.M., and Waterman-Storer, C.M. (2003) Conserved microtubule-actin interactions in cell movement and morphogenesis. Nat. Cell Biol. 5, 559-609.

Rogalski, A.A. and Singer, S.J. (1984) Association of elements of the Golgi apparatus with microtubules. J. Cell Biol. 99, 1092-1100.

Rohde, H.M., Cheong, F.Y., Konrad, G., Paiha, K., Mayinger, P., and Boehmelt, G. (2003) The human phosphatidylinositol phosphatase SAC1 interacts with the Coatomer I complex. J. Biol. Chem. 278, 52689-52699.

Sahlender, D.A., Roberts, R.C., Arden, S.D., Spudich, G., Taylor, M.J., Luzio, J.P., Kendrick-Jones, J., and Buss, F. (2005) Optineurin links myosin VI to the Golgi complex and is involved in Golgi organization and exocytosis. J. Cell Biol. 169, 285-295.

Schmitz, K.R., Liu, J., Li, S., Setty, T.G., Wood, C.S., Burd, C.G., and Ferguson, K.M. (2008) Golgi localization of glycosyltransferases requires a Vps74p oligomer. Dev. Cell 14, 523-534.

Scott, K.L., Kabbarah, O., Liang, M.-C., Ivanova, E., Anagnostou, V., Wu, J., Dhakal, S., Wu, M., Chen, S., Feinberg, T., Huang, J., Saci, A., Widlund, H.R., Fisher, D.E., Xiao, Y., Rimm, D.L., Protopopov, A., Wong, K.-K., and Chin, L. (2009) GOLPH3 modulates mTOR signaling and rapamycin sensitivity in cancer. Nature 459, 1085-1090.

Seaman, M.N.J., Marcusson, E.G., Cereghino, J.L., and Emr, S.D. (1997) Endosome to Golgi retrieval of the vacuolar protein sorting receptor, Vps10p, requires the function of the *VPS29*, *VPS30*, and *VPS35* gene products. J. Cell Biol. 137, 79-92.

Seaman, M.N.J., McCaffery, J.M., and Emr, S.D. (1998) A membrane coat complex essential for endosome-to-Golgi retrograde transport in yeast. J. Cell Biol. 142, 665-681.

Short, B., Haas, A., and Barr, F.A. (2005) Golgin and GTPases, giving identity and structure to the Golgi apparatus. Biochim. Biophys. Acta 1744, 383-395.

Snyder, C.M., Mardones, G.A., Ladinsky, M.S., and Howell, K.E. (2006) GMx33 associates with the *trans*-Golgi matrix in a dynamic manner and sorts within tubules exiting the Golgi. Mol. Biol. Cell 17, 511-524.

Stapleton, M., Liao, G., Brokstein, P., Hong, L., Carninci, P., Shirake, T., Hayashizaki, Y., Champe, M., Pacleb, J., Wan, K., Yu, C., Carlson, J., George, R., Celniker, S., and Rubin, G.M. (2002) The *Drosophila* Gene Collection: Identification of putative full-length cDNAs for 70% of *D. melanogaster* genes. Genome Res. 12, 1294-1300.

Strahl, T., Hama, H., DeWald, D.B., and Thorner, J. (2005) Yeast phosphatidylinositol 4-kinase, Pik1, has essential roles at the Golgi and in the nucleus. J. Cell Biol. 171, 967-979.

Takeda, T., McQuistan, T., Orlando, R.A., and Farquhar, M.G. (2001) Loss of glomerular foot processes is associated with uncoupling of podocalyxin from the actin cytoskeleton. J. Clin. Invest. 108, 289-301.

Tan, I., Yong, J., Dong, J.M., Lim, L., and Leung, T. (2008) A tripartite complex containing MRCK modulates lamellar actomyosin retrograde flow. Cell 135, 123-136.

Tu, L., Tai, W.C.S., Chen, L., and Banfield, D.K. (2008) Signal-mediated dynamic retention of glycosyltransferases in the Golgi. Science 321, 404-407.

Varnai, P. and Balla, T. (2007) Visualization and manipulation of phosphoinositide dynamics in live cells using engineered protein domains. Pflugers Arch. 455, 69-82.

Wagner, S., Carpentier, I., Rogov, V., Kreike, M., Ikeda, F., Löhr, F., Wu, C.-J., Ashwell, J.D., Dötsch, V., Dikic, I., and Beyaert, R. (2008) Ubiquitin binding mediates the NF-κB inhibitory potential of ABIN proteins. Oncogene 27, 3739-3745.

Walch-Solimena, C. and Novick, P. (1999) The yeast phosphatidylinositol-4-OH kinase Pik1 regulates secretion at the Golgi. Nat. Cell Biol. 1, 523-525.

Wang, Y.J., Wang, J., Sun, H.Q., Martinez, M., Sun, Y.X., Macia, E., Kirchhausen, T., Albanesi, J.P., Roth, M.G., and Yin, H.L. (2003)

Phosphatidylinositol 4 phosphate regulates targeting of clathrin adaptor AP-1 complexes to the Golgi. Cell 114, 299-310.

Wong, K., Meyers, R., and Cantley, L.C. (1997) Subcellular locations of phosphatidylinositol 4-kinase isoforms. J. Biol. Chem. 272, 13236-13241.

Wu, C.C., Taylor, R.S., Lane, D.R., Ladinsky, M.S., Weisz, J.A., and Howell, K.E. (2000) GMx33: a novel family of *trans*-Golgi proteins identified by proteomics. Traffic 1, 963-975.

Yoshino, A., Rao Gangi Setty, S., Poynton, C., Whiteman, E.L., Saint-Pol, A., Burd, C.G., Johannes, L., Holzbaur, E.L., Koval, M., McCaffery, J.M., and Marks, M.S. (2005) tGolgin-1 (p230, golgin-245) modulates Shiga-toxin transport to the Golgi and Golgi motility towards the microtubule-organizing centre. J. Cell. Sci. 118, 2279-2293.

Zhou, W., Ryan, J.J., and Zhou, H. (2004) Global analyses of sumoylated proteins in *Saccharomyces cerevisiae*. J. Biol. Chem. 279, 32262-32268.

Zhu, G., Wu, C.-J., Zhao, Y., and Ashwell, J.D. (2007) Optineurin negatively regulates TNFα-induced NF-κB activation by competing with NEMO for ubiquitinated RIP. Curr. Biol. 17, 1438-1443.

Chapter 2: Ubp3p Functions in the Endocytosis of Integral Plasma Membrane Proteins

Introduction

Plasma membrane protein down-regulation and internalization is a fairly well characterized process, but many of the fine regulatory events associated with the endocytosis and turnover of these proteins have not been fully elucidated.

As mentioned in the previous chapter, Can1p is an amino acid permease found at the plasma membrane in yeast (Grenson et al., 1966; Hoffmann, 1985). After synthesis in the endoplasmic reticulum (ER), it travels via membrane transport through the Golgi secretory pathway (Roberg et al., 1997) to the plasma membrane (Figure 2.1) where it imports arginine. Upon uptake by endocytosis, it is sorted through the MultiVesicular Body (MVB) pathway and delivered to the vacuole where it is degraded (Figure 2.1; Opekarová et al., 1998).

Canavanine is a toxic arginine analogue. One way it causes harm to cells is by substituting for arginine in peptide chains during protein synthesis. This causes essential proteins to misfold, inactivating them or resulting in their degradation. Another means by which canavanine can cause damage is through inhibition of the cytochromes in the mitochondria, thereby reducing respiratory activity (Rosenthal, 1977).

A screen of approximately 4,700 viable yeast deletion mutants in the BY4741 collection was conducted to identify genes which when deleted result in slow growth or lethality in the presence of levels of canavanine in which wild type cells can grow normally. The goal of this screen was to identify uncharacterized factors involved in the turnover of proteins from the plasma membrane. Cells defective in this process would presumably have more of the Can1p permease stabilized at the cell surface, and thus import greater amounts of canavanine, producing harmful or lethal effects.

Working with a subset of canavanine hypersensitive deletions, a visual screen was performed using GFP-tagged Can1p and fluorescence microscopy. Can1p-GFP is found at the plasma membrane in log-phase wild type cells (Figure 2.1). Upon treatment with cycloheximide, a drug shown to trigger endocytosis of multispan plasma membrane proteins (Volland et al., 1994), or rapamycin, which mimics starvation conditions (Beck et al., 1999), Can1p-GFP is internalized and sorted to the vacuole for degradation (Figure 2.1). Deletion of genes encoding proteins involved in endocytosis or ESCRT (Endosomal Sorting Complex Required for Transport) components results in the inability of the cell to turn over Can1p-GFP (Figure 2.1).

Three genes encoding DeUBiquitinating enzymes (DUBs) were found to confer canavanine hypersensitivity when deleted in the yeast strain BY4741. Sixteen DUBs have been identified in yeast. They process ubiquitin precursors to form mature ubiquitin and catalyze the cleavage of mono- and/or

polyubiquitin from proteins, recycling ubiquitin for reuse. The UBP (UBiquitin-specific Protease) domain is the only common trait among this group of proteins, and consists of catalytic histidine, cysteine, and aspartic acid residues (Figure 2.2; Amerik and Hochstrasser, 2004).

Results

Deletion of *UBP3* leads to canavanine hypersensitivity and defective endocytosis

Ubp3p, Ubp4p/Doa4p, and Ubp15p were each identified in our lab's canavanine hypersensitivity screen of the BY4741 deletion collection. Another lab had previously found three other DUB deletions, *Δubp6*, *Δubp10*, and *Δubp14*, to be canavanine hypersensitive in a different yeast strain (Amerik et al., 2000b) in addition to the three from our screen. In order to test the sensitivity of each of these six DUB deletions in the strain SEY6210, homologous recombination was used to delete the chromosomal copy of each. Of the six, only *Δubp3*, *Δubp4*/*doa4*, *Δubp10*, and *Δubp15* showed any degree of canavanine hypersensitivity in the strain SEY6210 (Figure 2.3), thus repeating the results of the screen. (Deletion of *UBP10* is not a part of the BY4741 deletion collection used and so would not have been identified in the screen.)

The next step was to determine which of these canavanine hypersensitive UBP deletions showed mistrafficking of Can1p-GFP. As

previously mentioned, upon treatment of wild type cells with cycloheximide or rapamycin, Can1p-GFP is internalized from the plasma membrane. Both *Δubp3* and *Δubp4*/*doa4* stabilized Can1p-GFP at the plasma membrane with either treatment, but *Δubp10* and *Δubp15* sorted Can1p-GFP normally (Figure 2.4 and data not shown). Because the involvement of Ubp4p/Doa4p in MVB sorting is well-characterized (Amerik et al., 2000a), the role of Ubp3p in plasma membrane protein downregulation was further studied.

To show that treatment of cells with rapamycin or cycloheximide is not simply causing mass internalization of integral plasma membrane proteins in wild type cells and the deletion of *UBP3* causing this to stop, the trafficking of other endocytic cargoes was followed by fluorescence microscopy. Fur4p-GFP and Mup1p-GFP are permeases for uracil and methionine respectively, and in wild type cells, turnover is triggered by the addition of the transported substrates of each (Séron et al., 1999; Lin et al., 2008). Upon addition of substrate amino acid, each permease was internalized in wild type cells, but stabilized at the plasma membrane in *Δubp3* cells (Figures 2.5 and 2.6), demonstrating that rapamycin and cycloheximide are likely not causing generalized plasma membrane turnover that is stopped by deletion of *UBP3*.

Next, it was determined whether the deubiquitinating activity of Ubp3p is needed for endocytosis. A construct was made in which the catalytic cysteine was mutated to alanine (Ubp3p C469A) in single copy plasmid-borne *UBP3* by site directed mutagenesis. Wild type and mutant constructs were

transformed into *Δubp3* cells, and the canavanine sensitivity and Can1p-GFP trafficking examined. Ubp3p C469A did not rescue the canavanine hypersensitivity (Figure 2.7) or the Can1p-GFP trafficking defect (Figure 2.8) found in *Δubp3* cells, whereas the wild type construct rescued both. Thus, it is the deubiquitinating activity of Ubp3p that is necessary for endocytosis.

Deletion of *UBP3* does not result in decreased free ubiquitin in the cell

The ubiquitination of Can1p is essential to the turnover of Can1p-GFP at the plasma membrane and mutations of lysines predicted to be ubiquitinated to alanine results in stabilization of Can1p-GFP at the plasma membrane (Matejcková-Foretová et al., 1999; Lin et al., 2008). Because of this and because the deubiquitinating activity of Ubp3p is required for Can1p endocytosis, a deletion of Ubp3p could lead to limited free ubiquitin in the cell, causing an endocytic defect. A construct overexpressing ubiquitin upon induction with Cu^{2+} (Ellison and Hochstrasser, 1991) was transfected into wild type and *Δubp3* cells. Overexpression of ubiquitin had no effect on the trafficking of Can1p-GFP in wild type cells, but did not rescue the Can1p-GFP trafficking defect in *Δubp3* cells (Figure 2.9).

Another possible explanation of the indirect involvement of Ubp3p in Can1p-GFP trafficking is the lack of mature ubiquitin in the cell if Ubp3p is solely involved in ubiquitin precursor processing as described in Baker et al., 1992. CarboxyPeptidase S (CPS) is a vacuolar protease requiring

monoubiquitination to be sorted into the MultiVesicular Body (MVB) pathway and delivered to the vacuole (Katzmann et al., 2003). To determine if this could be the case, GFP-tagged CPS was observed in *Δubp3* cells and seen to have no defect in sorting (Figure 2.10).

Ubp3p may deubiquitinate endocytic machinery, activating it or preventing its proteasomal degradation

Intuitively, the Ubp3p substrate probably would not be the cargo, since Can1p-GFP requires ubiquitination to be endocytosed (Lin et al., 2008). If a DUB were acting directly on the cargo, it would presumably lead to stabilization at the plasma membrane. Deleting this DUB would result in increased turnover from the plasma membrane.

The target of Ubp3p could be part of the endocytic machinery. The role of Ubp3p would likely be positive regulation of its substrate, possibly by rescue of it from degradation by the proteasome. Such an example of this can be found in *Drosophila*. Epsin is an ENTH (Epsin N-Terminal Homology) domain-containing protein that induces curvature of clathrin-coated pits during endocytosis (reviewed in Horvath et al., 2007; Itoh and De Camilli, 2006). The *Drosophila* epsin homolog Liquid facets is deubiquitinated by the DUB Fat facets, reversing its polyubiquitination and rescuing it from proteasomal degradation. Knockdown of Fat facets leads to a defect in endocytosis (Cadavid et al., 2000; Chen et al, 2002).

Another possible role for Ubp3p could entail the deubiquitination of a monoubiquitinated endocytic machinery component, positively activating it. Several mammalian endocytic proteins have been shown to be monoubiquitinated (Dupré et al., 2004). One idea is that ubiquitination recruits proteins to the site of endocytosis through binding of ubiquitin binding domains found in other endocytic machinery proteins. Alternatively, a DUB could be used to deubiquitinate these ubiquitinated proteins, breaking them away from the endocytic complex after completion of endocytosis, thus allowing another cycle of activity. Deubiquitination could also activate an endocytic machinery component by preventing self-inhibition through binding to its own ubiquitin-binding domain.

To test for mono- or polyubiquitination of endocytic machinery components, SDS lysates were made from wild type or *Δubp3* cells expressing HA-tagged endocytic proteins. Western blotting with an antibody to HA allowed comparison of banding patterns from wild type and *Δubp3* cells. Monoubiquitination would show, in addition to a band at the predicted molecular weight of a protein, a band 8.5kDa higher than the predicted molecular weight. Polyubiquitination typically shows a ladder of bands above the band at the predicted molecular weight. Cells with chromosomally HA-tagged *EDE1*, *END3*, *ENT1*, and *RVS167*, genes encoding proteins with homologues ubiquitinated in other organisms were used (Dupré et al., 2004). Rvs167p has been shown to be ubiquitinated in yeast (Stamenova et al.,

2004), but showed no difference in ubiquitination status between wild type and *Δubp3* cells (Figure 2.11). End3p did not appear to be ubiquitinated or modified in any way (Figure 2.11). Ent1p and Ede1p showed ladder banding patterns above the bands at the predicted molecular weight, but this signal was stronger in*Δubp3* cells only for Ede1p (Figure 2.11). Blotting with an antibody to ubiquitin would be required to determine if any modification seen was actually ubiquination.

Ubp3p interacts with Bre5p, which is also necessary for endocytosis

Glycerol velocity sedimentation and gel filtration analysis indicated that Ubp3p is part of a complex of at least 400kDa and possibly 1.5MDa (Figure 2.12). It is likely that the protein is part of many different complexes, as Ubp3p has been implicated in various cellular processes (Auty et al., 2004; Cohen et al., 2003a and 2003b; Baxter et al., 2005; Moazed and Johnson, 1996). Additionally, interactions with several different proteins have been reported in large-scale screens, but with exception of one well-established interaction with Bre5p, the lists do not match (Gavin et al., 2006; Krogan et al., 2006).

A wider search for Ubp3p substrates or regulators was undertaken. To look for components of a Ubp3p complex, TAP-tagged Ubp3p (Cheeseman et al., 2001) was purified and co-purifying proteins identified by mass spectrometry. Unfortunately, the only protein identified as a Ubp3p interactor

with any degree of certainty was Bre5p (Figure 2.13), the previously-identified Ubp3p co-factor.

I wondered if in addition to its role in anterograde and retrograde trafficking between the ER and Golgi (Cohen et al., 2003a, Cohen et al., 2003b), Bre5p could be involved in endocytosis. Examination of Can1p-GFP trafficking in cells deleted for *BRE5* showed that its depletion also stabilizes Can1p at the plasma membrane (Figure 2.14).

Further reading indicated that a mammalian homologue of Bre5p, G3BP, was found to bind an SH3 domain-containing protein (Parker et al., 1996). The yeast genome encodes 23 SH3 domain-containing proteins, many of which are involved in endocytosis. Furthermore, Bre5p has 2 PxxP motifs, the minimal necessity for SH3 domain binding (Saksela et al., 1995). Using site-directed mutagenesis, these motifs were changed to AxxA, each separately and both together, in *BRE5* carried on a single-copy plasmid. All three mutant constructs rescued the *Δbre5* Can1p-GFP trafficking defect as well as the wild type *BRE5*, indicating that the Bre5p PxxP motifs are likely not necessary for endocytic function (Figure 2.15).

Additional experiments

Because mass spectrometry of purified Ubp3p did not provide desired results, a 2-hybrid screen was conducted to find Ubp3p and Bre5p interactors. Yeast 2-hybrid could possibly identify weak interactions that are broken upon

cell lysis or during the stringent conditions of the purification process, as the interaction between a catalyst and its target is likely transient. Unfortunately, no known endocytic proteins were identified using either protein as bait (data not shown).

Also investigated was a reported genetic interaction involving *Δubp3*. The deletion of *FKS1* is synthetic lethal with deletion of *UBP3*. Deletion of *FKS1* is also synthetic lethal with deletion of *SLA1*, *RVS167*, or *EDE1*, genes encoding three well-characterized endocytic proteins. (Lesage et al., 2004; Tong et al., 2004) Fks1p is the catalytic subunit of the β-glucan synthase, activated by Rho1p. Its deletion has been shown to result in a defect in radiolabeled α-factor uptake, indicating failure to endocytose Ste2p, the yeast α-factor receptor. Even in the absence of a cell wall, wild type cells take up α-factor normally, whereas *Δfks1* cells do not, indicating that endocytosis could be a function for Fks1p separate from that of maintaining cell wall integrity (de Hart et al., 2003). *FKS1* was deleted in SEY6210 and found that when replaced with the gene for *HIS3,* the deletion resulted in no canavanine hypersensitivity or Can1p-GFP trafficking defect (Figures 2.16 and 2.17). When *FKS1* was replaced with *TRP1*, canavanine hypersensitivity resulted equivalent to that seen in *Δubp3* cells (Figure 2.16), but Can1p-GFP trafficking was not examined in that strain.

Summary and Conclusion

Ubp3p is involved in the turnover of Can1p-GFP and other cargoes from the plasma membrane, a process for which its catalytic activity is essential. Its deletion does not lead to a shortage of mature ubiquitin. Ubp3p is a component of a large complex or complexes. Identification of substrate(s) for Ubp3p deubiquitinating activity or physical interaction with known endocytic proteins was sought by purification of TAP-tagged Ubp3p followed by mass spectrometry and a two-hybrid screen. The previously described Ubp3p cofactor Bre5p is also involved in endocytosis. No endocytic substrate for Ubp3p has been found.

Acknowledgements

Thank you to Christopher Stefan for starting this project and to Scott Emr for his guidance. Thank you to Charles Lin and members of the Emr lab for helpful discussions.

Figures

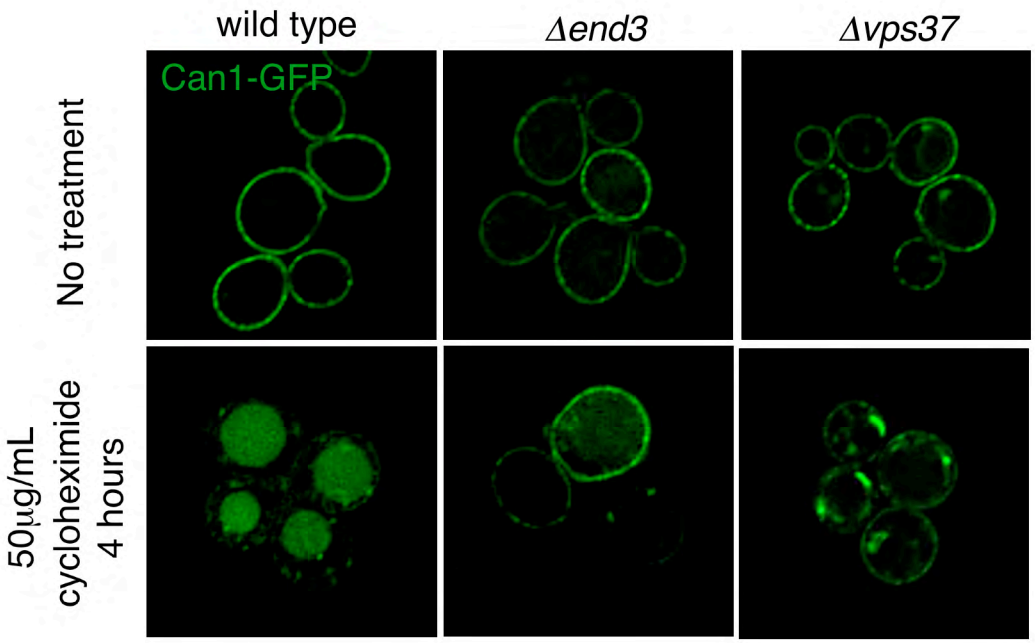

Figure 2.1. Can1p-GFP is found at the plasma membrane in log phase cells. Upon treatment with 50μg/mL cycloheximide for 4 hours, Can1p-GFP is trafficked to the vacuole. Can1p-GFP is not internalized in cells deleted for endocytic machinery proteins (*Δend3*) or ESCRT proteins (*Δvps37*).

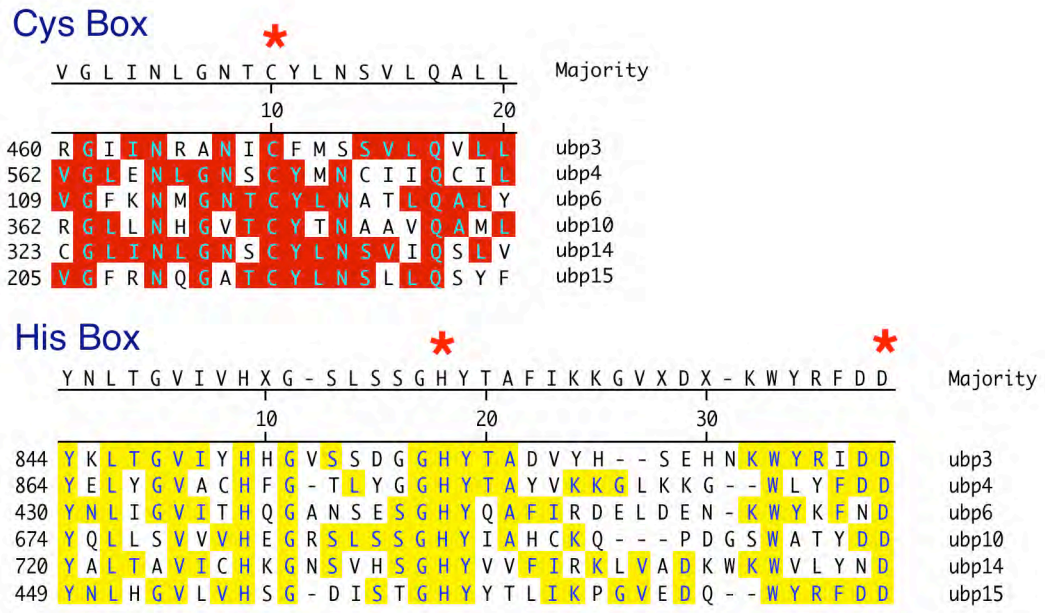

Figure 2.2. The UBP domain consists of catalytic Cys and His boxes. Red asterisks mark conserved cysteine, histidine, and aspartic acid residues essential to proteolytic activity.

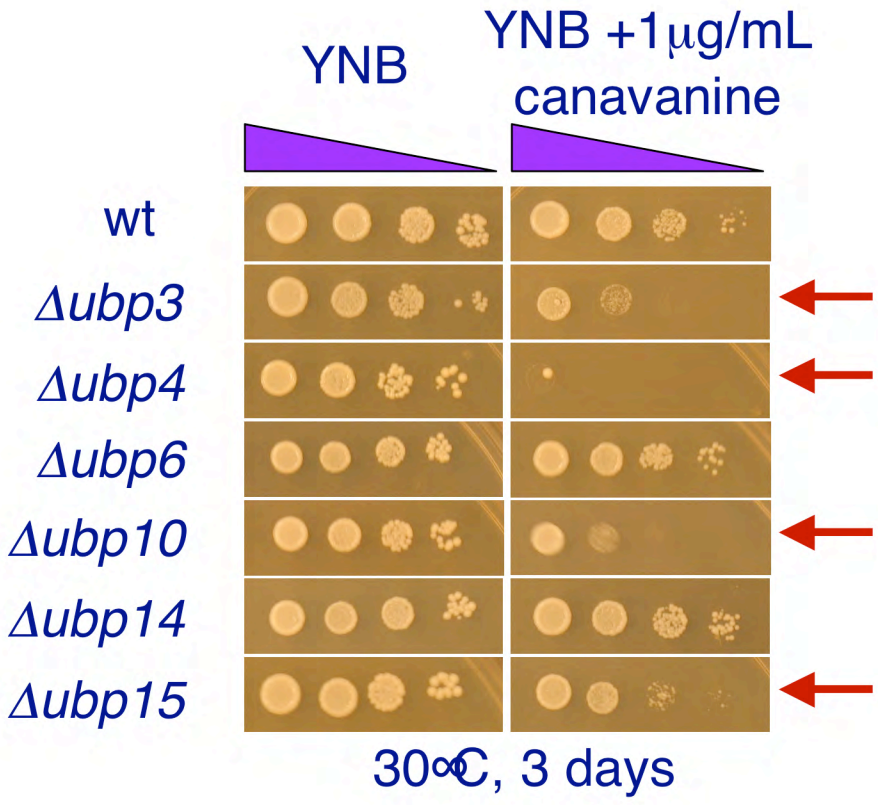

Figure 2.3. Wild type yeast strain SEY6210 can grow on plates containing 1μg/mL canavanine. SEY6210 yeast cells deleted for the DUBs *UBP3, UBP4, UBP10,* or *UBP15* cannot grow on plates containing 1μg/mL canavanine.

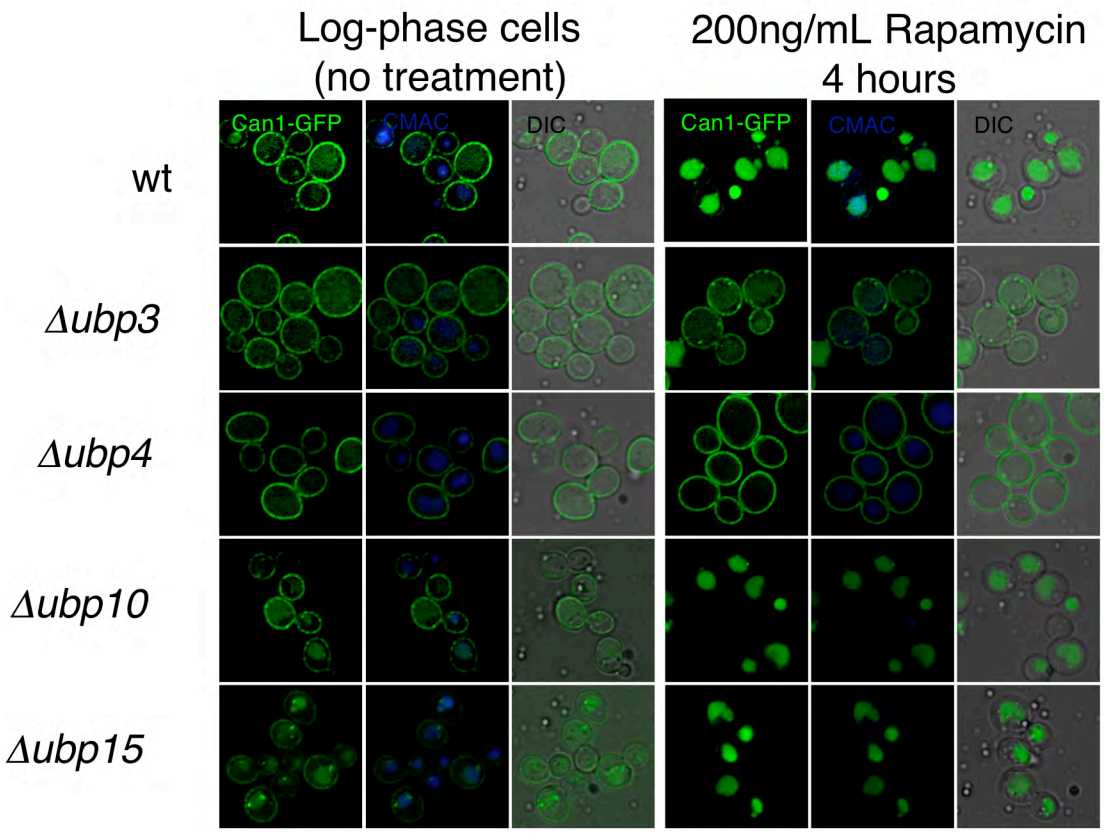

Figure 2.4. Can1p-GFP is stabilized at the plasma membrane in cells deleted for *UBP3* or *UBP4*. Can1p-GFP is trafficked normally in cells deleted for *UBP10* or *UBP15*.

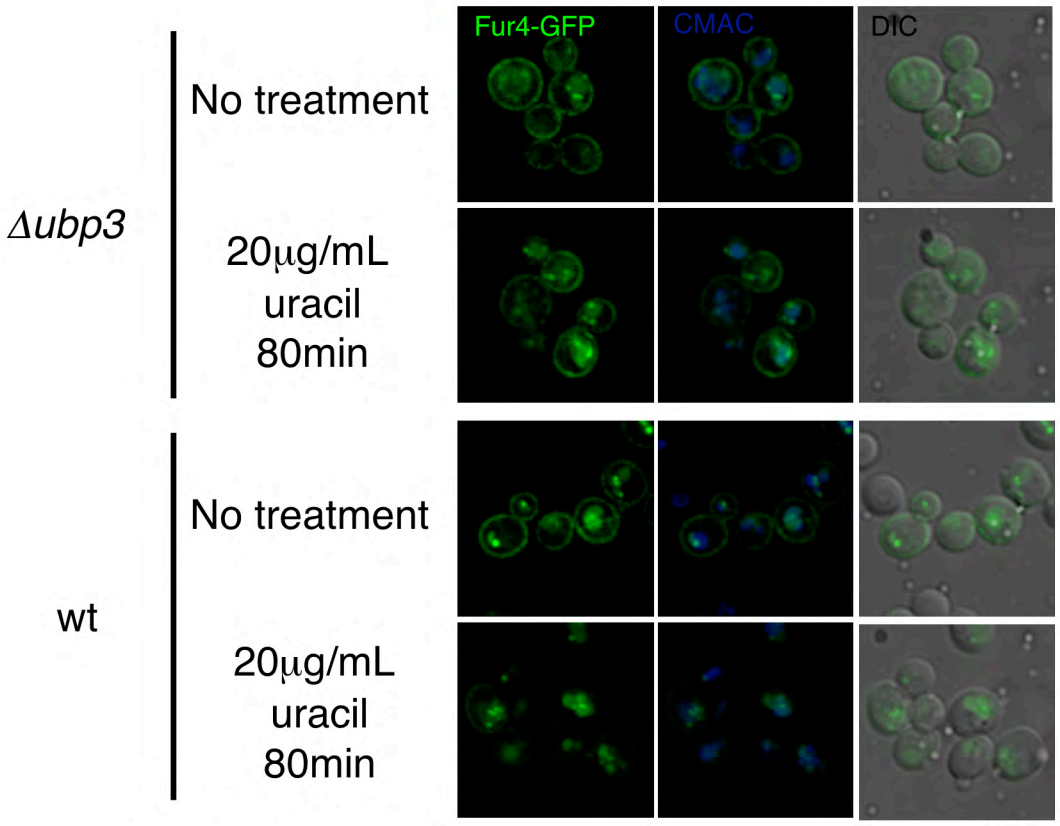

Figure 2.5. Fur4p-GFP is stabilized at the plasma membrane in cells knocked down for *UBP3.* CMAC stains the vacuole.

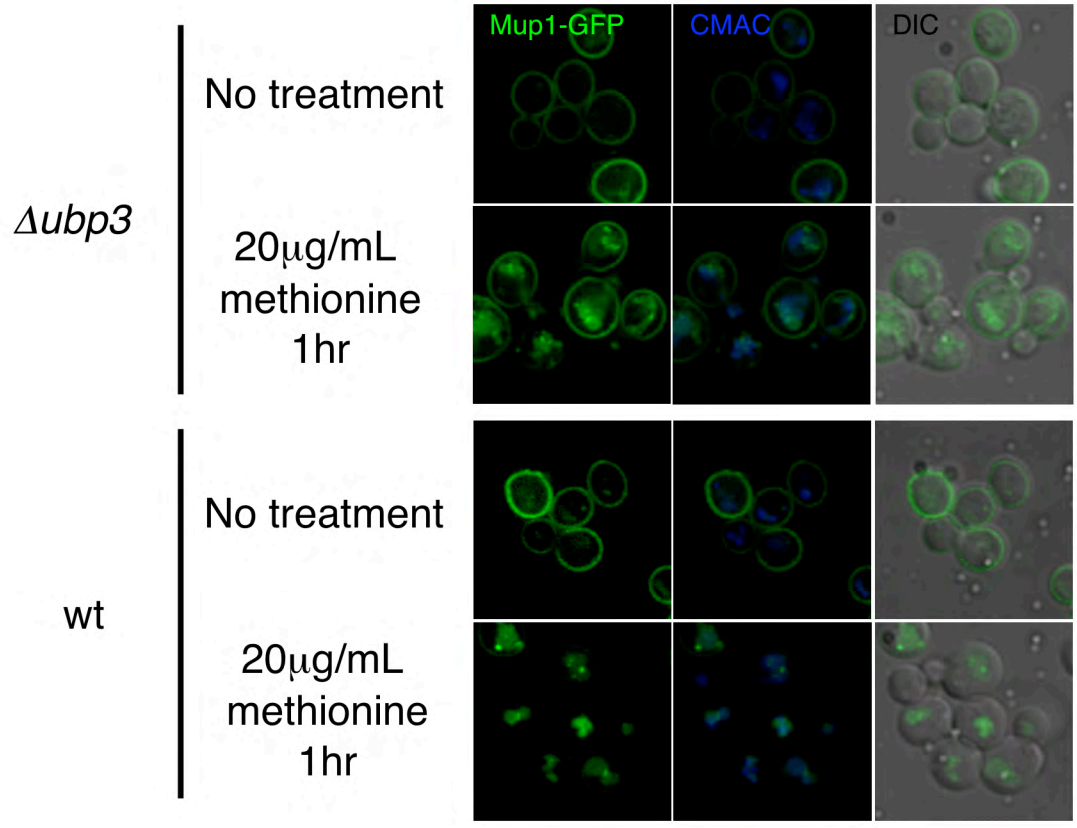

Figure 2.6. Mup1p-GFP is stabilized at the plasma membrane in cells deleted for *UBP3*. CMAC stains the vacuole.

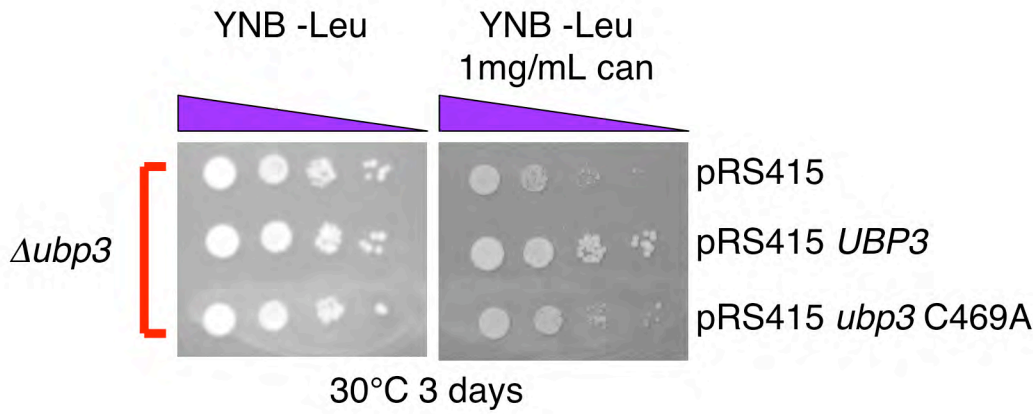

Figure 2.7. Wild type *UBP3* expressed on a single copy plasmid rescues the canavanine hypersensitivity of *UBP3* deletion. Ubp3p with the catalytic cysteine mutated to alanine does not rescue the canavanine hypersensitivity of *UBP3* deletion.

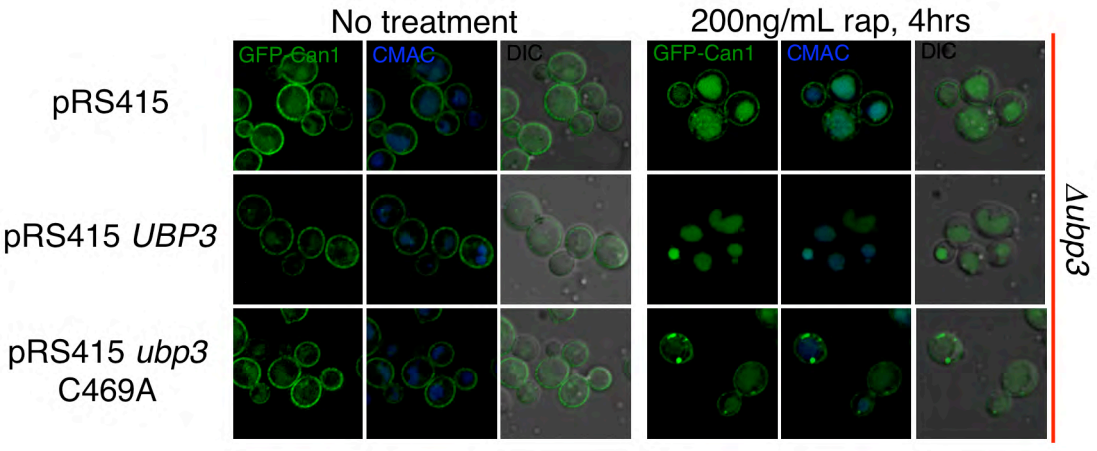

Figure 2.8. Catalytically inactive Ubp3p does not rescue the Can1p-GFP trafficking defect in *Δubp3* cells.

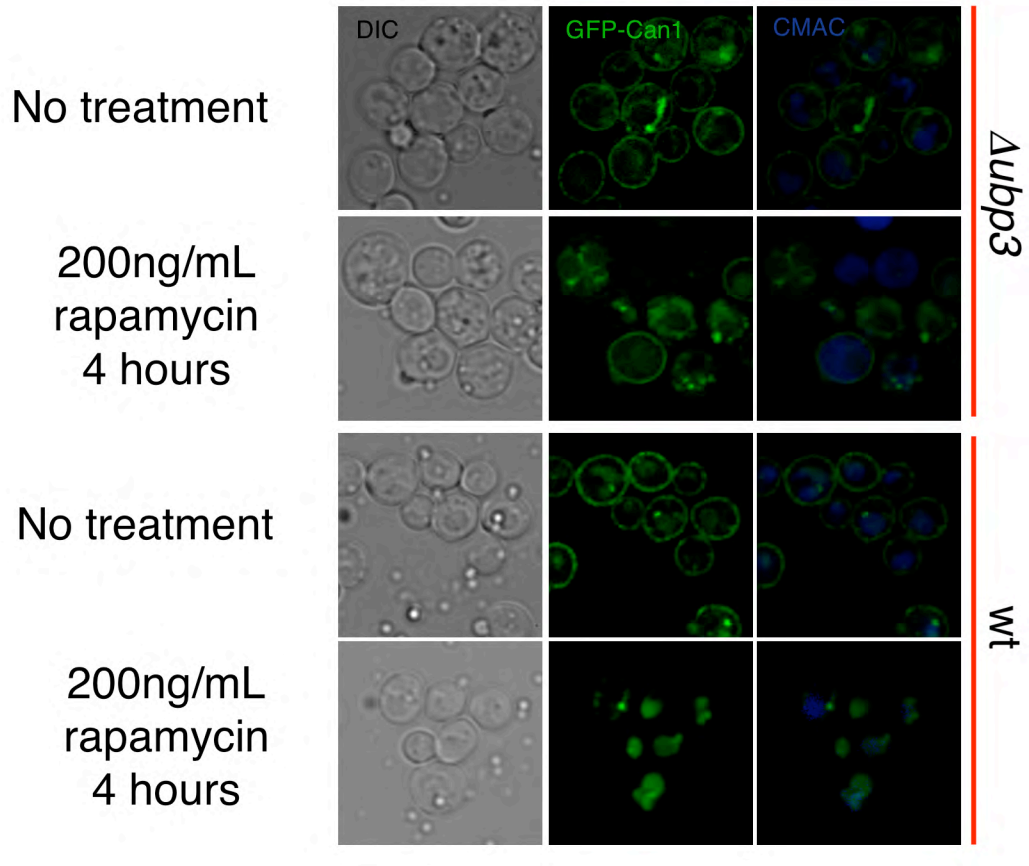

Figure 2.9. Overexpression of ubiquitin in *Δubp3* cells does not rescue the Can1p-GFP trafficking defect. Cells were transformed with YEp105 myc-Ub and grown in the presence of 100μM $CuSO_4$.

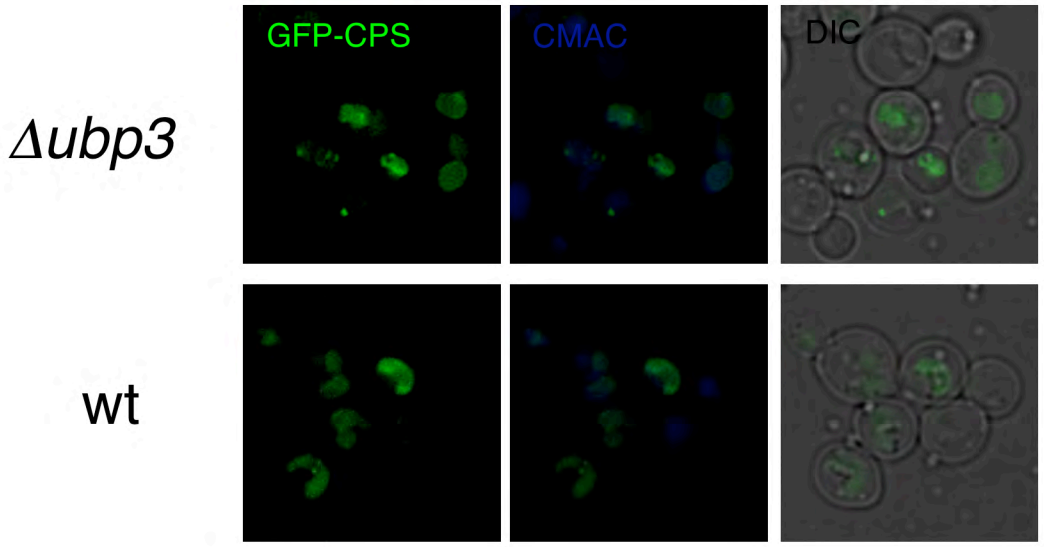

Figure 2.10. GFP-tagged vacuolar protease carboxypeptidase S (CPS) is sorted to the vacuole in *Δubp3* cells. CMAC stains the vacuole.

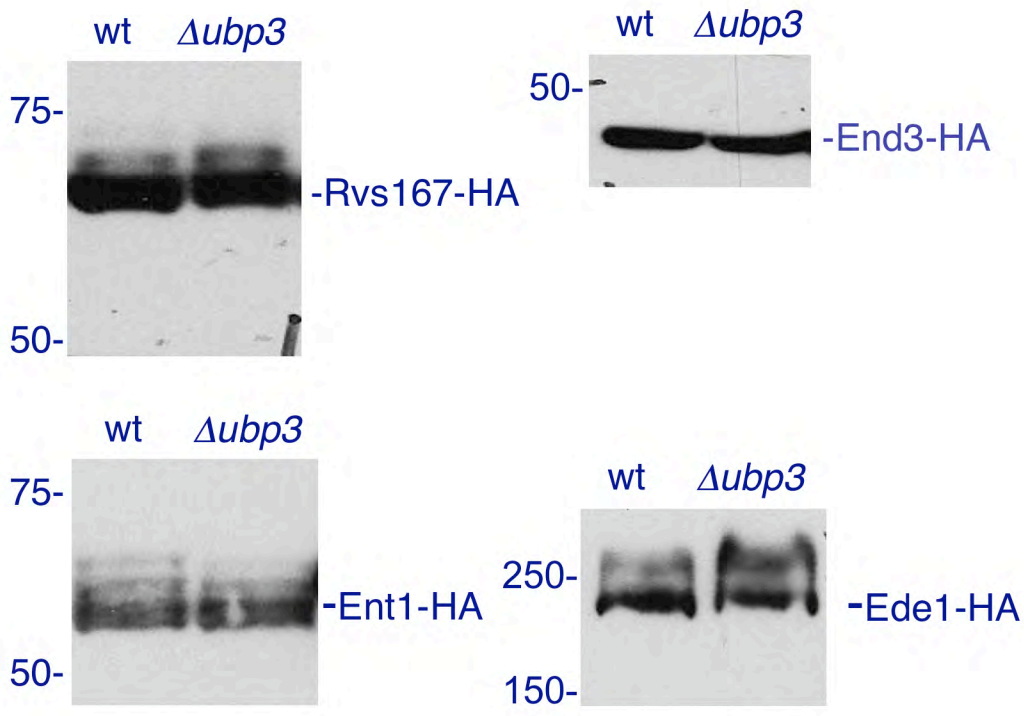

Figure 2.11. Comparison of lysates from cells with chromosomally HA-tagged endocytic machinery proteins. Blot for HA.

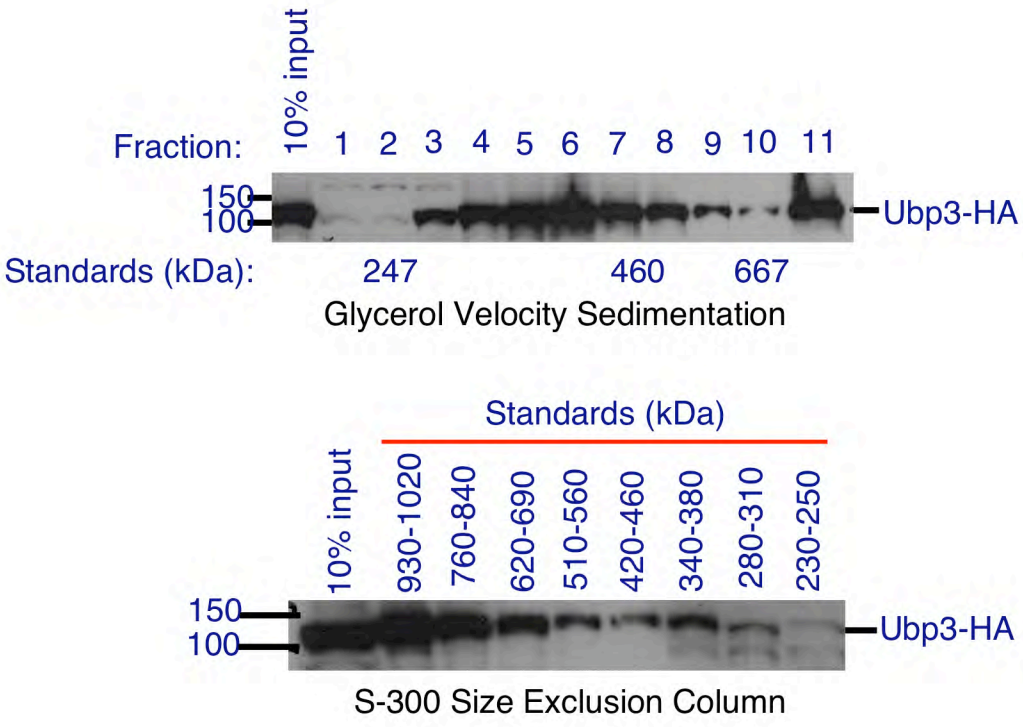

Figure 2.12. Glycerol velocity sedimentation (top) and size exclusion chromatography (bottom) indicate that Ubp3p is part of a large complex.

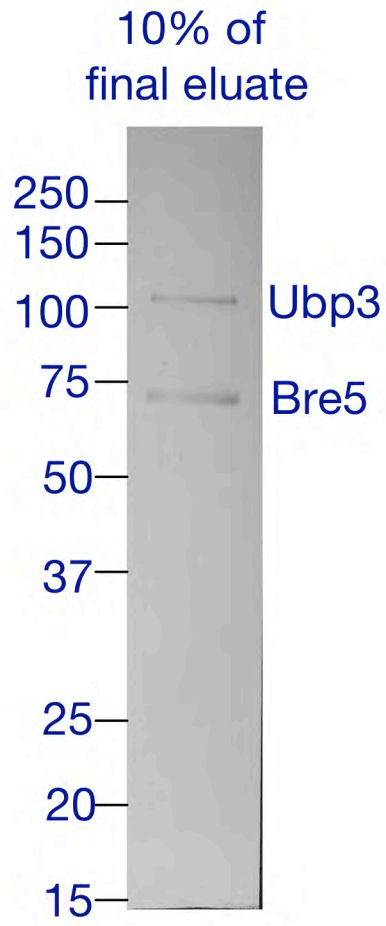

Figure 2.13. Mass spectrometry of purified Ubp3p-S tag-TEV-ZZ identifies Bre5p as a Ubp3p interactor.

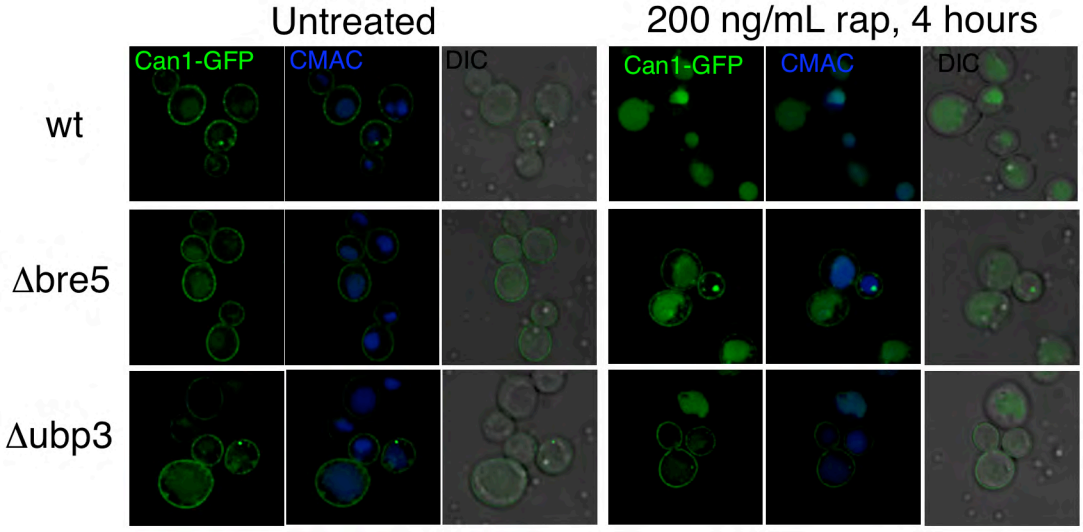

Figure 2.14. Can1p-GFP is stabilized at the plasma membrane in *Δbre5* cells. CMAC stains the vacuole.

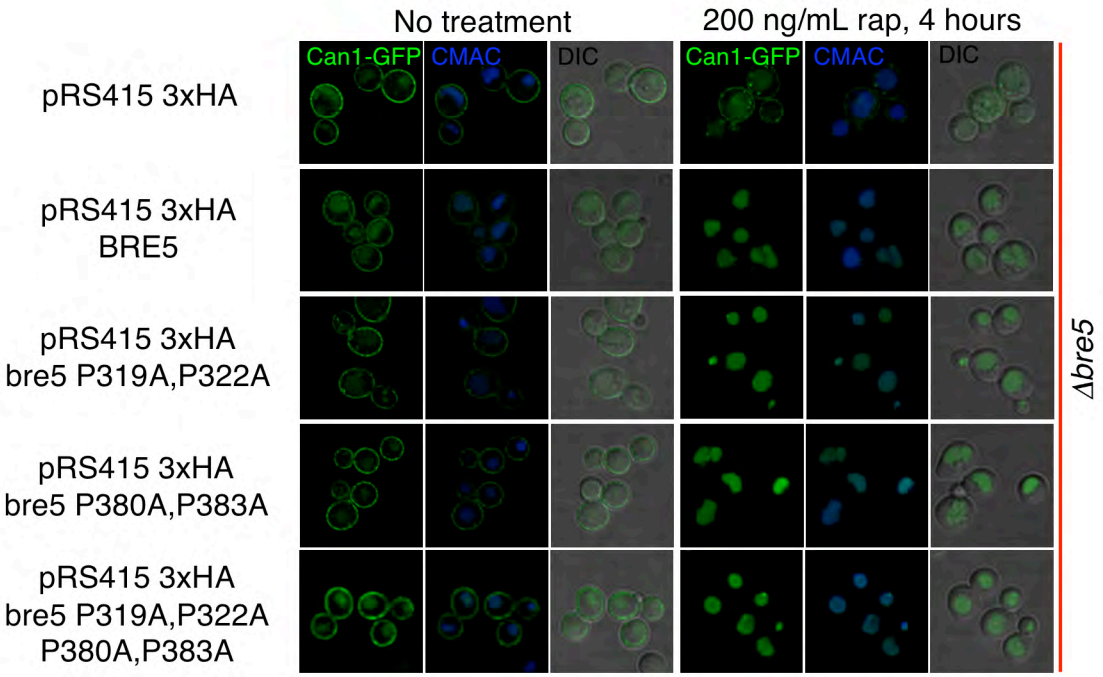

Figure 2.15. The Can1p-GFP trafficking defect in *Δbre5* cells is rescued by expression of wild type *BRE5* on a single copy plasmid. Bre5p with mutations in PxxP motifs also rescue the defect.

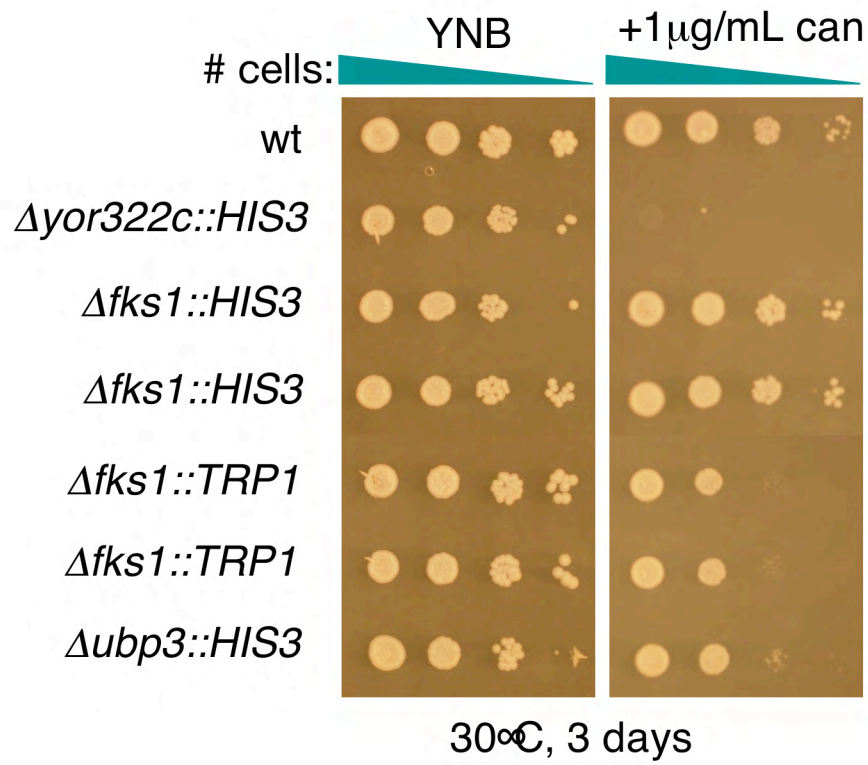

Figure 2.16. Deletion of *FKS1* results in canavanine hypersensitivity when replaced with *TRP1*, but not when replaced with *HIS3*. Experiment was repeated with identical results. *Δyor322c* used as positive control for canavanine hypersensitivity.

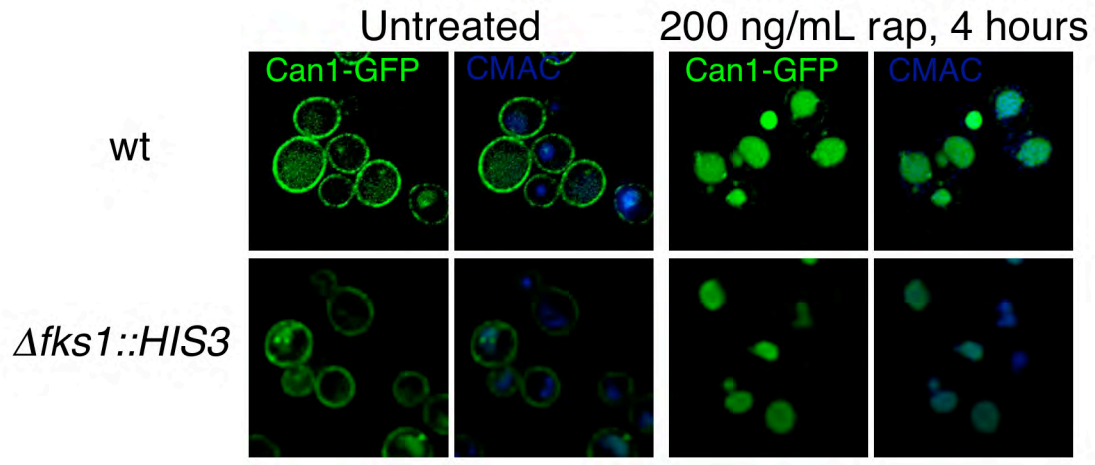

Figure 2.17. Cells deleted for *FKS1* do not stabilize Can1p-GFP at the plasma membrane when *FKS1* is replaced with *HIS3*.

References

Amerik, A.Y., Nowak, J., Swaminathan, S., and Hochstrasser, M. (2000a) The Doa4 deubiquitinating enzyme is functionally linked to the vacuolar protein-sorting and endocytic pathways. Mol. Biol. Cell 11, 3365-3380.

Amerik, A.Y., Li, S.-J., and Hochstrasser, M. (2000b) Analysis of the deubiquitinating enzymes of the yeast *Saccharomyces cerevisiae*. Biol. Chem. 381, 981-992.

Amerik, A.Y. and Hochstrasser, M. (2004) Mechanism and function of deubiquitinating enzymes. Biochim.Biophys. Acta 1695, 189-207.

Auty, R., Steen, H., Myers, L.C., Persinger, J., Bartholomew, B., Gygi, S.P., and Buratowski, S. (2004) Purification of active TFIID from *Saccharomyces cerevisiae*. J. Biol. Chem. 279, 49973-49981.

Baker, R.T., Tobias, J.W., and Varshavsky, A. (1992) Ubiquitin-specific proteases of *Saccharomyces cerevisiae*: Cloning of *UBP2* and *UBP3*, and functional analysis of the *UBP* gene family. J. Biol. Chem. 267, 23364-23375.

Baxter, B.K., Abeliovich, H., Zhang, X., Stirling, A.G., Burlingame, A.L., and Goldfarb, D.S. (2005) Atg19p ubiquitination and the cytoplasm to vacuole trafficking pathway in yeast. J. Biol. Chem. 280, 39067-39076.

Beck, T., Schmidt, A., and Hall, M.N. (1999) Starvation induces vacuolar targeting and degradation of the tryptophan permease in yeast. J. Cell Biol. 146, 1227-1237.

Cadavid, A.L.M., Ginzel, A., and Fischer, J.A. (2000) The function of the *Drosophila* Fat facets deubiquitinating enzyme in limiting photoreceptor cell number is intimately associated with endocytosis. Development 127, 1727-1736.

Cheeseman I.M., Brew, C., Wolyniak, M., Desai, A., Anderson, S., Muster, N., Yates III, J.R., Huffaker, T.C., Drubin, D.G., and Barnes, G. (2001) Implication of a novel multiprotein Dam1p complex in outer kinetochore function. J. Cell Biol. 155, 1137-1145.

Chen, X., Zhang, B., and Fischer, J.A. (2002) A specific protein substrate for a deubiquitinating enzyme: Liquid facets is the substrate of Fat facets. Genes Dev. 16, 289-294.

Cohen, M., Stutz, F., Belgareh, N, Haguenauer-Tsapis, R, and Dargemont, C. (2003a) Ubp3 requires a cofactor, Bre5, to specifically deubiquitinate the COPII protein, Sec23. Nat. Cell Biol. 5, 661-667.

Cohen, M., Stutz, F., and Dargemont, C, (2003b) Deubiquitination, a new player in Golgi to endoplasmic reticulum retrograde transport. J. Biol. Chem. 278, 51989-51992.

deHart, A.K.A., Schnell, J.D., Allen, D.A., Tsai, J.-Y., and Hicke, L. (2003) Receptor internalization in yeast requires the Tor2-Rho1 signaling pathway. Mol. Biol. Cell 14, 4676-4684.

Dupré, S., Urban-Grimal, D., and Haguenauer-Tsapis, R. (2004) Ubiquitin and endocytic internalization in yeast and animal cells. Biochim. Biophys. Acta 1695, 89-111.

Ellison, M.J. and Hochstrasser, M. (1991) Epitope-tagged ubiquitin. J. Biol. Chem. 266, 21150-21157.

Gavin, A.C., Aloy, P., Grandi, P., Krause, R., Boesche, M., Marzioch, M., Rau, C., Jensen, L.J., Bastuck, S., Dümpelfeld, B., Edelmann, A., Heurtier, M.A., Hoffman, V., Hoefert, C., Klein, K., Hudak, M., Michon, A.M., Schelder, M., Schirle, M., Remor, M., Rudi, T., Hooper, S., Bauer, A., Bouwmeester, T., Casari, G., Drewes, G., Neubauer, G., Rick, J.M., Kuster, B., Bork, P., Russell, R.B., and Superti-Furga, G. (2006) Proteome survey reveals modularity of the yeast cellular machinery. Nature 440, 631-636.

Grenson, M., Mousset, M., Wiame, J.M., Bechet, J. (1966) Multiplicity of the amino acid permeases in *Saccharomyces cerevisiae*. I. Evidence for a specific arginine-transporting system. Biochim. Biophys. Acta. 127, 325-38.

Hoffmann, W. (1985) Molecular characterization of the CAN1 locus in Saccharomyces cerevisiae. A transmembrane protein without N-terminal hydrophobic signal sequence. J. Biol. Chem. 260, 11831-7.

Krogan, N.J., Cagney, G., Yu, H., Zhong, G., Guo, X., Ignatchenko, A., Li, J., Pu, S., Datta, N., Tikuisis, A.P., Punna, T., Peregrín-Alvarez, J.M., Shales, M., Zhang, X., Davey, M., Robinson, M.D., Paccanaro, A., Bray, J.E., Sheung, A., Beattie, B., Richards, D.P., Canadien, V., Lalev, A., Mena, F., Wong, P., Starostine, A., Canete, M.M., Vlasblom, J., Wu, S., Orsi, C., Collins, S.R., Chandran, S., Haw, R., Rilstone, J.J., Gandi, K., Thompson, N.J., Musso, G., St Onge, P., Ghanny, S., Lam, M.H., Butland, G., Altaf-Ul, A.M., Kanaya, S., Shilatifard, A., O'Shea, E., Weissman, J.S., Ingles, C.J., Hughes, T.R.,

Parkinson, J., Gerstein, M., Wodak, S.J., Emili, A., and Greenblatt, J.F. (2006) Global landscape of protein complexes in the yeast *Saccharomyces cerevisiae*. Nature 440, 637-643.

Lesage, G., Sdicu, A.-M., Ménard, P., Shapiro, J., Hussein, S., and Bussey, H. (2004) Analysis of β-1,3-Glucan assembly in *Saccharomyces cerevisiae* using a synthetic interaction network and altered sensitivity to caspofungin. Genetics 167, 35-49.

Lin, C.H., MacGurn, J.A., Chu, T., Stefan, C.J, and Emr, S.D. (2008) Arrestin-related ubiquitin-ligase adaptors regulate endocytosis and protein turnover at the cell surface. Cell 135, 714-725.

Link, A.J., Eng, J., Schieltz, D.M., Carmack, E. Mize, G.J., Morris, D.R., Garvik, B.M. and Yates III, J.R. (1999) Direct analysis of protein complexes using mass spectrometry. Nat. Biotechnol.17, 676-682.

Matejcková-Foretová, A., Kinclová, O., and Sychrová, H. (1999) Degradation of *Candida albicans* Can1 permease expressed in *Saccharomyces cerevisiae*. FEMS Microbiol. Lett. 176, 257-262.

Moazed, D. and Johnson, A.D. (1996) A deubiquitinating enzyme interacts with Sir4 and regulates silencing in *S. cerevisiae*. Cell 86, 667-677.

Opekarová, M., Caspari, T., Pinson, B., Bréthes, D., and Tanner, W. (1998) Post-translational fate of Can1 permease of *Saccharomyces cerevisiae*. Yeast 14, 215-224.

Parker, F., Maurier, F., Delumeau, I., Duchesne, M., Faucher, D., Debussche, L., Dugue, A., Schweighoffer, F., and Tocque, B. (1996) A Ras-GTPase-activating protein SH3-domain-binding protein. Mol. Cell. Biol. 16, 2561-2569.

Roberg, K.J., Bickel, S., Rowley, N., Kaiser, C.A. (1997) Control of amino acid permease sorting in the late secretory pathway of Saccharomyces cerevisiae by SEC13, LST4, LST7 and LST8. Genetics 147, 1569-84.

Rosenthal, G.A. (1977) The biological effects and mode of action of L-canavanine, a structural analogue of L-arginine. Q. Rev. Biol. 52, 155-178.

Saksela, K., Cheng, G. and Baltimore, D. (1995) Proline-rich (PxxP) motifs in HIV-1 Nef bind to SH3 domains of a subset of Src kinases and are required for the enhanced growth of Nef^+ viruses but not for down-regulation of CD4. EMBO J. 14, 484-491.

Séron, K., Blondel, M.-O., Haguenauer-Tsapis, R., and Volland, C. (1999) Uracil-Induced Down-regulation of the yeast uracil permease. J. Bacteriol. 181, 1793-1800.

Stamenova, S.D., Dunn, R. Adler, A.S. and Hicke, L. (2004) The Rsp5 ubiquitin ligase binds to and ubiquitinates members of the yeast CIN85-Endophilin complex, Sla1-Rvs167. J. Biol. Chem. 279, 16017-16025.

Tong, A.H., Lesage, G., Bader, G.D., Ding, H., Xu, H., Xin, X., Young, J., Berriz, G.F., Brost, R.L., Chang, M., Chen, Y., Cheng, X., Chua, G., Friesen, H., Goldberg, D.S., Haynes, J., Humphries, C., He, G., Hussein, S., Ke, L., Krogan, N., Li, Z., Levinson, J.N., Lu, H., Ménard, P., Munyana, C., Parsons, A.B., Ryan, O., Tonikian, R., Roberts, T., Sdicu, A.M., Shapiro, J., Sheikh, B., Suter, B., Wong, S.L., Zhang, L.V., Zhu, H., Burd, C.G., Munro, S., Sander, C., Rine, J., Greenblatt, J., Peter, M., Bretscher, A., Bell, G., Roth, F.P., Brown, G.W., Andrews, B., Bussey, H., and Boone, C. (2004) Global mapping of the yeast genetic interaction network. Science 303, 808-813.

Volland, C., Urban-Grimal, D., Géraud, G., and Hagueneauer-Tsapis, R. (1994) Endocytosis and degradation of the yeast uracil permease under adverse conditions. J. Biol. Chem. 269, 9833-9841.